Dissertation

submitted to the
Combined Faculty of Natural Sciences and Mathematics
of the Ruperto-Carola University of Heidelberg, Germany
for the degree of
Doctor of Natural Sciences

presented by

M.Sc. Sebastian Brosig
born Henkel in Räckelwitz, Germany

Oral examination: November 14th, 2019

Single Cell microRNA Dynamics during Mouse Embryonic Stem Cell Differentiation

Referees: Dr. Alexander Aulehla

Prof. Dr. Michael Knop

This work has been carried out at the European Molecular Biology Laboratory in Heidelberg under the supervision of Dr. Pierre Neveu from October 2015 to September 2019.

"Es gibt nicht die Lösung – jeder strauchelt, so gut er kann"

(Der Psychologie-Podcast von Puls)

SUMMARY

miRNAs cooperate and fine tune gene expression on the post-transcriptional level and can therefore be seen as an additional regulatory layer during mouse embryonic stem cell (mESC) self-renewal and differentiation. However, the biological activity of conserved miRNAs during those processes is poorly understood, as most studies cannot uncouple miRNA activity from miRNA expression levels. Therefore, my PhD project focused on studying single cell miRNA dynamics during mESC differentiation towards the three major germ layers and measured miRNA affinities to a miRNA reporter *in vivo*. I established stable mESC lines expressing fluorescent reporters for the 162 miRNAs conserved in vertebrates and could show that the temporal miRNA activity profile is tightly regulated throughout mESC differentiation. Interestingly, miRNAs exhibit activity changes at early, mid and late stages of stem cell differentiation. Moreover, miRNAs seem to regulate differentiation in a cooperative manner on a global level rather than being germ layer specific. However, this does not exclude single miRNA clusters from being potentially germ layer specific as shown for the highly conserved miR-302 cluster. Strikingly, based on principle component analysis, miRNA activity diverged between germ layer fates already 48 hours after onset of differentiation.

In addition, this PhD project experimentally determined miRNA affinities for 119 conserved miRNAs by integrating measurements of miRNA activity and expression levels. I could show that miRNA affinities span several orders of magnitude and are negatively correlated to miRNA expression levels, which suggests that weakly expressed miRNAs can be as potent as highly expressed ones. Knowing the affinity and expression levels in a given cell type, enabled me to rank miRNAs according to their effective potency. This will potentially help to determine which genes are targets of a given miRNA.

In summary, this thesis project provides a comprehensive picture of changes in miRNA activity upon mESC differentiation in addition to experimentally determined miRNA affinities. Future gain and loss-of-function experiments of interesting miRNAs in fluorescently labeled fate marker cell lines will potentially reveal miRNAs indispensable for stem cell differentiation.

ZUSAMMENFASSUNG

microRNAs (miRNAs) spielen eine wichtige Rolle bei der Koordination und Feinjustierung der Genexpression auf post-transkriptionaler Ebene. Daher werden sie als zusätzlich regulatorische Ebene bei der Erneuerung und Differenzierung embryonaler Stammzellen betrachtet. Die biologische Aktivität evolutionär konservierter miRNAs ist jedoch unzureichend erforscht, da die meisten Studien nicht zwischen miRNA Genexpression und biologischer Aktivität unterscheiden. Daher liegt der Focus meiner Doktorarbeit auf der Untersuchung von miRNA Affinitäten und Dynamiken während der Erneuerung und Differenzierung von embryonalen Stammzellen in die drei Hauptkeimblätter Mesoderm, Endoderm und Ectoderm. Dazu habe ich 162 miRNA Sensor Ziellinien entwickelt, die spezifisch die Affinität zu einem fluoreszierenden Sensor sowie dessen biologische Aktivität messen. Der daraus resultierende Datensatz umfasst alle evolutionär konservierten miRNAs in Wirbeltieren.

Diese Daten zeigen, dass die Aktivität der miRNAs während der Differenzierung zeitlich sehr strikt geregelt ist. Aktivitätsänderungen sind dabei zu frühen, mittleren und späten Zeitpunkten der Stammzelldifferenzierung zu beobachten. Zudem scheinen miRNAs auf globaler Ebene zu kooperieren, statt Keimblatt spezifisch zu wirken. Dies schließt keineswegs die Funktionalität keimblattspezischer miRNA cluster aus, wie am Beispiel des miR-302 clusters gezeigt werden konnte. Die Hauptkomponentenanalyse (PCA) des miRNA Aktivitätsdatensatzes hat zudem ergeben, dass sich die drei Hauptkeimblätter bereits 48 Stunden nach Differenzierungsbeginn unterscheiden.

Ferner wird in dieser Doktorarbeit die Affinität von 119 evolutionär konservierten miRNAs experimentell bestimmt. Interessanterweise, variieren die Affinitäten über mehrere Größenordnungen und korrelieren zudem negativ mit der miRNA Menge. Daher können gering exprimierte miRNAs die gleiche oder eine stärkere Wirkung erzielen wie stark exprimierte miRNAs. Die Bestimmung von miRNA Expressionsmengen und miRNA Affinitäten ermöglichte eine Klassifizierung nach ihrer Wirkungsstärke. Eine solche Klassifizierung kann dazu beitragen, miRNA Kandidaten mit besonders hoher biologischer Relevanz zu identifizieren und in weiteren Studien deren target mRNAs sowie regulierter Signalwege zu bestimmen.

Das vorliegende Projekt gibt einen umfassenden Einblick in die dynamischen Aktivitätsänderungen von miRNAs während der Stammzelldifferenzierung und

beschreibt die experimentelle Bestimmung von bisher vernachlässigten miRNA Affinitäten. Zukünftige „gain and loss-of-function“ Experimente von vielversprechenden miRNA Kandidaten in fluoreszierenden „fate-marker“ Zellinien werden dazu beitragen, die für die Stammzelldifferenzierung essentiellen miRNAs zu identifizieren. Diese Erkenntnisse werden besonders für die regenerative Medizin von großem Nutzen sein.

CONTENTS

LIST OF FIGURES

LIST OF TABLES

LIST OF ABBREVIATIONS

2i	2 inhibitors
Ago2	argonaute 2
AP	alkaline phosphatase
αTUB	α-tubulin
βGpA	β-tubulin
BAC	bacteria artificial chromosome
BFP	blue fluorescent protein
BMP	bone morphogenetic protein
bp	base pairs
BSA	bovine serum albumin
CAG	CMV-enhancer β-actin
Cas9	CRISPR associated protein 9
CD	cluster of differentiation
cDNA	complementary DNA
ceRNA	competing endogenous RNA
CMV	cytomegalovirus
CRISPR	clustered regularly interspaced short palindromic repeats
DAPI	4',6-diamidino-2-phenylindole
Dgcr8	DiGeorge critical region 8
DMEM	Dulbecco's modified Eagle medium
DMSO	dimethylsulfoxide
DNA	deoxyribonucleic acid
dsRNA	double-stranded RNA
E	day of embryonic development
EDTA	ethylendiaminetetraacetic acid
EF1α	elongation factor 1α
EMBL	European Molecular Biology Laboratory
Epi	epiblast
EpiLC	epiblast like stem cell
EpiSC	epiblast stem cell
ERK	extracellular-signal regulated kinase
ES cells	embryonic stem cells
Esrrb	estrogen-related receptor beta
ExE	extra-embryonic ectoderm
FACS	fluorescence-activated cell sorting
FBS	fetal bovine serum
FCS	fetal calf serum
FGF	fibroblast growth factor
FOXA2	forkhead box protein A2
FRET	Förster resonance energy transfer
GDP	guanosine diphosphate
GFP	green fluorescent protein
GMEM	glasgow minimum essential medium
gp130	glycoprotein 130
GSK3	glycogen synthase kinase 3

GTP	guanosine 5'-triphosphate
H2B	histone 2B
hESC	human embryonic stem cells
HMG	high mobility group
HRP	horseradish peroxidase
HTS	high throughput sampler
ICM	inner cell mass
ID	inhibitor of differentiation
IDE-1	inducer of definitive endoderm 1
IgG	immunoglobin G
IL6	interleukin-6
ILR6	interleukin-6 receptor
JAK	janus kinase
kb	kilo base pairs
KLF4	krüppel-like factor 4
KO	knockout
KRAS	kirsten rat sarcoma viral oncogene homolog
KSR	knockout serum replacement
LB	lysogeny broth
LIF	leukemia inhibitory factor
LIFR	leukemia inhibitory factor receptor
mAb	monoclonal antibody
MAPK	mitogen-activated protein kinase
mCherry	monomeric Cherry
mESC	mouse embryonic stem cell
MEF	mouse embryonic fibroblast
MEK	mitogen activated protein kinase
miRNA	micro RNA
miRNA-Seq	micro RNA sequencing
mRNA	messenger RNA
NA	not applicable
NaCl	sodium chloride
NLS	nuclear localization signal
OCT4	octamer binding transcription factor 4
pA	polyadenylation signal
pAb	polyclonal antibody
PBS	phosphate buffered saline
PC	principal component
PCA	principal component analysis
PCR	polymerase chain reaction
PEST	proline-glutamic acid-serine-threonine
PFA	paraformaldehyde
PGK	phosphoglycerate-kinase 1
PI3K	phosphatidylinositol-3 phosphate kinase
PIP3	phosphatidylinositol (3,4,5)-triphosphate
PrE	primitive endoderm
pre-miRNA	precursor miRNA
pri-miRNA	primary miRNA transcript
RA	all-trans retinoic acid

RAF	rapidly accelerated fibrosarcoma
RAS	rat sarcoma viral oncogene
RISC	RNA induced silencing complex
RNA	ribonucleic acid
RNase	ribonuclease
RNA-Seq	RNA sequencing
RPMI	Roswell Park Memorial Institute
RT	room temperature
rtTA	reverse tetracycline transactivator
SDS	sodium dodecyl sulfate
sgRNA	single guide RNA
SH2	src homology 2 domain
αSMA	alpha-smooth muscle actin
SOB	super optimal broth
SOC	SOB with catabolic repressor
SOX2	SRY (sex determining region Y)-box2
SOX17	SRY (sex determining region Y)-box17
STAT3	signal transducer and activator of transcription 3
TDMD	target-directed miRNA degradation
T	Brachury
TE	trophectoderm
TF	transcription factor
TM	melting temperature
TGF-β	transforming growth factor-β
TRBP	Tar RNA binding protein
Tubb3	ß-III-tubulin
U	units
UTR	untranslated region
VE	visceral endoderm

1 INTRODUCTION

1.1 Embryonic stem cells as model system

Stem cells comprise the ability to self-renew and differentiate towards specialized cell types. Yet, their developmental potency varies considerably (De Los Angeles et al. 2015). A totipotent zygote, has the capacity to give rise to all embryonic and extraembryonic tissue (Nichols and Smith 2012). Moreover, zygotes are programmed to undergo a defined process of cleavage divisions which results in loss of pluripotency as the embryo develops (Niakan et al. 2012). This characteristic makes it challenging to study molecular basics of pluripotency *in vivo*, however, their developmental potential has not been captured *in vitro*. Therefore, blastocyst derived embryonic stem cells (ESCs) are used to study pluripotency and transient pluripotent cell populations *in vivo* (Evans and Kaufman 1981; Martin et al. 1981; Nichols and Smith 2012).

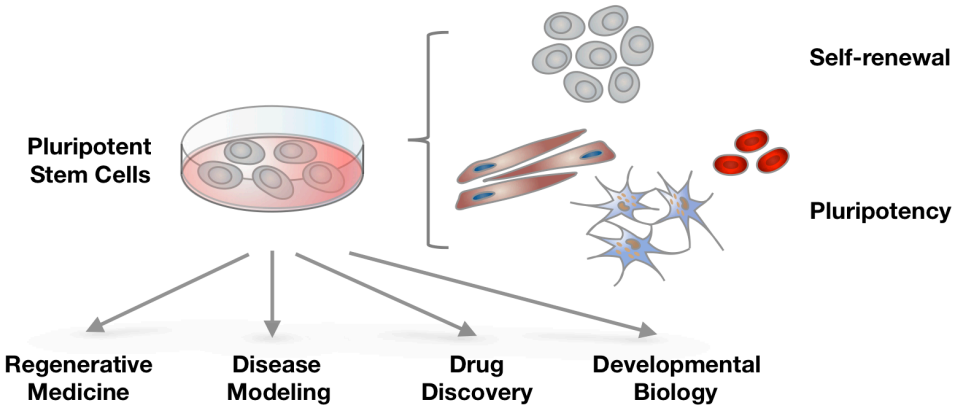

Figure 1: Pluripotent stem cells as model system.

Pluripotent stem cells are derived from the inner cell mas and can be kept indefinitely in culture. They have the capacity to self-renew and can differentiate towards any specialized tissue of an organism. In addition to disease modeling and drug discovery, pluripotent stem cells are used as model system in developmental biology and regenerative medicine, in order to delineate the molecular circuitries of pluripotency and fate choice. Adapted from Hu (2018).

Compared to zygotes, ESCs are developmentally more restricted as they do not contribute to extraembryonic tissues like the placenta (Condic 2014), they still comprise the potency to differentiate into all tissues of an organism. ESCs can be maintained *in vitro* for extended periods of time, without loss of their capacity to contribute to any germ layer of the developing embryo (Lanza and Atala 2014). Therefore, ESCs possess great potential for applications in regenerative medicine, disease modeling and developmental biology (**Figure 1**) (Loh et al. 2006). Moreover, they are the model system of choice to study the molecular circuitry of pluripotent state (Jaenisch and Young 2008) and cell fate choice (Yamanaka and Ralston 2010).

1.1.1 Transient pluripotency during embryonic development

Pre-implantation development of the mammalian embryo starts with fertilization of the oocyte and involves several distinct cellular events. The zygote is considered totipotent and gives rise to all embryonic and extraembryonic tissues (Chazaud and Yamanaka 2016). After the first cleavage division, the 2-cell stage is followed by the embryonic genome activation (EGA). After this transition, development is exclusively controlled by the embryonic genome as the maternal gene products have been degraded and embryonic transcription is evident (Saitou et al. 2012). EGA is a global activation of genes necessary to establish the pre-implantation developmental program. The next key developmental event occurs at the 8-cell morula stage, where polarization and compaction take place (Cockburn and Rossant 2010). Subsequent differentiation of the blastomeres' builds the inner cell mass (ICM) in addition to the trophectoderm (TE), which gives rise to the placenta. As the embryo develops into a hollow sphere known as blastocyst, the ICM differentiates into the epiblast (Epi) and primitive endoderm (PrE) (**Figure 2**) (Miguel et al. 2010). Generation of the first three lineages trophectoderm, epiblast and primitive endoderm, seem to be orchestrated by differences in cell-to-cell interaction, gene expression levels as well as the microenvironment of individual cells rather "than the active partitioning of maternal determinants" (Chazaud and Yamanaka 2016).

ESCs are derived from the ICM at embryonic day 3.5 (E 3.5) whereas EpiSCs are derived at later timepoints (E 5.5 – E 6.5). Pluripotency of epiblast cells is transient and persists for only few days in the developing embryo (Nichols and Smith 2012), which makes it difficult to study the molecular circuitries of primed pluripotency *in vitro*.

Interestingly, ESCs are the *ex vivo* equivalent of the epiblast stage in the preimplantation blastocyst and share the same developmental potential, therefore, ESCs can be differentiated into the three major germ layers endoderm, mesoderm and neuroectoderm (Czechanski et al. 2014).

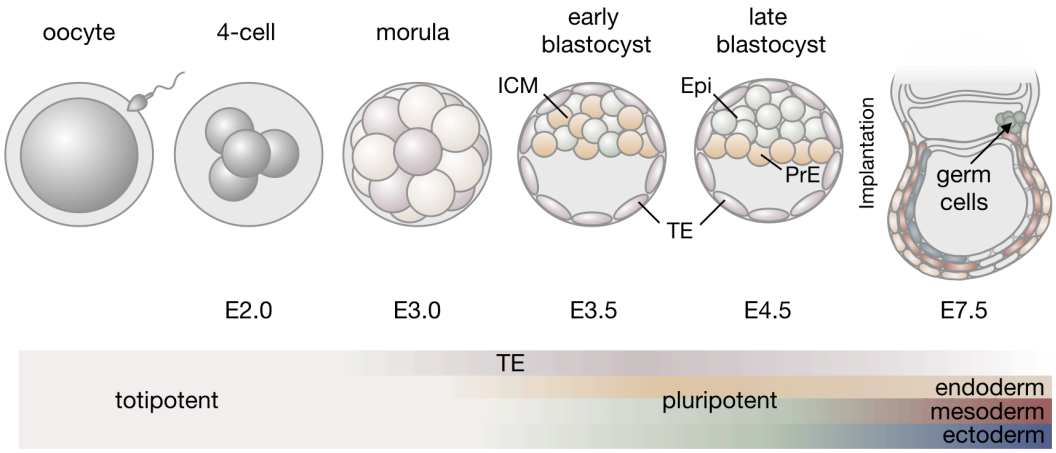

Figure 2: Origin of mESCs and mEpiSCs.

Fertilization of the oocyte forms a totipotent stem cell (zygote) with the capacity to derive all embryonic and extraembryonic tissue of an organism. The developmental potency thereafter declines as cells begin to specialize. After several rounds of cleavage divisions, the early blastocyst is formed. The inner cell mass (ICM) separates into pluripotent epiblast cells (Epi) and primitive endoderm (PrE). The resulting late blastocyst resembles the last stage of pre-implantation development and consists of developmentally restricted cells (TE, Epi, PrE). Embryonic stem cells (ESCs) are derived from the ICM at embryonic day E3.5. Epiblast derived stem cells (EpiSCs) are derived at E5.5 – E6.5. The blastocyst further develops into egg cylinder to prepare for germ layer specification.

1.1.2 Origin and definition of pluripotent states

Pluripotency is maintained by an interplay of extracellular signaling and intracellular gene expression circuits which keeps embryonic stem cells in an undifferentiated and self-renewing state (Miguel et al. 2010). As ESCs are derived from the ICM of the pre-implantation blastocyst, hallmarks of *ex-vivo* pluripotency should correspond to the properties of the preimplantation epiblast. This includes: i) teratoma and chimera formation with germline transmission, ii) unlimited self-renewal capacity and the potential to derive any somatic cell type, iii) expression of a specific set of genes

associated with pluripotency, iv) global DNA hypomethylation v) two functional X-chromosomes, vi) low level of bivalent histone marks, vii) the capability of metabolism through oxidative phosphorylation as well as glycolysis and viii) the lack of lineage priming (De Los Angeles et al. 2015).

Two pluripotent stem cell states can currently be stabilized in culture: naïve (or "ground state") and primed (EpiSCs) pluripotency (Nichols and Smith 2009). Naïve stem cells are derived from the pre-implantation embryo, whereas primed stem cells are derived from the post-implantation embryo (Najm et al. 2011). Although both cell types differentiate *in vitro* towards the three major germ layers, naïve and primed cells are distinct in their origins, biological characteristics, gene expression profiles, developmental potential and signal pathways dependences (Brons et al. 2007; Evans and Kaufman 1981; Tesar et al. 2007).

1.1.3 The naïve state ("ground state") of pluripotency

A complex circuit of transcription factors (TFs) in addition to epigenetic regulators holds ESCs in naïve pluripotent state, mostly by repression of lineage specific genes and activation of core pluripotency factors like Nanog, Oct4 and Sox2 (Thomson et al. 2011). Thus, transcription factors are the perfect proxy to determine pluripotent cell populations or mark the onset of differentiation (Hackett and Azim Surani 2014). In the advent of naïve pluripotency exit, levels of Nanog, Klf2 and Tfcp211 TFs decline earlier than Rex1 (Kalkan et al. 2017). Therefore, cells expressing Rex1 always maintain self-renewal capacity. Hence, Rex1 is considered to be one of the "real" naïve pluripotency markers, as its downregulation marks the irreversible exit from the naïve state (Kalkan and Smith 2014).

Stem cells are kept in "ground state" pluripotency (Ying et al. 2008) using 2i/LIF or Serum/LIF media conditions. 2i/LIF media contains the two inhibitors PD and CHIR (2i) which repress the extracellular-signal-regulated protein kinase (MEK/ERK) and glycogen synthase kinase-3 (GSK3) pathways. This results in the inhibition of the FGF pathways and activation of Wnt signaling (Sim et al. 2017). Therefore, 2i artificially rewires gene expression programs necessary to keep stem cells in an pluripotent state, which is usually transient in the developing embryo (Weinberger et al. 2016).

Serum/LIF media on the other hand, which is chemically undefined due to its serum content. Fetal bovine serum (FBS) provides a wide variety of embryonic growth promoting factors such as macromolecular proteins, nutrients, hormones and attachment factors (Jayme and Blackman 1985; Jayme, Epstein, and Conrad 1988). In addition, it adds buffering capacity to the media and neutralizes toxic components. On a molecular level Serum/LIF media is characterized by constitutively active MEK/ERK and GSK3 signaling (Graf et al. 2011). Although MEK/ERK drives necessary genes for proliferation (Zhang and Liu 2002) and GSK3 benefits the Wnt pathways needed for self-renewal (Singh et al. 2012), the ERK pathway is also activated and known to facilitate differentiation (Tee et al. 2014) which in turn might antagonize pluripotency. Moreover, serum is thought to be the underlying component for heterogeneity in mESCs which was shown to be absent when cells are cultured in 2i condition (Guo et al. 2016). Indeed, ESCs cultured in 2i/LIF are considered morphologically uniform and express naïve pluripotency genes whereas ESCs cultured in Serum/LIF are heterogeneous for both (Guo et al. 2016; Kumar et al. 2014). Of note, as opposed to 2i/LIF, Serum/LIF condition is not associated with genomic instability like karyotype changes over extended culture periods (Hassani et al. 2014; Choi et al. 2017).

Interestingly, epigenetic features like global DNA demethylation, missing X chromosome inactivation and low levels of bivalent (activator and repressor) histone marks on chromatin define naïve pluripotent ESCs. Even enhanced capacity for phosphorylation, or high mitochondria activity are considered hallmarks of naïve pluripotency (Hackett and Azim Surani 2014; Zimmerlin, Park, and Zambidis 2017; De Los Angeles et al. 2015). Therefore, switching of genetic and epigenetic features is used to convert naïve cells into primed pluripotent cells and vice versa (Bao et al. 2009; Silva et al. 2009; Tosolini and Jouneau 2015b). Intriguingly, cells cultured first in 2i/LIF and subsequently propagated in Serum/LIF adopt to the surrounding signaling cues which could be measured by gene expression changes. This shows that cell states exhibited in 2i or serum conditions are highly plastic (**Figure 3**) (Weinberger et al. 2016).

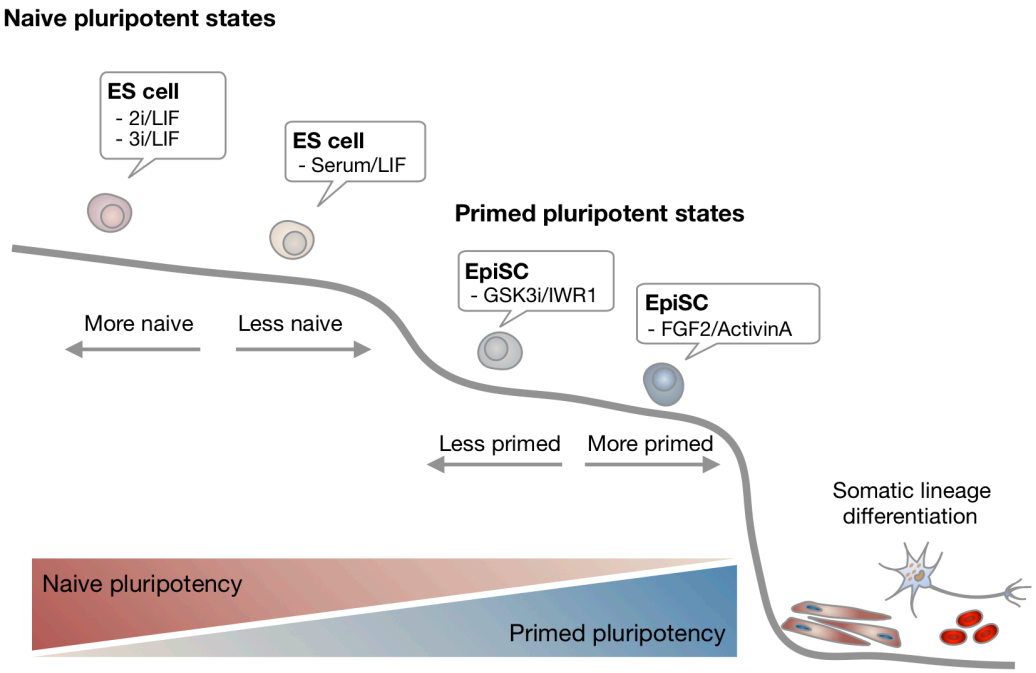

Figure 3: Developmental plasticity of naive and primed pluripotent stem cells.
ESC media is composed of signaling molecules in various combinations, all of which keep ESCs in a pluripotent state. The model depicts "relative naivity" within the spectrum of naïve and primed pluripotency. Naïve pluripotency cannot be described in absolute terms, as naïve cells can comprise features of primed pluripotent stem cells. Similarly, primed cells cultured in various conditions have different features and various degrees of naivety. As the naïve pluripotency feature decreases, the primed feature increases, which is reflected by the change in gene expression programs and epigenetic signatures as well as signaling circuitries. Adapted from Weinberger et al., (2016) with permission from Springer Nature under License Number 4653000646926.

1.1.4 The primed state (EpiSCs) of pluripotency

Mouse epiblast stem cells (EpiSCs) are established either by derivation from the post implantation epiblast (Brons et al. 2007; Tesar et al. 2007) or by ICM conversion *in vitro* using appropriate media conditions (**Figure 3**) (Guo et al. 2009; Tosolini and Jouneau 2015; Brons et al. 2007). EpiSCs originate from a slightly more differentiated state compared to ESCs, thus, ESCs correspond to embryonic day 4.5 (E4.5) of development (Boroviak et al. 2014) whereas EpiSCs are the equivalent of E5.5 to E7.5 (Han et al. 2010). This explains why pluripotent cells are categorized into "naïve" (ESCs) and "primed" (EpiSCs) pluripotency. Although both are considered pluripotent, their

epigenetic state, chromatin state, gene expression signature, transcriptional state, metabolism, and signaling mechanism differ vastly (Brons et al. 2007; Ying and Smith 2017; Kalkan and Smith 2014). Besides differences, much overlap can be found, especially in gene expression. This suggests that pluripotency is a highly dynamic rather than fixed individual state which is confirmed by different degrees of naivety or priming among naïve and primed cells (**Figure 3**) (Weinberger et al. 2016). Primed cells, for instance, overlap with naïve cells in expression levels of core pluripotency factors such as Nanog, Oct4, Sox2, but not Klf2,4,5, Tbx3, Dax1 or Esrrb, which are dramatically downregulated in primed cells. Intriguingly, fate specific TFs such as Brachyury, FoxA2 or Cer are only expressed in primed (Kalkan and Smith 2014) but not naïve cells. Taken together this suggests, that epiblast stem cells are a mixed population of lineage progenitors and pluripotent precursors.

Similar to ESCs, EpiSCs can be kept *in vitro* for an extended period of time (Najm et al. 2011), which makes them a model system to study pluripotency exit and entry into lineage specification. EpiSCs can form chimeras when injected into post-implantation embryos. Moreover, EpiSCs differentiate to derivatives of all three major germ layers (Brons et al. 2007; Huang et al. 2012), but lack the ability of chimera formation upon blastocyst injection (Tesar et al. 2007; Han et al. 2010). Among many factors, the characteristic epigenetic profile of EpiSCs might contribute to its reduced plasticity (Han et al. 2010). Intriguingly, EpiSCs share distinctive properties with human ESCs (Chenoweth et al. 2010), thus EpiSCs are one among other model systems to study signaling cues and cell fate decisions in the context of human development.

Since primed pluripotency is known to be dependent on Activin/Nodal signaling, EpiSCs are commonly cultured in Activin A and FGF2 containing media (Najm et al. 2011). Although FGF is not strictly required, it improves the overall quality of the culture by reinforcing the efficiency of activin signaling (Brons et al. 2007) and inhibits spontaneous neuronal differentiation (Gritti et al. 1996). In addition, Activin A activates SMAD2/3 transcription factors (**Figure 4**) (Pauklin and Vallier 2015) which positively regulate Nanog (Brons et al. 2007) and therefore promote pluripotency.

1.2 Extrinsic and intrinsic signaling of pluripotency

1.2.1 LIF dependent pluripotency

Originally, mESCs were cultured on mitotically inactive feeder cells (embryonic fibroblasts). In 1988, leukemia inhibitory factor (LIF) was discovered as paracrine signal produced by these cells (Williams et al. 1988; Smith et al. 1988). Moreover, LIF mRNA was detected in both, the trophectoderm and blastocyst stage, which shows its pivotal role during early mouse embryogenesis (Nichols et al. 1996). Since then, LIF is the key media component for derivation and cultivation of mouse embryonic stem cells. As an interleukin 6 class cytokine, LIF sustains and facilitates the self-renewing and undifferentiated state of stem cells (Yoshida et al. 1994). In addition to paracrine signaling, LIF functions through an autocrine manner as it is produced by the LIF gene of mESCs (Yue et al. 2015).

LIF affects three major signaling pathways in mESCs which were shown to maintain the pluripotent state of stem cells. The STAT3 signaling pathways, which facilitates self-renewal of pluripotent stem cells (Tai et al. 2014), the ERK signaling pathway, which promotes proliferation and differentiation (Cartwright 2005), and the AKT pathway, which was shown to foster cell survival through ß-catenin (Niwa et al. 2009).

On a molecular basis LIF binds to the low affinity LIF receptor (LIFR) which induces heterodimerization with the glycoprotein 130 (gp130) subunit. This heterodimerization results in the activation of the receptor associated Janus kinase (JAKs), phosphorylation of receptor docking sites and recruitment of STAT3 through Src-homolgy-2 (SH2) domains. In turn, signal transducer and activator of transcription 3 (STAT3) is phosphorylated, translocates to the nucleus, and drives the expression of self-renewal genes (**Figure 4**) (Yue et al. 2015). STAT3 also inhibits the differentiation of stem cells into mesoderm and endoderm progenitors by preventing the activation of lineage specific differentiation programs (Graf et al. 2011). At the same time the extracellular signal-regulated kinase pathway (ERK-pathway) is activated by LIF signaling where ERK phosphorylates itself in addition to cytoplasmic targets. Upon phosphorylation, ERK interacts with importin 7, which facilitates ERK translocation to the nucleus (Berti and Seger 2017). Nuclear ERK indirectly regulates gene expression

through TFs that in turn facilitate cellular proliferation (**Figure 4**) (Cartwright 2005). The third pathway activated by LIF signaling is the phosphatidylinositol-3 phosphate kinase/AKT pathway (PI3K/AKT pathway). Activated receptors proceed via stimulation of a lipid kinase PI3K which is bound by regulatory subunits or adapter molecules such as the insulin receptor substrate (IRS) (Hemmings and Restuccia 2012). PI3K phosphorylates phosphatidylinositol lipids in the plasma membrane, creating docking sites for PH-domain (pleckstrin-homology domains) containing kinases PDK1 and AKT (Burdon et al. 2002). As AKT becomes enriched, it is phosphorylated by PDK1 and gains full activity (Alessi et al. 1997). Activation of AKT results in substrate specific phosphorylation events in the cytoplasm and nucleus which mediates numerous cellular functions including growth, proliferation and survival (Hemmings and Restuccia 2012). In addition, the PI3K pathway has been shown to be involved in the maintenance of pluripotency (S. Watanabe et al. 2006; Paling et al. 2004).

As media components were established empirically, LIF is used in various combinations with signaling cascade inhibitors such as GSK3, MEK or other inhibitors (Hassani et al. 2019). Therefore, it has to be kept in mind that depending on the media supplements used, cells respond differently to the signaling environment, which results in different wiring of pluripotency programs. These differences can be measured in transcriptional gene expression, epigenetic states or developmental potency.

1.2.2 Chemically defined mESC culture conditions

Pluripotency media supplemented with FBS is chemically undefined as it originates from animals and the exact content of signaling molecules cannot be determined, thus, FBS-lots might vary (Zheng et al. 2006). In order to reduce the complexity of media formulations, chemically defined media were developed (Yasuda et al. 2018). Transcriptional profiling and RNA-Seq experiments on single cell level suggest that stem cells respond differently to the surrounding signaling cues depending on which media they are being cultured in (Hackett and Surani 2014). Examples for chemically defined media containing various combinations of signaling molecules are: 2i/LIF, BMP4/LIF or Wnt/LIF (**Figure 4**) (Ogawa et al. 2006; Tosolini and Jouneau 2015a; Qi et al. 2004).

Interestingly, mESC pluripotency can be maintained under standard stem cell culture conditions, by dual inhibition (2i) of the GSK3 and MAP-kinase pathway (Sim et

al. 2017). Although the combination of CHIR (GSK3 inhibitor) and PD (MEK inhibitor) is known to facilitate pluripotency without the addition of exogenously supplied cytokines, LIF is still present in pluripotent cells due to autocrine signaling (Graf et al. 2011). Of note, although 2i/LIF media conditions recapitulate gene expression programs of the preimplantation embryo (Nichols and Smith 2012; Navarro 2018), one has to keep in mind that a hypomethylated DNA state exists only for few days in the developing embryo (Smith et al. 2014). Hence, increasing passage numbers of stem cell lines might increase the frequency of unwanted damaging events due to DNA hypomethylation (Oliveira et al. 2014; Gaztelumendi and Nogués 2014; Imreh et al. 2006). Indeed, ESCs cultured in 2i/LIF for extended periods of time were shown to have increased tendencies of acquiring genomic abnormalities (Choi et al. 2017; Hassani et al. 2014). It remains unclear whether these abnormalities are a by-product of nonspecific inhibitor activity or a result from intrinsically naïve pluripotency features like global DNA hypomethylation (Leitch et al. 2013).

LIF supplemented serum free culture media is not sufficient to maintain mESC pluripotency (Ying et al. 2003). Interestingly, bone morphogenic protein 4 (BMP4) was characterized as the crucial component of serum which facilitates pluripotency in mESCs. Moreover, BMP4 was shown to be expressed from mouse embryonic fibroblasts (MEFs) which have been used as feeder layers to culture mESCs (Qi et al. 2004). As BMP4 belongs to the transformation growth factor beta (TGFß) superfamily which also includes Activin, Nodal, Lefty, it is involved in the regulation of proliferation and differentiation (Ying et al. 2003). Therefore, BMP4 play essential roles during embryonic development (Massagué 1998) and is a crucial media component if Serum is absent.

On a molecular level BMP4 binds to type I receptors which leads to a signaling cascade with phosphorylation of downstream proteins known as SMADs. Once activated, SMADs translocate to the nucleus where they function as transcription factors with coactivators to regulate ID (inhibitor of differentiation) gene expression (Ying et al. 2003). Intriguingly, BMP4 supports mESC self-renewal by inhibition of ERK and p38 MAP kinase pathways. Moreover, BMP4 and LIF were shown to have synergistic effects on the self- renewal of ES cells (Qi et al. 2004), preserve “multilineage differentiation, chimera colonization, and germ line transmission properties” (Wobus and Boheler 2005, p1). Thus, BMP4/LIF is an established pluripotency medium.

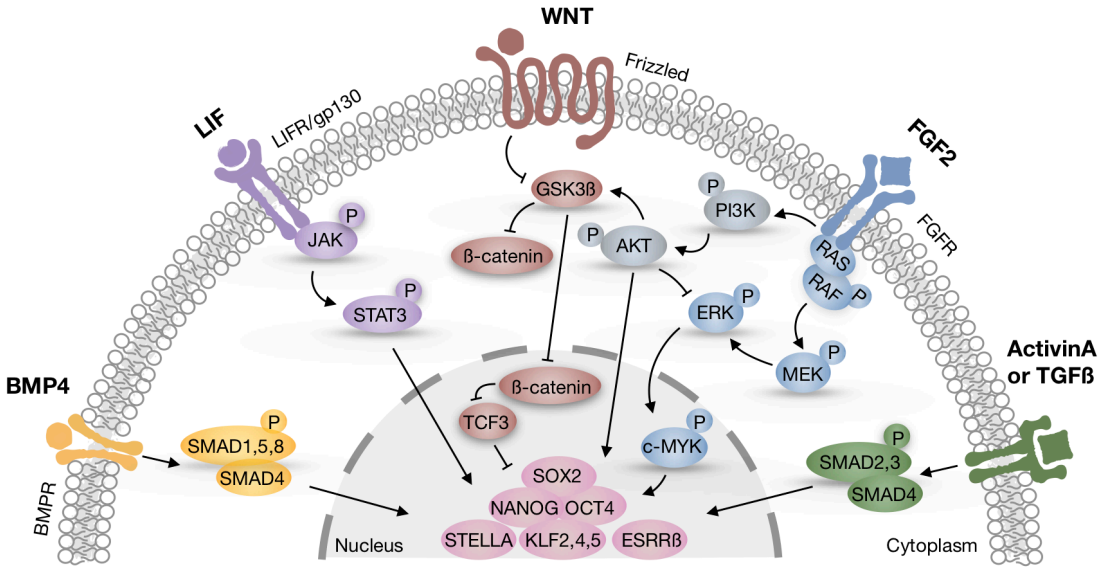

Figure 4: Extrinsic and intrinsic signaling of naive and primed pluripotency.

Schematic representation of BMP4, LIF, WNT, FGF2 and Activin signaling in naïve and primed pluripotency. ***A)*** *BMP signaling: BMP4 binds the type I BMP receptor which leads to a signaling cascade and phosphorylation of SMAD proteins. Activated SMADs translocate to the nucleus and drive the expression of ID genes.* ***B)*** *LIF signaling: LIF binds to the low affinity LIF receptor which induces dimerization with the gp130 subunit. In turn STAT3 is phosphorylated, translocates to the nucleus and promotes the expression of self-renewal genes. In addition, LIF induces the ERK and PI3K-pathway.* ***C)*** *Wnt signaling: During Wnt/ß-catenin signaling, Wnt interact with Frizzled through the cysteine-rich domain (CRD) which causes the inhibition of the ß-catenin destructive Axin complex (APC, CK1, GSK3) and accumulation of ß-catenin in the cytoplasm. ß-catenin then translocates to the nucleus and acts as transcriptional coactivator for transcription factors of the TCF family to activate Wnt responsive genes.* ***D)*** *FGF2 signaling: FGF2 binds the FGF receptor and results in autophosphorylation of the intracellular receptor region. The signal cascade is conveyed through JAK/STAT3, PI3K and ERK pathways which results in phosphorylation of c-MYC and activation of c-MYC responsive genes.* ***E)*** *Activin A signaling: Activin binds the Activin receptor and results in activation of the serine/threonine receptors which in turn trigger the phosphorylation of SMADs which act as transcriptional regulators by inducing or repressing transcription of their target loci.*

The search of chemically defined pluripotency media led to the discovery of Wnt proteins (Nusse 2008). In the absence of MEFs, mESCs were able to self-renew due to high production of Wnt proteins. In combination with LIF, autocrine Wnt signaling was sufficient for ESC self-renewal *in vitro* (MacDonald et al. 2009). Wnt proteins bind to the Frizzled receptor which results in inhibition of glycogen-synthease kinase-3 (GSK3) and subsequent accumulation of ß-catenin in the nucleus which facilitates expression of target genes (**Figure 4**) (Sokol 2011). Intriguingly, Wnt signaling was documented to block neurogenesis and promote mesendodermal differentiation. It seems counterintuitive that Wnt signaling can promote both, self-renewal and differentiation (Berge et al. 2011). Yet, the interaction of Wnt signaling pathway with other spatially and temporally restricted pathways triggered by Nodal/Activin, FGF or BMP affects the outcome of signaling. This underlines the complexity of keeping the pluripotency network active and visualizes that independent signaling cues can be used to keep stem cells in pluripotent state.

1.2.3 Core pluripotency factors

Signaling pathways eventually result in the induction or repression of target gene expression in the nucleus (**Figure 4**). Pioneering work in delineating pluripotency networks identified three core pluripotency factors Oct4, Sox2 and Nanog (Loh et al. 2006). This triad of TFs does not only form a pluripotency network of "autoregulatory and feedforward loops" (Boyer et al. 2005), they additionally downregulate their own genes to prevent overexpression. Indeed, overexpression of Oct4 and Sox2 is known to impair the homeostasis of mESCs by triggering differentiation (Niwa et al. 2000; Mitsui et al. 2003), whereas the inactivation of Sox2 or Oct4 resulted in embryonic lethality during pre-implantation stage *in vivo* (Chew et al. 2005). *In vitro*, reduced levels of Oct4 resulted in trophectoderm differentiation (Nichols et al. 1998) whereas a 2-fold increase in Oct4 levels facilitated differentiation towards progenitor cells, positive for extraembryonic endoderm and mesoderm markers (Niwa et al. 2000). In addition, gain and loss-of-function experiments have shown, that Nanog-loss results in mESC differentiation whereas Nanog-gain facilitates pluripotency (Chambers et al. 2003; Mitsui et al. 2003). Therefore, TF levels of Nanog, Sox2 and Oct4 must be regulated precisely in order to maintain self-renewal of mESCs.

1.3 Transcriptional heterogeneity in mESCs

1.3.1 Transcriptional heterogeneity in naïve mESCs

Heterogenous gene expression is observed *in vivo* (Hupalowska et al. 2016) and *in vitro* (Torres-Padilla and Chambers 2014), albeit in lower levels *in vivo*. Transcriptional heterogeneity within pluripotent cells is indicative of dynamic changes that might occur when cells "drift between different states" (Singh et al. 2013, p1). The functional role of heterogeneity is heavily debated in the field with contrasting hypotheses. One hypothesis suggests that heterogeneity is transcriptional noise (Eldar and Elowitz 2010) with essentially no relevant function for cells (Allison et al. 2018), hence, random fluctuations of gene expression. The other hypothesis suggests that heterogeneity has a crucial role for a subset of cells within the pluripotent population (Torres-Padilla and Chambers 2014). Those cells either self-renew or commit towards differentiation.

It has been shown that ESCs respond differently to external cues, thus, their ultimate fate depends on a combination of intrinsic and extrinsic factors (Chambers et al. 2007; Toyooka et al. 2008). Indeed, dynamic regulation of transcription factors and its co-expression with lineage specific genes has been suggested to create a "window of opportunity" for cells and their fate choice (Abranches et al. 2014). Depending on the sum of extracellular signaling and intracellular transcriptional heterogeneity, cells would either differentiate or continue to self-renew (Graf and Stadtfeld 2008). This plasticity in transient gene expression programs would allow the existence of timely restricted subpopulations within a culture (Abranches et al. 2013; Hackett and Azim Surani 2014). Therefore, "the pluripotent state is not well defined at the single-cell level but rather a statistical property of stem cell populations" (MacArthur and Lemischka 2013, p1). The origin of heterogeneity cannot be pinpointed to just one mechanism within cells. It is most probably a result of many cell features including transcriptional burst of genes (Suter et al. 2011; Raj and van Oudenaarden 2008), monoallelic or biallelic gene expression (Miyanari and Torres-Padilla 2012), multiple locations of TFs within the genome (Torres-Padilla and Chambers 2014), post-transcriptional regulation via protein synthesis rather than mRNA production (Gambardella et al. 2017), or the modulation of signaling pathways (Hastreiter et al. 2018).

Transcriptional profiling of ESCs at bulk and single cell level revealed that stem cells routinely display heterogeneous gene expression (Messmer et al. 2019) especially with regard to transcription factors such as Rex1, Tbx3, Esrrb, Klf4, Stella (DPPA), Prdm14 or Nanog (Singer et al. 2014; Kumar et al. 2014). Absence of Nanog expression in Oct4 positive cells led to the discovery of TF heterogeneity using fluorescent Nanog reporter knock in cell lines (Chambers et al. 2007). Indeed, cells in $Nanog^{high}$ state comprised pluripotent gene expression and self-renewal whereas $Nanog^{low}$ cells were prone to undergo spontaneous differentiation (Chambers et al. 2007; Singh et al. 2007). Single cell sorting and subsequent culture of $Nanog^{low}$ cells revealed that cells can indeed revert back into a $Nanog^{high}$ state, although in lower rates than vice versa (Singh et al. 2007; Abranches et al. 2013). Lower switching rates are explained by spontaneous differentiation of $Nanog^{low}$ cells which in turn do not participate to the emerging undifferentiated population. Similar results were shown for $Rex1^{high}$ or $Rex1^{low}$ subpopulations. Cell sorting and re-plating of either $Rex1^{high}$ and $Rex1^{low}$ cells regained its counterpart (Toyooka et al. 2008). Similar to Nanog, conversion rates of $Rex1^{low}$ to $Rex1^{high}$ were lower than $Rex1^{high}$ to $Rex1^{low}$. Which might be explained by epigenetic marks that may be partly reversible (Tompkins et al. 2012) and therefore regulate the transcriptional activity of Rex1 and Nanog genes.

Compelling studies hint to functional relevance of heterogeneity in mESCs. Yet, heterogeneity continues to be controversially discussed in the field, especially since individual studies try to explain heterogeneity as an artifact of knock in reporters (Faddah et al. 2013), a result of monoallelic regulation (Miyanari and Torres-Padilla 2012) or as a result of poor cell culture conditions (Smith 2013). Indeed, TFs were shown to be more heterogeneously expressed in Serum/LIF as compared to 2i/LIF conditions. Bimodal genes expressed in Serum/LIF became unimodal expressed in 2i/LIF, suggesting that 2i might suppress one of the previously encountered cellular states (Zakary 2014). Moreover, recent findings from Hastreiter *et al*. show in a quantitative manner the 2i specific and selective effect against $Nanog^{low}$ cells. Not only does 2i enrich for $Nanog^{high}$ populations, it also upregulates Nanog expression in $Nanog^{low}$ cells and prevents its downregulation (Hastreiter et al. 2018). This selection of $Nanog^{high}$ cells would explain the homogeneous TF expression in 2i media as opposed to Serum/LIF conditions.

Additional sources of heterogeneity are epigenetic regulations such as DNA methylation, histone tail modification or chromatin structure remodeling (Hayashi et al. 2008; Toyooka et al. 2008; Yamaji et al. 2013). Interestingly, differentially methylated regions (DMRs) such as enhancers and promoters were shown to bear lineage specific methylation patterns (Nakanishi et al. 2010; Hattori et al. 2007). Indeed, locus specific bisulfate sequencing at known targets of methylation in Rex1^{low} and Rex1^{high} cells has shown that promoter methylation is elevated in Rex1^{low} cells compared to its counterpart (Singer et al. 2014). Intriguingly, after state switching (Rex1^{low} to Rex1^{high}) cells recovered the methylation levels of Rex1^{high} cells, demonstrating the reversibility in promoter methylation levels (Singer et al. 2014). Rex1^{low} cells efficiently differentiate into somatic lineages *in vitro* but failed to contribute to chimeras upon blastocyst injection (Toyooka et al. 2008). Moreover, regulation of local chromatin structure by posttranslational modification of histone tails additionally affects gene expression which might explain in part heterogeneous gene expression.

In addition to TFs, germ layer specific genes such as Gata6, Hex or Hes1 have been shown to be bimodally expressed (Graf and Stadtfeld 2008; Kobayashi et al. 2009). Indeed, Gata 6 and Nanog are known to be expressed at the 8-to-16-cell stage, with some cells expressing both markers (Bessonnard et al. 2014). Slightly later in development, Nanog and Gata6 are expressed in an random but mutually exclusive “salt and pepper” fashion which marks the initiation of lineage segregation (Chazaud et al. 2006; Singh et al. 2007). This suggests that heterogeneity has a functional role in embryonic stem cells.

1.3.2 Nanog heterogeneity in mESCs – a case study

Nanog was one of the first pluripotency associated TFs discovered to be heterogeneously expressed both *in vivo* and *in vitro* (Macarthur et al. 2012; Abranches et al. 2014). Whether Nanog heterogeneity is an intrinsic property of mESCs (Abranches et al. 2014), pivotal for their developmental potency, or merely a culture induced phenomenon (Smith 2013) is controversially discussed in the field. Still, recent data on Nanog heterogeneity suggest a functional role in stem cells (Abranches et al. 2014). Indeed, cells in Nanog^{high} state have been shown to self-renew whereas Nanog^{low} cells were prone to differentiate

(Singh et al. 2007). Where this Nanog heterogeneity originates from remains to be elucidated.

Pioneering studies on Nanog heterogeneity suggest monoallelic expression in both, pre-implantation embryos and mESCs, cultured in Serum/LIF conditions (Miyanari and Torres-Padilla 2012). In addition, Nanog is believed to switch to biallelic expression in the naïve epiblast and mESCs, when cultured in 2i/LIF (Miyanari and Torres-Padilla 2012). Thus, biallelic Nanog expression is proposed to result in homogeneous Nanog levels (Filipczyk et al. 2013), marking truly naïve stem cells. This notion was challenged by studies showing that biallelic Nanog expression varies as much in expression levels as other pluripotency factors (Faddah et al. 2013). Monoallelic Nanog expression seems to be functionally irrelevant as a central mechanism of regulating TF heterogeneity (Filipczyk et al. 2013). Instead it has been suggested, that regulatory mechanisms such as inherently noisy gene expression in stochastic bursts (Singer et al. 2014), Nanog autorepression (Fidalgo et al. 2012) or topology of pluripotency TFs and signaling networks (Macarthur et al. 2012) are the origin of Nanog heterogeneity. Indeed, studies on quantitative measurements of Nanog expression suggested that Nanog is biallelically expressed (Filipczyk et al. 2013) with stochastic promoter activation significantly contributing to the expression variability of Nanog (Ochiai et al. 2014). Therefore, bursty transcription (Suter et al. 2011) could explain dynamic fluctuations of TFs such as Nanog, Rex1 and Stella in mESCs. Interestingly, quantitative Nanog measurements showed that Nanog heterogeneity is observed in both, 2i/LIF and Serum/LIF conditions (Ochiai et al. 2014; Abranches et al. 2014). These findings would be in line with *in vivo* data suggesting Nanog heterogeneity in the early and late stage blastocyst as an intrinsic feature (Ohnishi et al. 2014).

Although the majority of studies agrees on the necessity of Nanog downregulation for the differentiation of stem cells (Ohnishi et al. 2014; Torres-Padilla and Chambers 2014; Trott and Martinez Arias 2013), the capacity of $Nanog^{low}$ cells to interconvert remains to be elucidated. Studies on stochastic switching suggest that $Nanog^{low}$ cells can indeed revert back to $Nanog^{high}$ state although in lower rates than vice versa (Singer et al. 2014). Nair *et al*. questions the state switching potential of Nanog (Nair et al. 2015) and other pluripotency TFs. The authors suggest, that $Nanog^{low}$ cells might be in fact low at the Nanog protein level but high at the Nanog mRNA level, which was neglected in

previous quantifications. Single cell sorting of Nanog^{low} cells, would eventually result in Nanog^{high} populations because of their high Nanog mRNA levels. Suggesting that those cells have never been Nanog^{low} to begin with (Nair et al. 2015).

Intriguingly, results from transcription factor binding site analysis have shown that fate marker gene expression is not under direct control of the pluripotency associated network. This suggests the presence of spontaneously differentiating cells (Nair et al. 2015). It has to be kept in mind that the pluripotent state is transient in the developing embryo and artificially stabilized in stem cell cultures (Weinberger et al. 2016). Therefore, stem cells could be in an unstable equilibrium allowing cells to exit pluripotency without any option to reverse lineage priming (Nair et al. 2015).

1.3.3 Transcriptional heterogeneity in primed mESCs

EpiSCs are believed to be less heterogeneous then ESCs. Yet, characterization of EpiSC cultures revealed heterogeneity for pluripotency (Han et al. 2010) and lineage specific factors (Kalkan and Smith 2014). The core pluripotency factor Oct4 has been shown to mark functionally different subpopulations in EpiSCs (Han et al. 2010). Intriguingly, Oct4^{low} and Oct4^{high} EpiSCs are functionally different in chimera contribution. Oct4^{low} EpiSCs did not contribute to chimeras whereas Oct4^{high} cells contributed normally to chimeras, albeit in lower rates then ESCs (Han et al. 2010). Therefore, EpiSCs comprise functionally distinct subpopulations in culture that resemble cells of early- and late stage post-implantation embryos. In addition to Oct4, lineage specific factors such as T, FoxA2 and Cer were shown to be heterogeneously expressed in EpiSCs (Kojima et al. 2014; Han et al. 2010). This suggests that similar to ESC heterogeneity, EpiSC heterogeneity might have a functional role in development.

1.4 Cell fate choice of naïve and primed mESCs

1.4.1 Developmental potency of naïve mESCs

ESC differentiation *in vitro* is believed to recapitulate *in vivo* developmental programs (Keller 1995). Yet, molecular mechanisms underlying cellular differentiation that yield both, mature and functional cell types, are still poorly understood. Current literature highlights TFs (Nanog, Oct4 and Rex1) as suitable markers for the differentiation state of stem cells as they are believed to act as molecular switches in activating or repressing differentiation gene expression programs (Niwa et al. 2000). Indeed, transcriptional profiling has shown that pluripotency associated TFs (Rex1, Oct4, Nanog, Klf5, Tbx3 or Sox2) comprise signatures of fate specific regulation (Weidgang et al. 2016). Thus, naïve pluripotency markers might be implicated in both, maintenance of self-renewal and lineage commitment.

Oct4 and Sox2 targets, for example, were shown to create heterogeneities that bias cells to become either pluripotent or commit towards an differentiated fate (Hupalowska et al. 2016). In addition, Nanog levels affect self-renewal and differentiation propensities. $Nanog^{high}$ cells maintain self-renewal whereas $Nanog^{low}$ cells facilitate differentiation (Abranches et al. 2014). Similar effects have been shown for $Rex1^{high}/Oct4^{high}$ cells, which differentiated into primitive ectoderm and contributed to chimera formation as opposed to $Rex1^{low}$ /$Oct4^{low}$ cells, which differentiated towards fates of the somatic lineage with poor chimera contribution (Toyooka et al. 2008). Intriguingly, epigenetic and posttranscriptional regulations are also believed to be functionally relevant for stem cells differentiation and contribute to heterogeneity (Singer et al. 2014). Substantial differences in promoter methylation of Oct4 and Nanog have been shown to have major regulatory impact on stem cell self-renewal and differentiation (Hattori et al. 2007; Athanasiadou et al. 2010).

In vitro differentiation of mESC (**Figure 5**) faces the major challenge to uncover the dynamics of gene expression programs implicated in cell fate choice. Current endoderm differentiation protocols use IDE1 (inducer of definitive endoderm) as pharmacological ingredient to activate the endoderm gene expression program (Borowiak et al. 2009). Successful endoderm derivation is quantified by FoxA2 or Sox17 expression levels (Sulzbacher et al. 2009). Mesoderm germ layer differentiation, on the other hand,

is mainly facilitated by LIF withdrawal in basal GMEM medium containing knock out serum replacement. Characteristic fate markers expressed upon mESC differentiation are Brachyury, EOMES, Vimentin or Mixl1 (Torres et al. 2012). Along the ectodermal lineage, retinoic acid and a signaling cocktail of N2B27 in neurobasal media pushes stem cells towards ectoderm progenitors. ES cells lose the pluripotent status and commit to neuronal fate over a 6-8-day period, which can be monitored by Tubb3 (ß-III-tubulin) expression (Ying and Smith 2003).

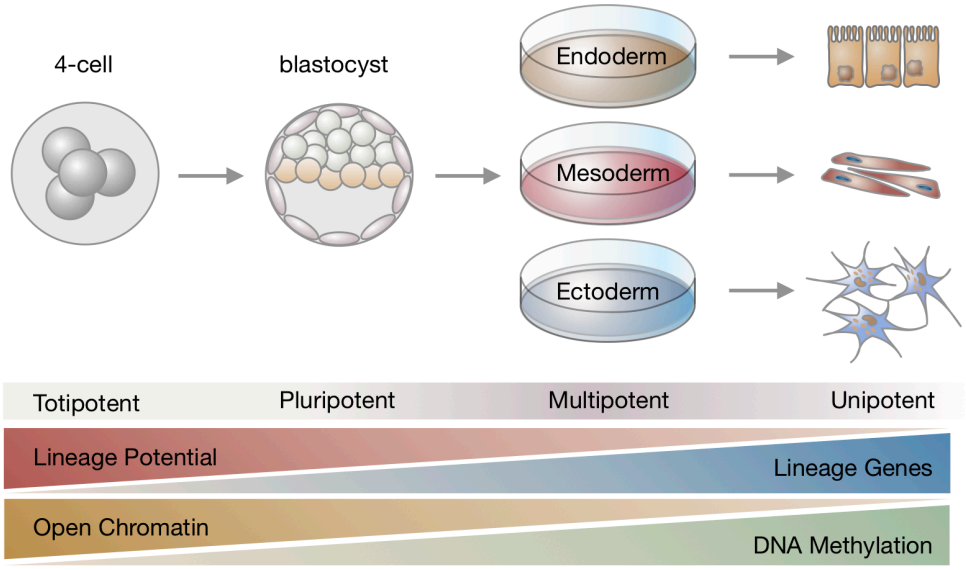

Figure 5: In vitro differentiation of mESCs.

Developmental potency of stem cells decreases upon differentiation from totipotentcy to unipotentcy. mESCs have the capacity to differentiate into the three major germ layers (endoderm, mesoderm, ectoderm), and beyond towards terminally differentiated cell types. Stem cell properties such as lineage potential and chromatin accessibility become more restricted, and expression of lineage specific genes in addition to DNA methylation increases throughout the differentiation process. Adapted from Berdasco and Esteller (2011).

1.4.2 Developmental potency of primed mESCs (EpiSCs)

Hallmarks of pluripotency are the formation of teratomas and the contribution to chimeras *in vivo* (De Los Angeles et al. 2015). EpiSCs form teratomas and can be differentiated towards all three major germ layers *in vitro* (**Figure 5**) (Gardner 1968), but rarely contribute to chimera formation (Huang et al. 2012). Therefore, EpiSCs comprise limited developing potency (Brons et al. 2007). The functional difference of ESCs and EpiSCs is explained by global DNA methylation and differing signaling pathways. EpiSCs maintain their pluripotency through Activin/Nodal signaling (Brons et al. 2007) whereas mESCs are LIF dependent (Onishi and Zandstra 2015).

Despite the notion that EpiSCs rarely contribute to chimera formation after blastocyst injection (Gardner 1968; Brons et al. 2007; Tesar et al. 2007), a growing body of literature suggests that EpiSCs can contribute to chimeras when injected into the post-implantation epiblast (Huang et al. 2012). The inability of chimera contribution can be explained by their incompatibility with the environment of the pre-implantation epiblast (Huang et al. 2012). Blastocysts comprise embryonic day 3.5 (E3.5) whereas EpiSCs correspond to E5.5 ~ E7.5 of the developing embryo (**Figure 2**). Therefore, epiblast stem cells indeed form low-contribution chimeras when injected into the post-implantation epiblast (Huang et al. 2012).

Since EpiSCs have the propensity to differentiate towards any cell type of the developing embryo (Brons et al. 2007), they should be unbiased in their fate choice. Yet, transcriptome profiling suggests a predisposition towards the endoderm lineage in differentiation assays (**Figure 5**), especially when Mixl1 was upregulated (Kojima et al. 2014). Whether an endodermal fate bias is inherent to all EpiSCs or only present in a subpopulation of EpiSCs remains elusive. Current data suggest that Mixl1-early epiblast lines seem to be primed for endoderm differentiation due to a more efficient response to TGF-ß signaling (Kojima et al. 2014). Intriguingly, Liu *et al*. showed that Nodal inhibited EpiSCs differentiated preferentially towards the ectodermal fate (Liu et al. 2018). Inhibition of Wnt activity had no effect on fate choice whereas inhibition of Nodal activity enhanced ectoderm lineage propensity (Liu et al. 2018). This suggests that lineage specific stem cell lines could be generated by mimicking the signaling condition in the embryo for *in vitro* derivation and maintenance of EpiSCs.

Altered molecular characteristics and differences in signaling make EpiSCs a more advanced developmental stage in comparison to naïve ESCs (Nichols and Smith 2009). The methylation status of pluripotency genes such as Stella and Rex1 is a perfect proxy to separate naïve (ESC) from primed (EpiSC) stem cells. These genes would be hypomethylated in ESCs but hypermethylated in EpiSCs (Bao et al. 2009; Hayashi et al. 2008). Similar effects have been shown for germ cell specific gene promoters like Vasa or Fragilis (Iftm3) (Han et al. 2010). Therefore, the methylation status of genes is used as hallmark of ESC to EpiSC conversion. It is well accepted that ESCs can be directly converted to EpiSCs when FGF2 and Activin signaling is activated (Tosolini and Jouneau 2015b), however, reverting EpiSCs back to ESCs is highly debated. Current literature suggests that switching the culture media of primed cells to 2i/LIF reverts EpiSCs back to a naïve pluripotency (Tosolini and Jouneau 2015a). Alternatively cells can be reverted by transgenic expression of key naive inducers such as E-Cadherin (Murayama et al. 2015), Esrrb (Festuccia et al. 2012), the Krüppel-like factors Klf2/4/5 (Guo et al. 2009; Gillich et al. 2012; Jeon et al. 2016), cMyc (Hanna et al. 2009), or Nanog (Silva et al. 2009). These findings suggest, that naïve and primed pluripotency is interconvertible but stabilized by their respective signaling environment.

1.5 miRNAs in pluripotency and differentiation

1.5.1 miRNA biogenesis

microRNAs (miRNAs) are 21-25 nt long non-coding small regulatory RNAs implicated in stem cell self-renewal and differentiation by negatively regulating gene expression at the post-transcriptional level (Bartel et al. 2004; Lai 2003). miRNAs are either found as single gene insertions or miRNA clusters which contain two or more members originated from duplication events (Tanzer and Stadler 2004). Especially mammalian miRNA clusters contain miRNAs from different families which can be distinguished by their miRNA seed sequence (Kim and Nam 2006).

Canonical miRNAs are located in introns of protein coding and non-coding genes, or at independent non-coding gene loci (Kim et al. 2009), either as individual genes or entire miRNA clusters. miRNAs can be transcriptionally regulated through their host gene promoters (Lagos-Quintana et al. 2003) or their own miRNA promoters. Expression

of the developmentally important miR-17/92 (Concepcion et al. 2012) and miR-379/miR-410 (Labialle et al. 2014) clusters, for instance, is driven by their own miRNA promoter.

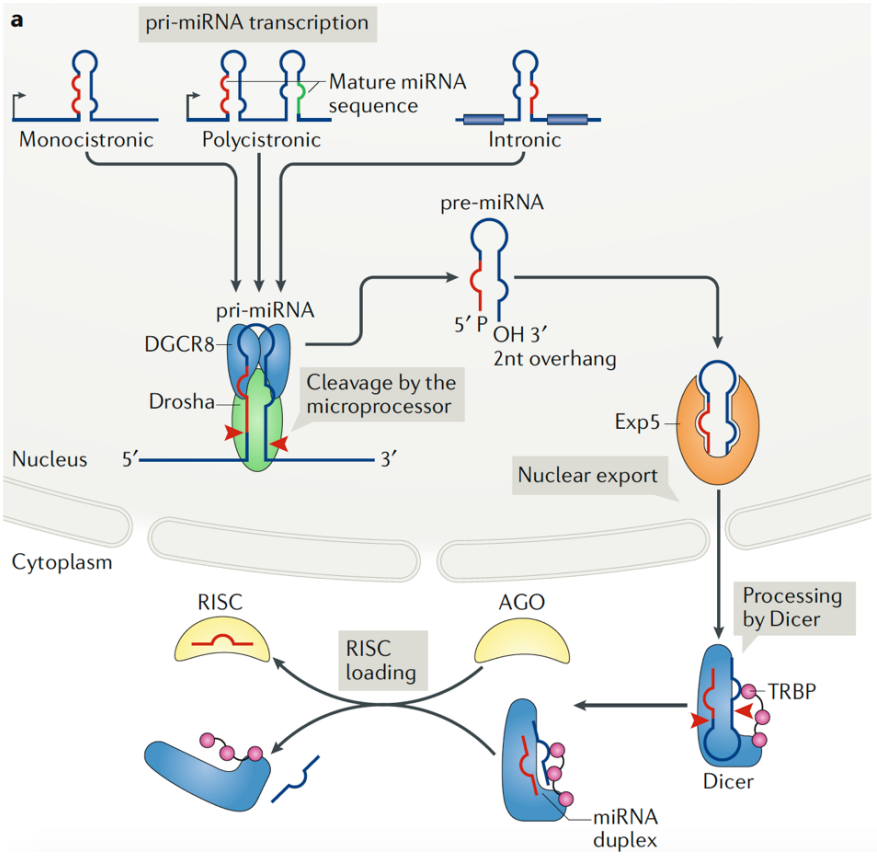

Figure 6: Canonical miRNA biogenesis and post-transcriptional gene regulation. *miRNAs are encoded as individual genes (monocistronic) or gene clusters (polycistronic) in introns and exons of protein coding and non-coding genes (intronic) or at independent non-coding gene loci. Endonuclear Drosha and its cofactor Dgcr8 cleave the nascent pri-microRNA (pri-miRNA) transcripts into ~70 nucleotide pre-miRNAs. Pre-miRNAs are shuttled from the nucleus to the cytoplasm by Exportin 5 and processed by Dicer into dsRNA duplexes, containing the mature miRNA (guide strand) and its complementary strand (passenger strand). Only one strand of the dsRNA is loaded onto Ago protein, forming the active RNA-induced silencing complex (RISC), while the passenger strand is degraded. Active RISC acts on its target by translational repression or mRNA cleavage depending on the level of complementarity between miRNA and its complementary sequence in the target 3'UTR. The figure was reprinted from* Treiber, Treiber, and Meister (2019) *with permission from Springer Nature under License Number 4653001047582.*

Clustered miRNAs are transcribed as polycistronic transcripts, which are processed to individual miRNAs. Mature miRNAs are derived by two subsequent cleavage stages catalyzed by RNase-II enzymes, Drosha and Dicer (Winter et al. 2009). After transcription of the nascent pri-miRNA transcript, endonuclear Drosha and its cofactor Dgcr8 cleave the RNA into a ~ 70 nt precursor (pre-miRNA) which is exported from the nucleus to the cytoplasm by Exportin 5, a Ran/GTP dependent nocleo/cytoplasmic cargo transporter (Lund et al. 2004). Cytoplasmic cleavage is performed by Dicer and its cofactor TRBP8, which yields the imperfect dsRNA duplex that contains the mature miRNA (guide strand) and its complementary strand (passenger strand) (Ketting et al. 2001). The mature miRNA is loaded onto the Argonaute (Ago) protein forming the active RNA induced silencing complex (RISC) (Hutvagner and Simard 2008) (**Figure 6**).

1.5.2 miRNA activity is dependent on active RISC

The RISC complex is composed of the Argonaute protein and short interfering RNAs (siRNAs) or micro RNAs (miRNAs) (Pratt and MacRae 2009). Active RISC is formed when the cleaved dsRNA duplex is handed to the Ago protein, which upon thermodynamic properties selects the mature miRNA, while the passenger strand is degraded (Hutvagner and Simard 2008). In order to study protein:RNA interaction *in vitro*, single-molecule fluorescence has been widely used (Yeom et al. 2011; Karunatilaka et al. 2010). This technique uses FRET (Förster resonance energy transfer) sensors and total internal reflection fluorescence microscopy to shed light into the dynamic search process of miRNA targeting (Salomon et al. 2016; Chandradoss et al. 2015). Recombinant human Ago2 was purified and loaded with fluorescently labeled miRNA let-7a, in order to study the miRNA to target search process *in vitro* (Salomon et al. 2016). Single-molecule fluorescence directly visualizes how active RISC searches for and identifies complementary miRNA target sites that were labeled with an acceptor fluorophore. The annealing rates were compared to naked let-7a RNA which revealed that RNA:RNA binding kinetics are not comparable to Ago2-miRNA:target binding kinetics (Chandradoss et al. 2015). Ago2 reshapes the binding properties of its loaded miRNA (Wee et al. 2012; Chandradoss et al. 2015; Salomon et al. 2016) in a way that miRNAs behave like an RNA binding protein rather than a free RNA (Salomon et al.

2016). Therefore, in-silico predictions of miRNA binding affinities give no valuable insights into target binding and miRNA affinities need to be experimentally determined.

The Argonaute protein comprises three functional domains (Song et al. 2004): i) the mid domain, which binds the 5'anchor of the miRNA (Wang et al. 2008), ii) the PAZ domain, which binds the 3'end of the miRNA facilitating Ago loading (Song et al. 2003) and iii) the PIWI domain, which catalyzes target cleavage (Liu et al. 2004). The Ago bound miRNA sequence on the other hand is separated into five functional domains that affect miRNA to target recognition. Namely, the 5' anchor (nt 1), the seed sequence (nt 2-8), the mid or central region (nt 9-12), the 3' supplementary region (nt 13-16), and the 3' tail (nt 17-22) (Wee et al. 2012). The 5' anchor is bound to the MID domain of Ago2 whereas the seed sequence is crucial for the initial targeting. The mid region, has the least functional role in target binding whereas the 3' supplementary region has a role in miRNA to target stabilization. Nucleotides beyond 16th do not participate in target binding and are called the tail region (Klein et al. 2017). Intriguingly, the bottleneck of miRNA activity is RISC loading rather than miRNA expression itself (Hausser et al. 2014). Therefore, miRNA activity cannot be inferred from miRNA expression levels.

The seed sequence has been shown to determine the binding specificity of the active Ago complex (Lewis et al. 2005). Active RISC undergoes a conformational change that exposes the miRNA seed in a prehelical structure that lowers the entropic barrier to target binding (Schirle et al. 2014; Parker et al. 2009; Wang et al. 2008). Indeed, mismatches in the seed sequence (nt 2-8) but not central (nt 9-12) or 3' supplementary region (nt 13-16), have been shown to negatively affect miRNA to target binding (Wee et al. 2012). Moreover, biochemical and structural studies (Chandradoss et al. 2015; Schirle et al. 2014; Salomon et al. 2016) suggest a step wise target recognition process, where the 5' anchor (nt1) promotes the initial target recognition followed by sub-seed binding of the first three nucleotides (nt2-4), maintaining weak target interaction as an initial search process. Sub-seed binding is followed by full seed binding (nt 2-8) after Ago2 "undergoes a conformational change leading to the displacement of the helix-7 loop" (Klein et al. 2017, p24), which promotes final seed binding of nt 6-8 (**Figure 7**) (Salomon et al. 2016; Schirle et al. 2014). Therefore, Ago2 changes from initial search mode (weak binding) into stable target recognition (strong binding) when the base pairing extends to the length of the entire seed (nt 2-8) (Chandradoss et al. 2015; Klein et al. 2017). Interestingly, a six-meer seed match has been shown to be not sufficient for mRNA

target regulation *in vivo* (Brennecke et al. 2005). Therefore, the rule of seven applies (Cisse et al. 2012), where seven contiguous base pairs are needed for miRNA silencing. A larger seed sequence would impair with the function of the silencing complex, whereas a shorter seed sequence might result in a drop of the initial Watson-Crick base-pairing interaction (Cisse et al. 2012).

Interestingly, siRNAs promote direct target cleavage; whereas miRNAs guide target binding, allowing Ago to recruit proteins that either trigger mRNA degradation or inhibit translational initiation or elongation (Huntzinger and Izaurralde 2011). RISC mediated target cleavage is frequent in plants, but infrequent in mammals. Therefore, the vast majority of miRNA targets in mammals are silenced through the recruitment of GW182 and co-factors, which result in translational repression or deadenylation and decay of target mRNAs (Guo et al. 2010; Meister 2013)

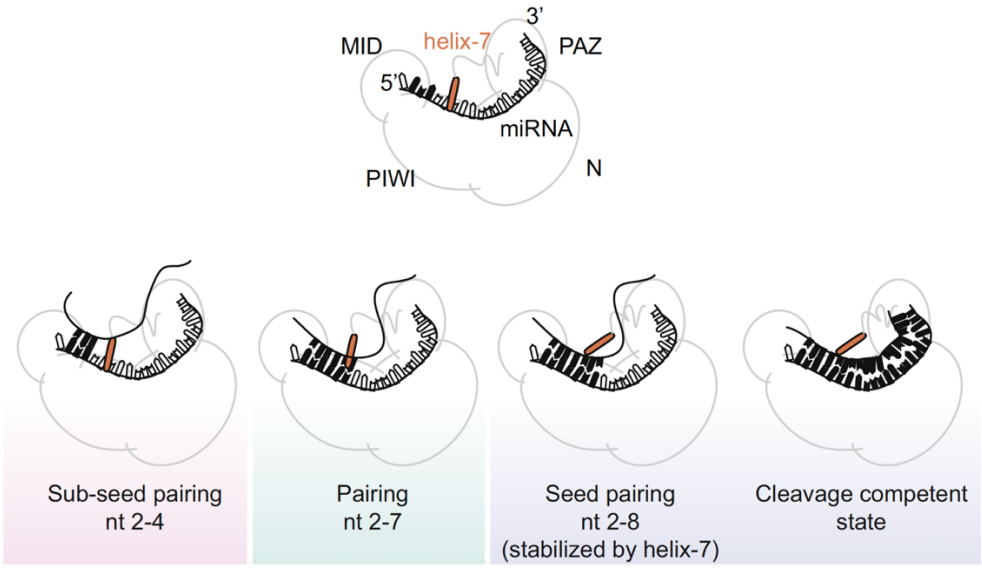

Figure 7: Two-step target search process by Ago2.

The 5'anchor of the mature miRNA binds the MID-domain of Ago and is stabilized in the functional RISC complex by the PAZ-domain. miRNA target search is a two-step process where the 5'anchor and sub-seed of nt 2-4 pair weakly complementary regions of potential targets for a quick search. Once bound, Ago2 undergoes a conformational change leading to a displacement of the helix-7 loop, allowing base pairing of nt 6-8. After full seed binding, more conformational changes take place before the bound Ago-miRNA complex becomes cleavage competent. This figure was reprinted from Klein et al. (2017) *with permission from Elsevier under creative common license CC BY-NC-ND 4.0.*

1.5.3 miRNAs in pluripotency

miRNAs modulate pluripotency by directly regulating the 3'UTRs of TFs such as Oct4, Sox2, Nanog and Klf4 (Xu et al. 2009; Tay et al. 2008). Likewise, TFs directly regulate miRNA expression in ESCs, by either occupying miRNA gene promoter regions, to activate ESC specific miRNAs, or to silence a subset of miRNAs that are expressed in differentiated cell types (Tay et al. 2008). Chromatin immunoprecipitation (ChIP)-sequencing assays confirmed that Nanog, Sox2 and Oct4 bind promoter regions of pluripotency associated miRNAs like the miR-106a/363 and miR-290/295 clusters in mESCs (Marson et al. 2008).

The functional importance of miRNAs in the developing embryo and mESCs becomes apparent when the miRNA biogenesis machinery is impaired. Deletion of either Dgcr8, Dicer or Argonaute genes caused embryonic lethality before the post-implantation stage. Similarly, deletion of Dgcr8 in mESCs resulted in loss of self-renewal capacity (Kanellopoulou et al. 2005). Therefore, distinct miRNA signatures are indispensable for stem-cell self-renewal. Those signatures comprise miR-290, miR-106a, miR-200 and miR-142, which are upregulated in mESC pluripotency (Lichner et al. 2011; Sladitschek and Neveu 2015b; Balzano et al. 2018).

One of the best characterized pluripotency associated miRNA cluster is the miR290/295 cluster, encoding miR-290, miR-291a, miR-291b, miR-292, miR-293, miR-294 and miR-295 (Yuan et al. 2017). These miRNAs maintain self-renewal by targeting Dkk-1, a Wnt pathway inhibitor (Zovoilis et al. 2009) and regulate the shortened G1 phase in mESCs through the repression of key cell-cycle regulators, Rbl1 and Cdkn1a (Wang et al. 2008; Lichner et al. 2011). Furthermore, the transcriptional repressor retinoblastoma-like 2 (Rbl2) was identified as miR-290 target. Rbl2 recruits and targets histone methyltransferases, which leads to epigenetic transcriptional repression (Sinkkonen et al. 2008; Benetti et al. 2008). Thus, the miR-290 cluster indirectly controls the expression of methyltransferases which reduces heterochromatin formation, a hallmark of pluripotency.

Another pluripotency associated microRNA is miR-142. The bimodal expression of miR-142 results in miR-142^{high} cells with low ERK/Akt activity which keeps mESCs from differentiation, whereas mir-142^{low} cells are able to exit the self-renewal circuitry (Sladitschek and Neveu 2015b). Taken together these findings suggest that mESC

specific miRNAs regulate target networks with critical role in the maintenance of ESC pluripotency.

1.5.4 miRNAs in differentiation

miRNAs fine tune gene expression (Baek et al. 2008) rather than act as binary On/Off switches (Sevignani et al. 2006). Subtle changes in gene expression seems to be sufficient to prime stem cells towards differentiation (Gu et al. 2016; Li et al. 2018), thus, miRNAs promote the transition from self-renewal to differentiation by either directly suppressing ESC self-renewal or stabilizing the differentiated state (Ando et al. 2017).

Pluripotency associated transcription factors Nanog, Oct4 and Sox2 were shown to be negatively regulated by miR-134, miR-296 or miR-470 (Ong et al. 2015). Similarly, miR-200c, miR-203, and miR-183 cooperate to repress Sox2 and Klf4 (Wellner et al. 2009), which facilitates the pluripotency exit and onset of differentiation. Interestingly, the miR-290/302 cluster is highly expressed at the late post-implantation epiblast stage, both *in vivo* and *in vitro*. Studies on pluripotency associated miRNAs suggest miR-290 as key player in the transition from naïve to primed pluripotency, through downregulation of miR-290 (Marson et al. 2008), and upregulation of miR-302 (Gu et al. 2016) expression. On a molecular level, miR-290/302 represses AKT target genes and upregulates MEK, which promotes differentiation of stem cells. Therefore, miR-290/302 expression levels are high during ESC to EpiSCs transition (Gu et al. 2016).

As opposed to miR-290, let-7 miRNA family members are upregulated after pluripotency exit, and have been shown to be tightly regulated during ESC differentiation (Viswanathan et al. 2008). let-7 is proposed to acts as "anti-stemness" regulator with pro-differentiation properties by directly targeting the expression of stemness factors c-Myc, Sall4 and Lin28 (Melton et al. 2010). In addition to functional roles in pluripotency exit, miRNAs are implicated in terminal differentiation of mESCs (Ivey et al. 2008). miR-1 and miR-133 clusters, for instance, are highly expressed in mESCs and regulate the differentiation towards cardiac muscle cells (Ivey et al. 2008; Tao et al. 2015). Furthermore, miR-214 has been shown to target Ezh2, a polycomp group protein that occupies and represses promoters of mesoderm differentiation genes among others. Upregulation of miR-214 facilitates Ezh2 mRNA degradation which ensures the complete differentiation of skeletal muscle cells (Juan et al. 2009). Similar effects have

been reported for neuroectoderm differentiation, which is facilitated by miR-134 upregulation. miR-134 is highly expressed in retinoic acid and N2B27 induced mESC (Tay et al. 2008), resulting in negative regulation of Nanog and LRH1 promoting neuroectoderm differentiation.

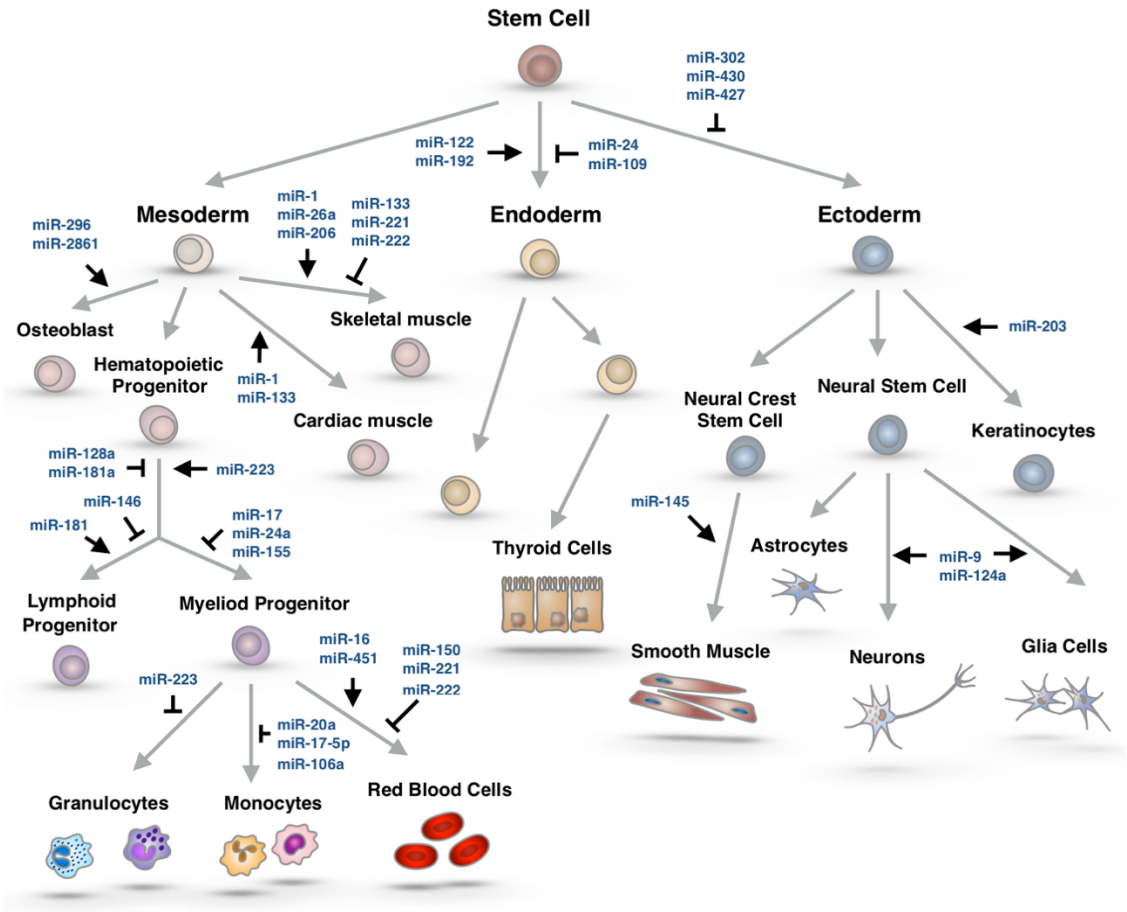

Figure 8: miRNAs as regulators of differentiation and lineage commitment.

Schematic representation of miRNAs promoting or inhibiting mESC differentiation. miRNAs regulate mESC differentiation at multiple levels: ***i)*** *at the exit of pluripotency,* ***ii)*** *during transition of pluripotent states (ESC to EpiSCs) and* ***iii)*** *during terminal differentiation into functional cell types. Arrows indicate a promoting function whereas "dead ends" highlight inhibitory function of the respective miRNAs. Adapted from* Ivey and Srivastava (2010) *with permission from Elsevier under License Number 4653010446697.*

Unlike mesoderm and ectoderm, definitive endoderm differentiation is facilitated by miR-338 and miR-340. CHIP-experiments revealed that promoter regions of endodermal fate marker Sox17 and FoxA2 are subject to histone acetylation (Fu et al. 2011). miR-338 and miR-340 negatively regulate histone deacetylase (HDAC) activity which in turn promotes endoderm differentiation. Interestingly, the list of regulatory miRNAs with functional roles in lineage commitment and terminal differentiation is constantly expanding (**Figure 8**) (Cordes et al. 2009; Ivey and Srivastava 2010; Krichevsky et al. 2006).

1.5.5 miRNA expression vs. miRNA activity

The mammalian genome encodes thousands of miRNAs (Hammond 2015), yet, activity studies suggest that the minority is biologically active. Therefore, the functional 'miRNome' of a cell is considerably smaller than currently presumed from miRNA expression analysis (Mullokandov et al. 2012). In order to identify miRNAs with biological impact in pluripotency and differentiation, miRNA activity rather than miRNA expression needs to be assessed.

Pioneering miRNA studies measured miRNA expression by northern blot, qPCR (Fiedler et al. 2010), miRNA oligo microarray (Kong et al. 2009) or RNA-sequencing (Wang et al. 2009). These techniques are invasive, destroy the sample and provide only a snapshot rather than dynamic information of miRNA activity. Moreover, the acquired data yield a population average of millions of cells, which might not reflect true miRNA expression levels at single-cell resolution. Therefore, non-invasive techniques such as miRNA reporter constructs were developed.

miRNA reporter constructs can be used at two stages of the miRNA biogenesis pathway: at the transcriptional level, using fluorescently labeled transcriptional reporter, or at the mature miRNA level (active RISC), using fluorescently labeled miRNAs target mimics. Traditional transcriptional reporter measure the expression rate of a given miRNA, but provide no information about its biological activity. Since the bottleneck of miRNA activity is RISC loading rather than miRNA expression (Hausser et al. 2014), transcriptional reporters yield no insights into the biological impact of miRNAs. Fluorescently labeled miRNA reporters that serve as miRNA target mimic, however, provide a direct readout for miRNA activity. One of the first miRNA activity reporters

was the luciferase assay, which assessed miRNA activity through complementary miRNA target sites placed downstream of the luciferase gene (Wang et al. 2011; Ji et al. 2008). This technique, however, is again invasive and does not yield single cell resolution data. Therefore, I will use a single-cell fluorescent miRNA reporter that consists of a bidirectional promoter driving the expression of a normalizer (mCherry) and a miRNA sensor (Citrine). This approach is non-invasive and yields single cell resolution data of miRNA activity in live cells (Sladitschek and Neveu 2016).

2 AIM

The mammalian genome encodes thousands of miRNAs, yet, only a minority is reported to have an impact on target gene expression. Therefore, the functional 'miRNome' of a cell is considerably smaller than currently presumed from miRNA expression analysis. miRNA expression data revealed that hundreds of miRNAs are differentially expressed during differentiation of embryonic stem cells (unpublished data). However, the biological activity of these miRNAs is poorly understood, as most studies cannot uncouple miRNA activity from miRNA expression levels. Therefore, my PhD project will focus on studying single cell miRNA dynamics during mouse embryonic stem cell differentiation towards the three major germ layers and measure miRNA affinities to a miRNA reporter *in vivo*. This will provide both, a comprehensive picture of the miRNA complement upon mESC differentiation and a determination of the affinity of individual miRNAs. In order to achieve these goals, I will subdivide my aim in the following steps:

1. Develop fluorescent mESC reporter lines for all 162 miRNAs broadly conserved in vertebrates, to systematically assess the dynamics of miRNA activity upon mESC differentiation at single cell resolution.

2. Experimentally determine miRNA affinities of conserved miRNAs in vertebrates using integrated measurements of miRNA activity and expression levels.

3. Establish and validate a functionality test for gain- and loss-of-function experiments of miRNAs identified in this study.

3 RESULTS

3.1 miRNA activity derived from miRNA reporter lines

The mammalian genome encodes thousands of miRNAs (Hammond 2015), but only few have been shown to be biologically active. This implies that the functional 'miRNome' of a cell is considerably smaller than currently presumed from miRNA expression analysis (Mullokandov et al. 2012). In order to identify conserved miRNAs with biological role in both, pluripotency and differentiation, I used a ratiometric fluorescent miRNA reporter based on a bidirectional promoter that was previously developed in our lab (Sladitschek and Neveu 2016).

The single-cell fluorescent miRNA reporter consists of a bidirectional promoter driving the expression of a normalizer (mCherry) and a miRNA sensor (Citrine) (**Figure 9**). The miRNA reporter relies on a target site perfectly complementary to the miRNA in question. Since miRNA binding sites in the 3'UTR of target genes were shown to elicit more efficient repression than target sites in the 5' or center regions of the respective target mRNA (Grimson et al. 2007), a fully complementary miRNA binding site was cloned into the multiple cloning site (MCS) which is located downstream of the sensor (Citrine) stop codon. The reporter was designed as such that the reporter ratio (R) is defined as the intensity of the Citrine signal ($I_{Detector}$) over the intensity of the mCherry signal ($I_{Normalizer}$) and serves as a direct readout for the miRNA activity in single cells.

$$R = \frac{I_{Detector}}{I_{Normalizer}}$$

Since miRNA activities will be measured every 24 hours during a 6-day differentiation protocol, the reporter needed to be stably integrated into the cellular genome. The reporter plasmid possesses a cassette expressing a hygromycin resistance gene in order to streamline the generation of stable cell lines. I chose random transgene integration over homologous recombination as the latter suffers from inherently low efficiency. More importantly, random transgene integration is time-efficient and yields multiple clones with distinct integration sites and various reporter expression levels which rules out clonogenicity of biological replicates. Furthermore, the ratiometric approach

(Mukherji et al. 2011) corrects for locus specific transcriptional noise that might create measurement artifacts of the randomly integrated miRNA reporters (**Figure 9**).

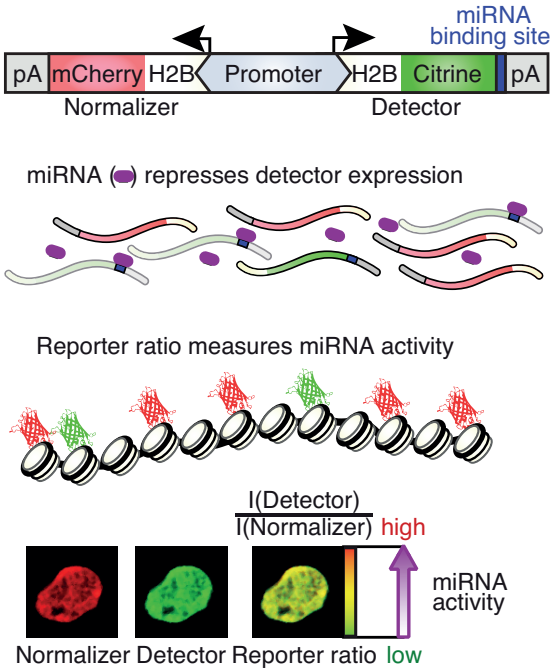

Figure 9: Ratiometric fluorescent miRNA reporter.

The ratiometric miRNA reporter relies on the co-expression of the fluorescent detector gene, sensing the miRNA presence whereas the fluorescent normalizer gene serves as internal expression control. The bidirectional CAG promoter drives the expression of the back to back oriented normalizer (mCherry) and miRNA detector (Citrine). The complementary miRNA binding site is cloned into the multiple cloning site which is located downstream of the citrine stop codon. The ratio of the fluorescence intensity of detector levels over normalizer levels is a direct readout for miRNA activity in single cells. This miRNA reporter was developed by the previous PhD student in the lab. The figure was reprinted with permission from Sladitschek and Neveu (2015).

The multiple cloning site downstream of the Citrine coding region enabled the time-efficient creation of miRNA reporter cell lines for all miRNAs conserved in vertebrates. Since this thesis project aimed to visualize the miRNA dynamics of all conserved miRNAs found in the mouse genome at single cell level, I successfully generated 162 stable transgenic reporter cell lines (**Table 1**).

Table 1: miRNAs conserved in vertebrates.

let-7a-5p	miR-96-5p	miR-139-5p	miR-190a-5p	miR-219-5p	miR-339-5p	miR-411-5p	miR-539-5p
miR-1a-3p	miR-99b-5p	miR-140-3p	miR-191-5p	miR-221-3p	miR-340-5p	miR-421-3p	miR-542-3p
miR-7a-5p	miR-101b-3p	miR-141-3p	miR-192-5p	miR-223-3p	miR-342-3p	miR-425-5p	miR-543-3p
miR-9-5p	miR-103-3p	miR-142a-5p	miR-193b-3p	miR-224-5p	miR-346-5p	miR-431-5p	miR-544-3p
miR-10b-5p	miR-122-5p	miR-143-3p	miR-194-5p	miR-290-5p	miR-34c-5p	miR-433-3p	miR-551b-3p
miR-15a-5p	miR-124-3p	miR-144-3p	miR-196a-5p	miR-292-5p	miR-361-5p	miR-448-3p	miR-590-3p
miR-17-5p	miR-124-5p	miR-145a-5p	miR-199a-5p	miR-293-3p	miR-365-3p	miR-450a-5p	miR-592-3p
miR-18a-5p	miR-125a-3p	miR-146b-5p	miR-200a-3p	miR-294-3p	miR-370-3p	miR-451a	miR-615-3p
miR-19a-3p	miR-125a-5p	miR-147-3p	miR-200b-3p	miR-295-3p	miR-374b-5p	miR-455-5p	miR-653-3p
miR-21a-5p	miR-126a-3p	miR-148a-3p	miR-202-3p	miR-296-3p	miR-375-3p	miR-486-5p	miR-708-5p
miR-22-3p	miR-127-3p	miR-149-5p	miR-203-3p	miR-299a-3p	miR-376b-3p	miR-487b-3p	miR-758-5p
miR-23a-3p	miR-128-3p	miR-150-5p	miR-205-5p	miR-301a-3p	miR-376c-3p	miR-488-3p	miR-873b
miR-24-3p	miR-129-5p	miR-153-3p	miR-208b-3p	miR-302b-3p	miR-377-3p	miR-490-3p	miR-874-3p
miR-26a-5p	miR-132-3p	miR-154-3p	miR-210-3p	miR-302c-3p	miR-378c	miR-491-5p	miR-875-5p
miR-27b-3p	miR-133b-3p	miR-155-5p	miR-211-5p	miR-320-3p	miR-379-5p	miR-494-3p	miR-876-5p
miR-29b-3p	miR-134-5p	miR-181a-5p	miR-212-5p	miR-324-5p	miR-381-3p	miR-495-3p	
miR-30c-5p	miR-135b-5p	miR-182-5p	miR-214-3p	miR-328-3p	miR-382-5p	miR-496a-3p	
miR-31-5p	miR-136-3p	miR-183-5p	miR-216a-5p	miR-329-5p	miR-383-5p	miR-499-5p	
miR-33-5p	miR-136-5p	miR-184-3p	miR-216b-3p	miR-330-5p	miR-384-3p	miR-503-5p	
miR-92a-3p	miR-137-3p	miR-186-5p	miR-217-3p	miR-335-5p	miR-410-3p	miR-504-5p	
miR-93-5p	miR-138-5p	miR-187-3p	miR-218-5p	miR-338-3p	miR-411-3p	miR-505-3p	

The single sequence fully complementary to the respective miRNA in question, served as a target mimic for each miRNA. Full miRNA-to-target complementarity would result in degradation of the detector mRNA (Citrine) and allowed the quantification of the respective miRNA activity (**Figure 9**), at each day of a 6-day differentiation protocol towards the three major germ layers endoderm, mesoderm and neuroectoderm.

miRNA reporter cell lines were established by transfection of Ab2.2 mESCs with the respective reporter plasmids. Hygromycin containing media was applied 24 hours after transfection in order to select for successfully transfected cells. After 7 days of antibiotic selection, clones positive for both, Citrine and mCherry expression were manually picked and propagated to constitute clonal cultures. 48 clones were picked for each reporter cell line and analyzed via flow cytometry analysis. Clones equally positive for Citrine and mCherry levels were propagated, frozen and subject to miRNA activity measurements in 6-day mESC differentiation protocols towards the three major germ layers (**Figure 10**).

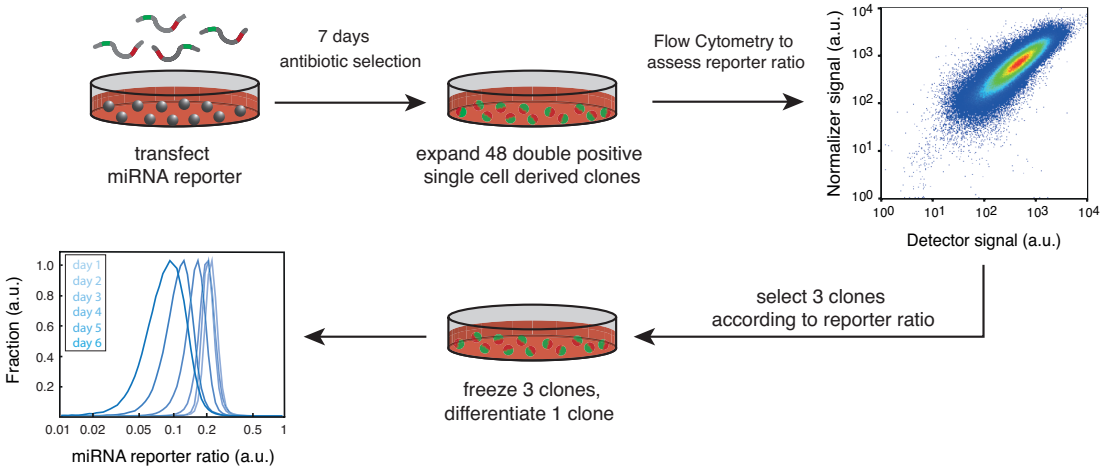

Figure 10: Workflow of generating stable transgenic miRNA reporter cell lines.

The scheme depicts the workflow for generating and screening clonal mESC lines stably expressing the respective miRNA reporter. Ab2.2 cells were transfected with the reporter plasmids. 7 days after Hygromycin selection, colonies positive for both, mCherry and Citrine were manually picked and propagated. Clones were assessed for equal expression of detector and normalizer using flow cytometry. Double positive clones were subject to activity measurements in a 6-day differentiation protocol, towards the three major germ layers.

3.2 miRNA seed drives miRNA to target recognition

The miRNA sequence can be separated into five functional domains: the 5' anchor, the seed sequence, the mid or central region, the 3' supplementary region, and the 3' tail (Wee et al. 2012). Several lines of evidence suggest that the seed sequence is the main driving force of miRNA to target specificity (Brennecke et al. 2005; Bartel 2009). In order to determine whether a seed-only sequence would result in miRNA reporter repression comparable to its full-length complementary control, I generated two scrambled miRNA binding sites for endogenous miR-136-5p. The first construct was composed of a full-length scrambled miRNA binding sequence (22 nt) which served as negative control. The second construct was composed of a functional seed binding region (nt 2-8) in an otherwise fully scrambled miRNA target sequence (scrambled 5'- and 3'region). miRNA activity of both reporter lines was compared to its full-length complementary control. miRNA to target specificity was measured by differentiation of stable transgenic miRNA and scrambled miRNA reporter cell lines, towards the endoderm lineage. Cells were differentiated in a 6-day differentiation protocol assessing the respective miRNA activity by flow cytometry analysis every 24 hours (**Figure 11**).

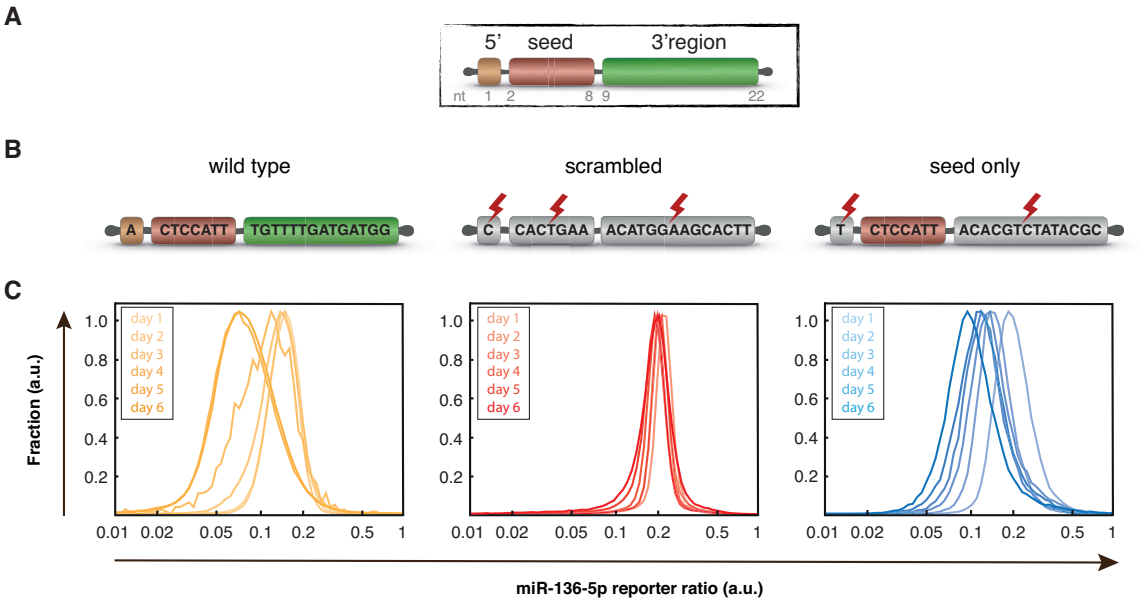

Figure 11: miRNA seed drives miRNA to target specificity.

A) *The miRNA sequence can be categorized into five functional domains: the 5' anchor (nt1), the seed sequence (nt 2-8), and the 3' region (nt 9-22) (which is further subdivided into central region (nt 9-12); supplementary region (nt 13-16) and 3' tail (nt 17-22)).* ***B)*** *Stable transgenic cell lines expressing full-length miR-136-5p reporter or scrambled versions of the miR-136-5p binding sites. The fully scrambled miRNA binding site served as negative control. The full complementary miRNA binding site served as positive control. The "seed only" binding site was the sample in question.* ***C)*** *Distribution of miRNA reporter ratios for each day of a 6-day endoderm differentiation are plotted. Distributions are overlaid according to their respective reporter cell line: wild type (yellow), scrambled (red) and seed-only (blue).*

miRNA activity was visualized by plotting the distribution of the reporter ratio for every day of differentiation. Since miR-136-3p expression levels are upregulated in RNA-Seq, I hypothesized that the miRNA reporter would be repressed upon mESC differentiation (**Figure 11**, C). Comparing the miRNA activity of the seed-only construct to its unedited control shows, that the seed sequence is indeed the main driver of target recognition. The seed-only reporter was downregulated in comparable range as the full complementary miRNA control. This confirms, that the miRNA seed sequence is sufficient to regulate its target mRNA. Next, I designed a prove-of-principle experiment to show that the miRNA reporter faithfully measures changes in miRNA expression levels.

3.3 Pluripotency associated miR-295 activity declines upon mESC differentiation

The pluripotency associated miR-290 cluster has been shown to be downregulated upon mESC differentiation (Lichner et al. 2011; Yuan et al. 2017). Intriguingly, the miR-290 cluster comprises seven miRNAs. As a representative of the cluster I chose miR-295-3p. Deep sequencing data of differentiated mESCs, suggested the downregulation of miR-295-3p upon mESC differentiation in all germ layers (**Figure 12**, A).

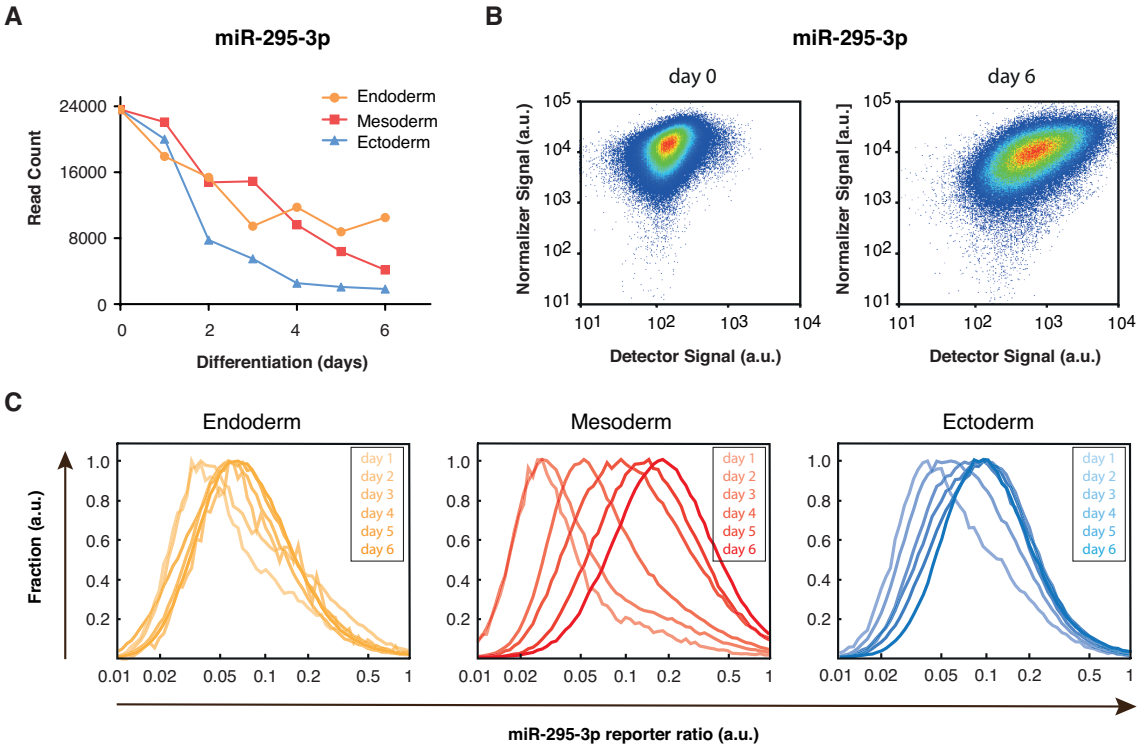

Figure 12: miR-295-3p activity decreases upon pluripotency exit.

A) *miRNA-295-3p expression levels were plotted for every day of a 6-day mESC differentiation towards the endoderm (yellow), mesoderm (red), and neuroectoderm (blue) lineage.* ***B)*** *miR-295-3p reporter cell line stably expressing normalizer (mCherry) and miR-295-3p detector (Citrine). Every dot in the plot depicts a single cell. The color code depicts the cell density in the dot plot (blue (low) to red (high)).* ***C)*** *Distribution of reporter ratios were plotted for every day of differentiation and overlaid according to its respective germ layer. Movement of the distributions to the right indicate the downregulation of miR-295-3p activity upon mESC differentiation.*

In order to demonstrate the general feasibility of miRNA activity measurements in mESC differentiation utilizing fluorescent miRNA sensors, I established the miR-295-3p reporter cell line which should recapitulate miR-295 downregulation upon mESC differentiation. Since the miRNA reporter is a direct readout of miRNA activity, I expected an increase in miRNA detector fluorescence upon mESC differentiation as miRNA expression levels are downregulated (**Figure 12**, B). Indeed, miR-295-3p reporter ratios increased over a 6-day differentiation period, which confirmed the downregulation of miR-295-3p activity in all three germ layers (**Figure 12**, C). This result shows, that the miRNA sensor is regulated upon changing miRNA levels and can be used as direct readout of miRNA activity.

3.4 miRNA crosstalk affects the miRNA-reporter

In section 3.2, I found that the miRNA seed sequence is the main driver of miRNA to sensor specificity. As miRNAs are known to share identical seed sequences with redundant biological functions (Grimson et al. 2007), I was interested to determine the influence of overlapping miRNA sequences on miRNA reporter repression of functionally different miRNAs. miR-295 and miR-302b share the same seed sequence (**Figure 13**, A) but are largely unique for the remaining functional miRNA domains such as 5' and 3' region. I hypothesized that the miR-302b reporter would be influenced by the miR-295 seed sequence and vice versa. Therefore, I measured the effect of miRNA crosstalk in miRNA activity measurements.

Deep sequencing data showed a downregulation of miR-295-3p and upregulation of miR-302b-3p expression levels upon mESC differentiation towards the endoderm lineage (**Figure 13**, B). Therefore, I expected a downregulation in miRNA reporter ratios for the miR-302b sensor. Surprisingly, miR-302b-3p reporter ratios, however, were upregulated (**Figure 13**, C). Moreover, miR-302b-3p activity profile recapitulated the miR-295-3p activity profile (**Figure 12**). This suggests, that miR-295-3p regulates the miR-302b reporter, probably due to miRNA crosstalk. The observed crosstalk might be explained by the high abundance of seven miR-290 cluster members as opposed to three members in the miR-302 cluster. A given miRNA reporter can therefore only faithfully measure the miRNA activity of unique and non-overlapping miRNA seed sequences.

Furthermore, this result visualizes how single miRNAs can regulate multiple mRNA targets (Bartel et al. 2004; Bartel 2009).

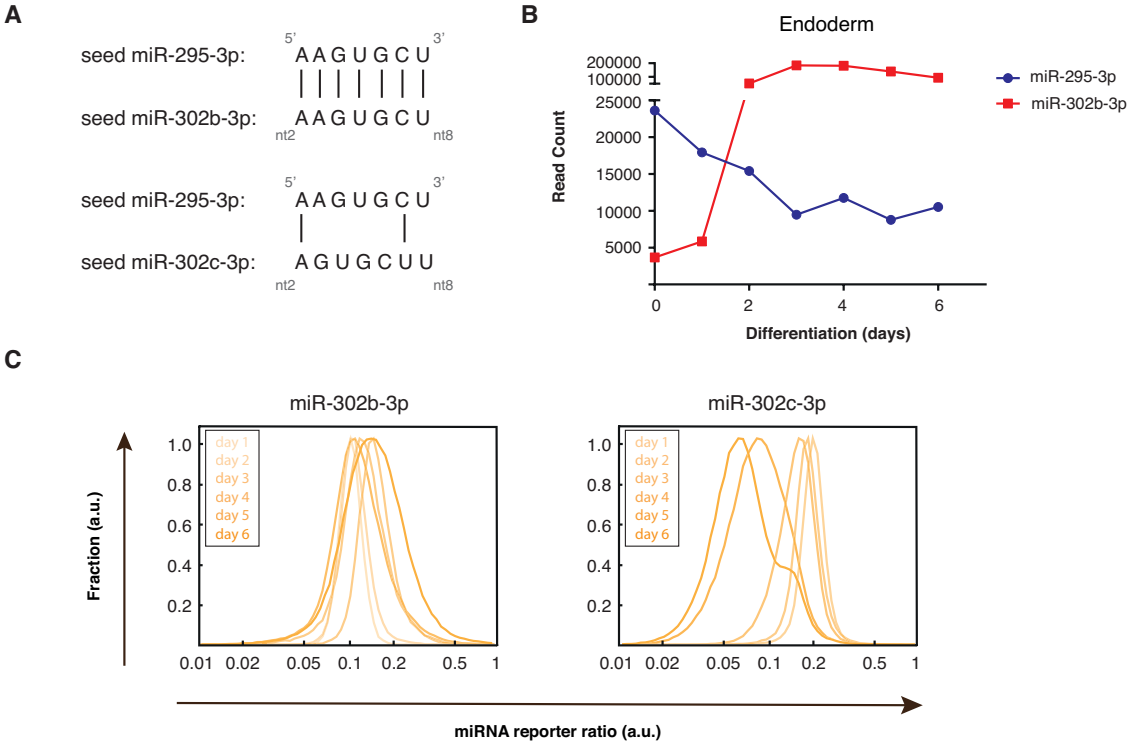

Figure 13: The miRNA reporter can be affected by miRNA crosstalk.

__A)__ The miRNA seed sequence (nt 2-8) alignment is depicted for miR-295-3p : miR-302b-3p, and miR-295-3p : miR-302c-3p, respectively. miR-302c-3p represents the miR-302 cluster as non-overlapping seed candidate. __B)__ miR-295-3p and miR-302b-3p expression levels are plotted over six days of mESC differentiation towards the endoderm germ layer. __C)__ Distribution of miRNA reporter ratio is plotted for every day of a 6-day differentiation protocol towards the endoderm lineage. Movement of the distributions to the right or left indicate the down- or upregulation of miRNA activity, respectively.

The encountered miRNA crosstalk of the miR-302b reporter cell line with miR-295, gave no valuable insight into miRNA activity of the miR-302 cluster. In order to still measure miRNA activity of the miR-302 cluster, I screened the five miRNA members for a unique and non-overlapping miRNA seed sequence. Seed sequence analysis revealed miR-302c-3p as candidate with non-overlapping and unique seed. Furthermore, sequence alignment revealed only a two nucleotide overlap of miR-302c-3p with miR-295-3p seed sequences (**Figure 13**, A). Since sub-seed pairing of nt 2-4 is postulated as initial seed to target binding but not target regulation (Schirle et al. 2014; Klein et al. 2017), I expected no crosstalk between miR-295-3p and the miR-302c-3p reporter. Indeed, miRNA activity data from mESC differentiation towards the endoderm lineage showed the expected upregulation of miR-302c-3p activity as suggested from the RNA-Seq dataset, with no measurable influence of the miR-295 seed (**Figure 13**, C).

3.5 miR-21a-3p heterogeneity in pluripotent mESCs

Heterogeneous expression of transcription factors (TFs) has been attributed a functional role in pluripotency and differentiation of mESCs (Tanaka 2009; Torres-Padilla and Chambers 2014; Martinez Arias and Brickman 2011). I postulate, that in addition to TFs, miRNAs might be heterogeneously expressed in stem cells. To address this question, I performed detailed mining of the RNA-Seq dataset acquired by the previous PhD student in the lab. Interestingly, miR-21a-3p was elevated in pluripotent state, which was surprising as miR-21a is known to have functional role in development, cancer (Kumarswamy et al. 2011) and mesenchymal stem cell differentiation (Sekar et al. 2015) but not pluripotency.

Similar to TF heterogeneity, I hypothesized that mESCs might cycle through different miRNA levels while keeping the pluripotent state. Temporal regulation of miRNA levels might open a “window of opportunity” for external stimuli that trigger pluripotency exit. Indeed, confocal analysis of mESCs stably expressing the miR-21a-3p reporter revealed miR-21a heterogeneity in pluripotent state. Cells expressing low levels of miR-21a-3p appeared green whereas cells expressing high miRNA levels appeared orange to red (**Figure 14**, A).

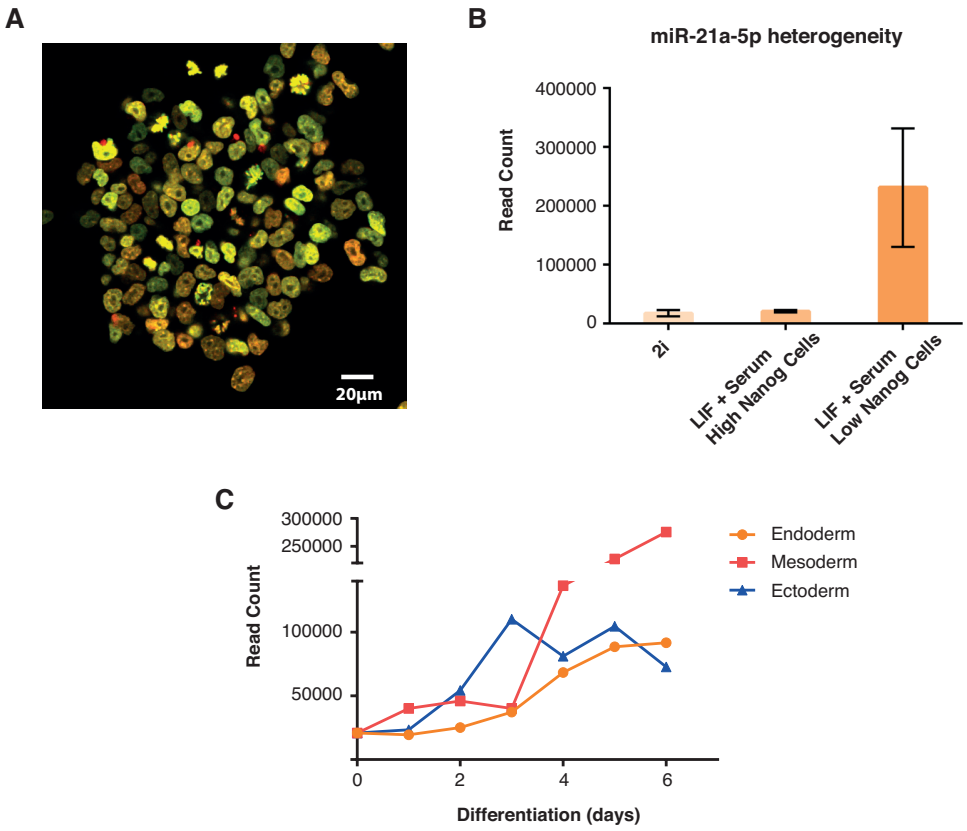

Figure 14: miR-21a-3p heterogeneity in pluripotent state.

A) *Confocal analysis of pluripotent mESCs stably expressing the miR-21a-3p reporter construct. Cells in miR-21a-3p low state appear green whereas cells in miR-21a-3p high state appear orange to red.* ***B)*** *miR-21a-3p expression levels of pluripotent cells maintained in 2i/LIF or Serum/LIF media are plotted. Cells cultured in Serum/LIF were further sub-divided into Nanog^{high} and Nanog^{low} cells.* ***C)*** *miR-21a-3p expression levels are plotted over six days of mESC differentiation towards the endoderm, mesoderm and neuroectoderm lineage.*

Several lines of evidence suggest that stem cells cultured in Serum/LIF are more advanced in their differentiation potential compared to cells cultured in 2i/LIF (Weinberger et al. 2016). Therefore, I screened the RNA-Seq dataset of Nanog^{low} and Nanog^{high} cells (unpublished data) for its respective miR-21a expression levels. Strikingly, Nanog^{low} cells showed high miR-21a expression levels whereas Nanog^{high} cells expressed low levels of miR-21a (**Figure 14**, B). This result is reminiscent of studies showing that Nanog heterogeneity has a functional role in keeping pluripotency or facilitating the onset of differentiation (Abranches et al. 2014; Miyanari and Torres-Padilla 2012). However, a comparable impact of miR-21a in mESC pluripotency would

need further investigation and was beyond the scope of this thesis project. Taken together these results suggest, that miR-21a-3p low cells maintain self-renewal while miR-21a-3p high cells are prone to exit pluripotency. Moreover, miR-21a-3p expression levels are strongly upregulated upon mESC differentiation towards endoderm, mesoderm and neuroectoderm lineage (**Figure 14**, C). Which suggests that miR-21a facilitates the differentiation process.

3.6 Potentially germ layer specific miRNAs

The previous chapter showed that miRNAs are implicated in pluripotency. Next, I was interested to determine miRNA dynamics upon stem cell differentiation. The pivotal role of miRNAs in terminal differentiated stem cells is well established in the field. miR-1 and miR-133, for instance, have distinct roles in modulating the differentiation of skeletal- and cardiac muscle cells (Zhao et al. 2005; Chen et al. 2006). Whereas, miR-9 and miR-142a were shown to be essential for the formation and proliferation of the neuronal lineage from ESCs (Krichevsky et al. 2006). Therefore, I hypothesized that in addition to terminal differentiation, miRNAs might be implicated in early cell fate decision making. To address this question, I screened the RNA-Seq data set (unpublished data) for outstanding and dynamically regulated miRNAs. I focused on conserved miRNAs with expression level changes of at least > 2 fold. In addition, I screened the dataset for potentially germ layer specific miRNAs.

The > 2 fold expression level change cut off resulted in 98 miRNAs candidates for endoderm, 59 miRNAs for mesoderm and 69 miRNAs for the neuroectoderm lineage. A more stringent cut off of > 4 fold resulted in 33 miRNAs for endoderm, 37 miRNAs for mesoderm and 45 miRNAs for the ectoderm lineage (**Figure 18**). Interestingly, almost all miRNAs were found to be regulated in more than one germ layer. This suggests, that conserved miRNAs might primarily regulate their targets globally in a cooperative manner (Bartel 2009), which does not exclude single candidates from potentially being germ layer specific.

miRNAs are considered germ layer specific if they are regulated in only one germ layer. Differentiation of mESCs towards the three major germ layers revealed that the miR-302 cluster is upregulated only in endoderm but not mesoderm nor neuroectoderm (**Figure 15**), which made this cluster an interesting candidate for further investigation.

The miR-302 cluster resides in an intron of the LARP7 gene and is encoded as single polycistronic transcriptional unit. The cluster is highly conserved among vertebrates and consist of five members: miR-302a, b, c, d and miR367. Interestingly, miR-302c and miR-367 do not share the miR-302 family seed sequence (Barroso et al. 2008; Chen et al. 2015).

Members of the miR-302 cluster seem to have a unique temporal expression profile throughout mESC differentiation as all miRNAs of the cluster peak in day 4 of differentiation whereas their magnitude of upregulation varied (**Figure 15**). Taken together the results suggest, that miR-302 is potentially germ layer specific, however, this finding needs further validation by gain- and loss-of-function experiments which were beyond the scope of this thesis project.

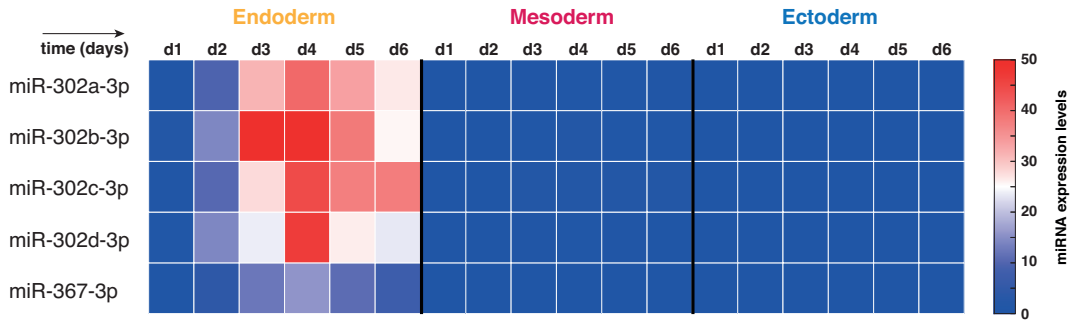

Figure 15: Potentially endoderm germ layer specific miR-302 cluster.

mESCs were differentiated towards the endoderm, mesoderm and neuroectoderm lineage, in a 6-day differentiation protocol. Samples were harvested every 24 hours and deep Sequencing was performed. miRNA expression levels of the miR-302 cluster were normalized to their levels in mESCs and visualized in a heat map for all major germ layers.

3.7 Dynamic regulation of developmentally important miR-17/92 and miR-379/410 cluster

The previous chapter showed that entire clusters can be regulated upon mESC differentiation. Therefore, I was interested in the dynamic regulation of the developmentally important miR-17/92 and miR-379/410 clusters upon stem cell differentiation towards the three major germ layers.

3.7.1 Upregulation of miR-17/92 cluster upon ESC differentiation

Genomic manipulation of the miR-17/92 cluster revealed its pivotal role in fine-tuning signaling cascades and developmental pathways (Concepcion et al. 2012) throughout normal mouse development (Lu et al. 2007; Ventura et al. 2008). Multiple integration sites within the mammalian genome and its high conservation among vertebrates corroborates the importance of this cluster (Concepcion et al. 2012). The primary polycistronic transcript is processed into six mature miRNAs: miR-17, miR-18a, miR-19a, miR-19b, miR-20a, and miR-92a (**Figure 16**, A). Intriguingly, miR-17 and miR-20a have been shown to directly target the TGF-ß receptor II, whereas miR-18a targets SMAD2 and SMAD4 (Mogilyansky and Rigoutsos 2013). SMAD proteins are known members of the TGF-ß/Nodal/Activin signaling pathway, which have a pivotal role in stem cell specification (Liu et al. 2018). Therefore, I was interested to determine previously unrepresented miRNA activity changes of the miR-17/92 cluster upon mESC differentiation (**Figure 16**).

Deep sequencing data of differentiated mESCs revealed a highly dynamic regulation of the miRNA cluster in both, expression levels and temporal profile of miRNA expression (**Figure 16**, B). The majority of miRNAs showed subtle changes in expression levels, whereas single members like miR-19a, miR-20b or miR-92b, were highly upregulated. Especially miRNAs expressed form chromosome X seemed to be highly regulated compared to members of chromosome 5 and 14. This suggests that miR17/92 cluster fine tunes target gene expression through subtle changes in its expression levels. Of note, specific miRNA targets were not identified and beyond the scope of this thesis project.

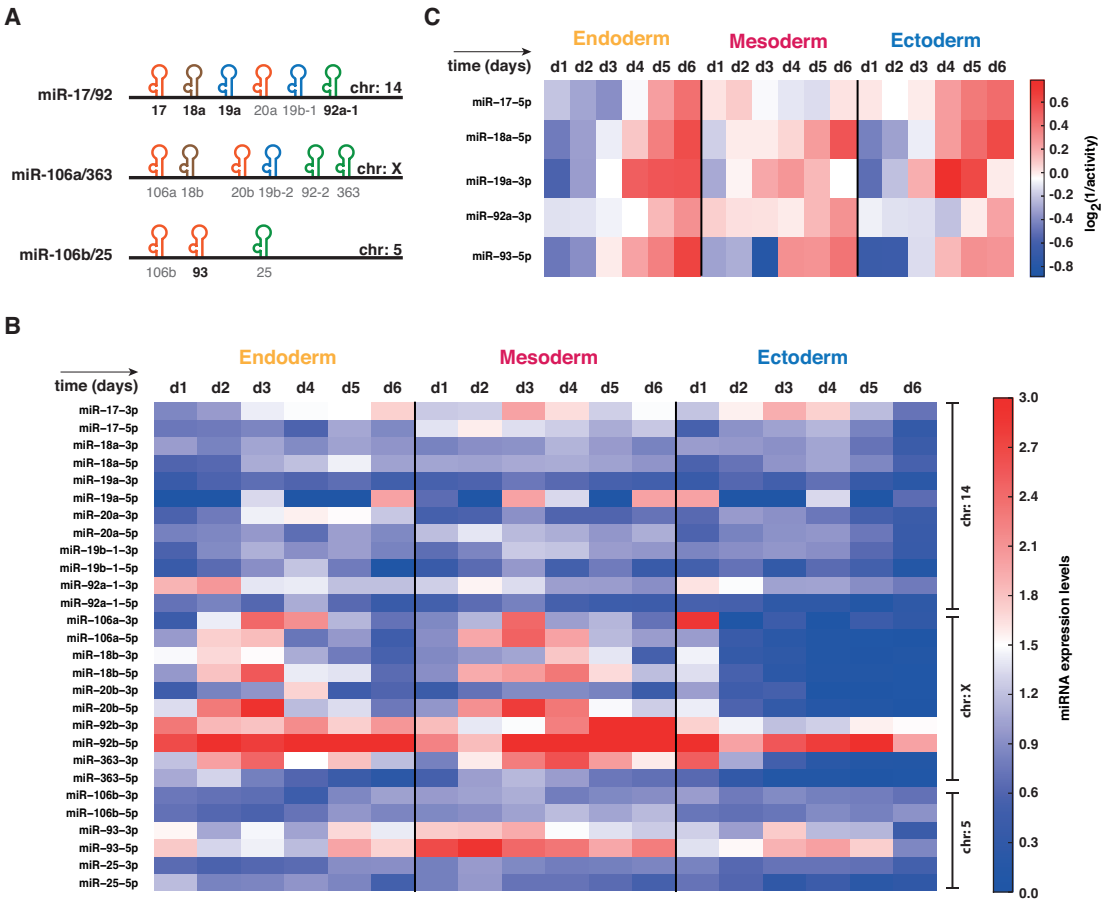

Figure 16: Dynamic regulation of the miR-17/92 cluster upon mESC differentiation.

A) *Schematic representation of the miR-17/92 polycistron. The miR-17/92 cluster encodes a pri-miR that yields 6 mature miRNAs. Based on seed sequence homology, these six miRNAs belong to four miRNA families (each color represents one family). miR-17/92 has two closely related homologues in mammals, the miR-106a/363 and miR-106b/25 clusters. These homologous clusters contain subsets of the miR-17/92 cluster with conserved genome arrangement on chromosome 5 and X. miRNAs highlighted in black represent each miRNA family in the screen (see C).* ***B)*** *mESCs were differentiated towards endoderm, mesoderm and neuroectoderm lineage in a 6-day differentiation protocol, where miRNA expression levels were assessed every 24 hours and depicted as heat map.* ***C)*** *mESCs were differentiated towards all major germ layers. miRNA activity was assessed using corresponding miRNA reporter cell lines which were analyzed via flow cytometry every 24 hours throughout a 6-day differentiation protocol. Resulting miRNA activity data were visualized as heat map. Each miRNA corresponds to a miRNA family (see A).*

The miRNA activity data recapitulate trends observed in deep sequencing data. Due to single cell resolution of the activity dataset, subtle changes in miRNA activity could be resolved which were previously unrepresented due to population average of deep sequencing data. The activity data show that miR-17/92 cluster was upregulated throughout mESC differentiation. Interestingly, miR-19 and miR-92a were upregulated right after onset of mesoderm differentiation as opposed to late regulation (d4-d5) in the endoderm lineage (**Figure 16**, C). Interestingly, miRNA activity peaked at different days of differentiation, which suggests that their temporal profile might play a role in development. Taken together, these data suggest a cooperative effect of the miR-17/92 cluster rather than germ layer specificity.

3.7.2 miR-379/410 activity dynamics upon mESC differentiation

Another developmentally important miR-379/410 cluster is located at the imprinted *DLK1-Dio3* region. Correct dosage of imprinted genes encoded by this locus have been shown to be crucial for embryonic growth and neuronal development (Rocha et al. 2008). Since the miR-379/410 locus is the largest known miRNA cluster in placental mammals and conserved among vertebrates, it was subject to further investigation.

The cluster comprises 40 miRNAs out of which 27 are represented in my miRNA activity dataset (**Figure 17**, A). Before assessing miRNA activities at single cell resolution, I was interested in miRNA expression dynamics of this cluster (**Figure 17**, B).

A

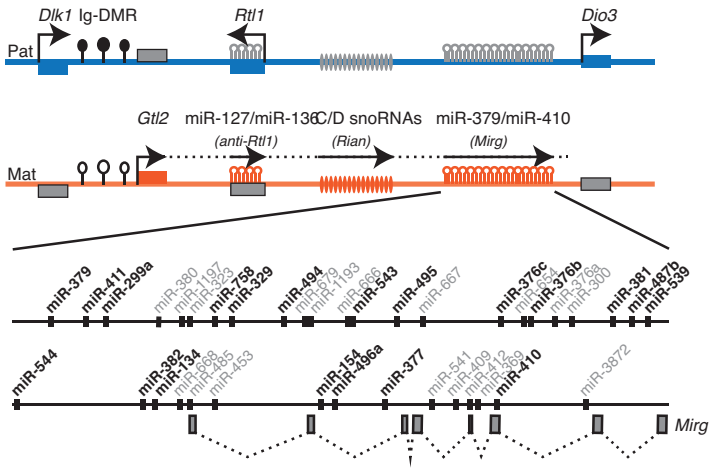

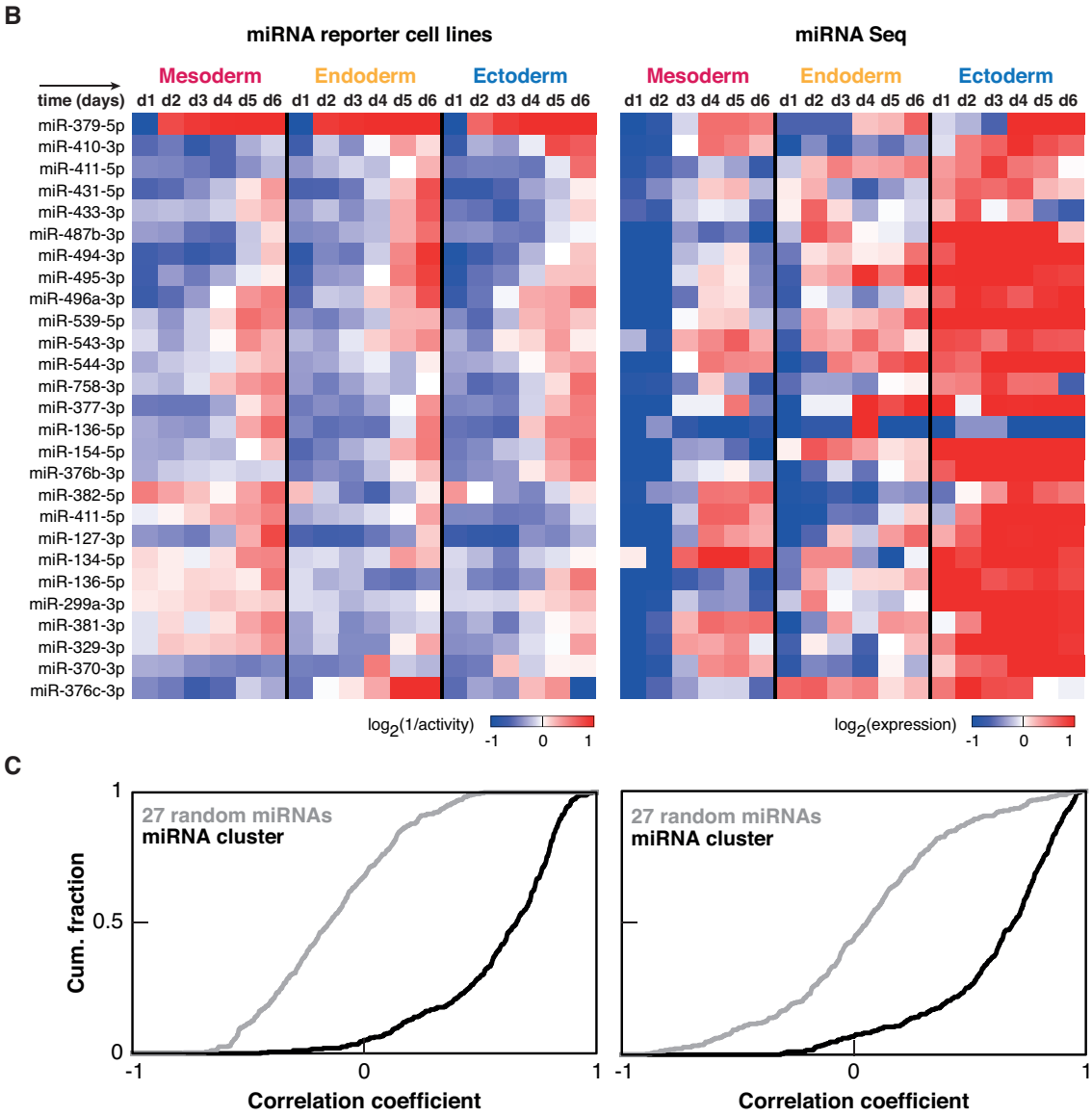

Figure 17: miRNA dynamics of the imprinted DLK1-Dio3 locus.

A) *Schematic representation of the imprinted Dlk1-Dio3 domain located on chromosome 12, harboring the miR-379/410 cluster. The cluster is conserved among vertebrates and comprises 40 miRNAs out of which 27 (bold) are represented in the miRNA activity dataset. Only miRNAs of the maternal strand are actively transcribed. Gtl2 (lncRNA), anti RTL1, Rian and Mirg are poorly characterized ncRNAs. Paternally expressed protein coding genes (Dlk1, RTL1, Dio3) are symbolized in blue rectangles, whereas maternally transcribed miRNAs are depicted in pink stem loops.* ***B)*** *miRNA activity data derived from corresponding reporter cell lines and miRNA expression levels derived from deep-sequencing are visualized in heat maps.* ***C)*** *The cumulative fraction was plotted over the corresponding correlation coefficient for 27 randomly chosen conserved miRNAs (grey) and 27 miRNAs of the miR-379/410 cluster (black), for both miRNA activity and RNA-Seq data.*

Similar to miR-17/92, also miR-379/410 cluster expression levels were overall upregulated in mESC differentiation. Surprisingly, almost all miRNAs were elevated throughout neuroectoderm differentiation, whereas miRNAs were tightly regulated in their temporal profile for mesoderm and endoderm differentiation. Furthermore, miRNA expression levels were on average earlier upregulated (from day 2) in endoderm as compared to mesoderm germ layer (from day 3). This suggests that the temporal profile of miRNA expression might impact mESC differentiation.

The miRNA activity dataset recapitulated RNA-Seq results, with overall upregulation of miRNA activity for the entire cluster. However, the temporal profile differed dramatically comparing miRNA activity and expression levels (**Figure 17**, B). miRNA expression levels were elevated right after onset of differentiation in the neuroectoderm lineage, whereas miRNA activity was ramped up from day 3 of differentiation. Interestingly, miRNA activity in endoderm germ layer was upregulated even later, it increased significantly from day 5 onwards. Less stringent was the upregulation of miRNA activity in mesoderm germ layer. Here miRNAs could be categorized into early, mid and late regulated miRNAs. Taken together, these results show that miRNA activity cannot be inferred from miRNA expression analysis alone. Moreover, the comparison of miRNA activity and corresponding miRNA expression levels indicates that the temporal regulation of miRNA activity might have a crucial role in stem cell differentiation.

The co-expression of a large number of miRNAs from the same cluster offers the opportunity to test the reproducibility of my miRNA activity dataset. Indeed, it relies on independent measurements of individual stable reporter mESC lines, as opposed to miRNA-Seq, which measures the expression levels of all miRNAs in one sample. Changes in activity levels of miRNAs from the miR-379/410 cluster were highly correlated, whereas activity levels of 27 miRNAs taken at random from the list of 162 conserved miRNAs, did not show any correlation in their activity changes during differentiation. A similar result was obtained when analyzing miRNA-Seq data (**Figure 17**, C). This result shows, that miRNA expression from the same cluster is highly correlated and not random. In addition, my miRNA activity measurements could be reliably compared across miRNAs.

3.8 Dynamic regulation of conserved miRNAs upon mESC differentiation

Having shown that developmentally important miRNA clusters are upregulated upon mESC differentiation, I was interested in the global miRNA activity dynamics of 162 conserved miRNAs and their temporal regulation throughout a 6-day differentiation process. Therefore, I established 162 stable transgenic miRNA reporter cell lines and differentiated each line towards mesoderm, endoderm and neuroectoderm fate. miRNA activity was assessed every 24 hours throughout a 6-day differentiation protocol using flow cytometry analysis. The resulting miRNA activity was depicted in a heat map, where every column represents a condition and every line the respective miRNA.

The results indicate that the majority of conserved miRNAs are upregulated upon mESC differentiation. Surprisingly, the number of upregulated miRNAs in the activity dataset almost matched the number of > 2-fold upregulated miRNAs in the expression level dataset (**Figure 18**, A). This shows, that even weakly expressed miRNAs have detectable changes in activity during stem cell differentiation. miRNA expression levels derived from RNA-Seq might mask interesting miRNA candidates due to population average data. To overcome this obstacle, I used miRNA reporter cell lines analyzed via flow cytometry which give access to germ layer specific single cell resolution data. The reporter cell lines revealed that miRNA activity is gradually upregulated upon differentiation for the majority of conserved miRNAs. Few miRNA candidates also peaked in intermediate days of differentiation. Based on temporal resolution of miRNA activity, miRNAs can therefore be grouped into early, mid and late regulated candidates. Furthermore, specific groups of miRNAs seem to be either upregulated in all three or in a combination of at two germ layers (**Figure 18**, B). Taken together, these data suggest a cooperative miRNA effect with specific temporal activity profile which might be pivotal to drive cell fate choice and stem cell differentiation. Yet, the impact on fate choice would need further validation.

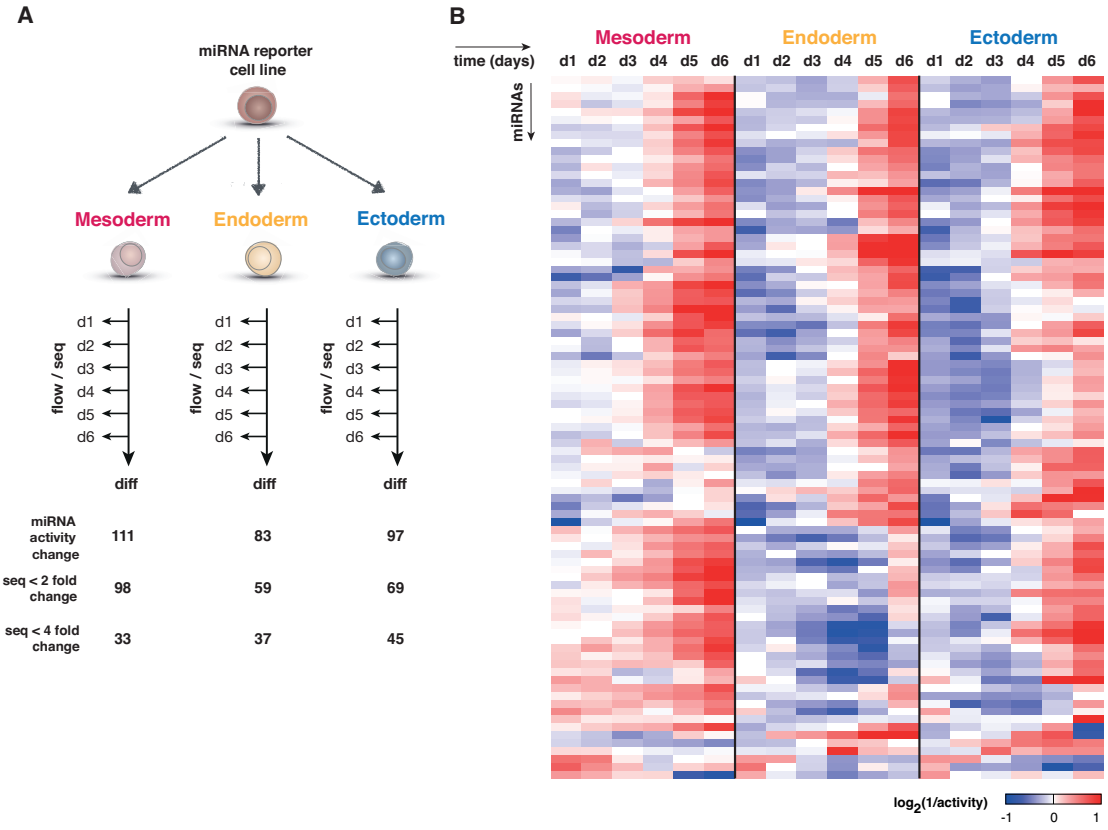

Figure 18: Dynamic miRNA activity regulation upon mESC differentiation.

A) *Schematic representation of generating both, the miRNA activity dataset and the miRNA expression level dataset. mESCs were differentiated towards the mesoderm, endoderm and neuroectoderm lineage in a 6-day differentiation protocol. miRNA expression levels and miRNA activity were assessed every 24 hours. The table summarizes the number of miRNAs with changing miRNA activity, in addition to the number of miRNAs upregulated in expression levels (2-fold and 4-fold).* ***B)*** *162 miRNA reporter cell lines were differentiated towards the major germ layers. miRNA activity data were depicted in a heat map where every column represents an experimental condition and every line represents a given miRNA.*

To further investigate whether changes in miRNA activity could distinguish fate choices, principle component analysis (PCA) was performed on the miRNA activity dataset. Divergence in miRNA profiles occurred 48 hours after onset of differentiation, where each germ layer followed a specific trajectory (**Figure 19**). This result is in line with Waddington's concept of "progressive restriction of cell differentiation potential during normal development" (Ladewig et al. 2013, p1).

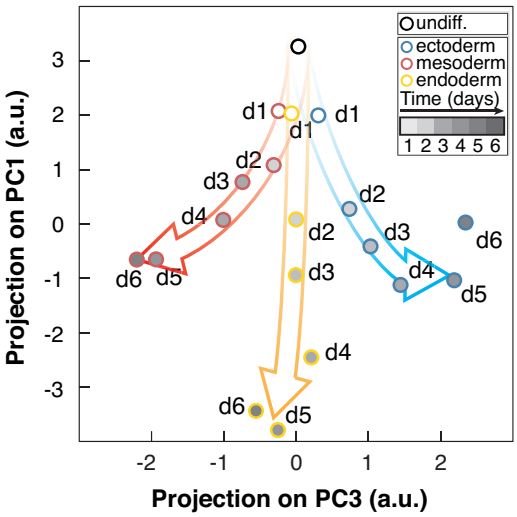

Figure 19: miRNA activity data distinguish cell fate choice.

PCA analysis was performed on miRNA activity data (Figure 17) of conserved miRNAs in vertebrates. miRNA activity was derived from reporter cell lines differentiated towards mesoderm, endoderm and neuroectoderm germ layer.

3.9 miRNA activity vs. miRNA expression levels

miRNA dynamics in stem cell differentiation is currently studied on the basis of miRNA expression levels using large RNA-Seq datasets (Li et al. 2018; Castel et al. 2018). However, miRNA activity cannot be inferred from expression analysis alone since the bottleneck of miRNA activity is Ago loading rather than miRNA expression (Hausser et al. 2014). Moreover, miRNA expression does not prove discernable activity as the 3'UTR of a potential target mRNA might not be accessible (Szostak and Gebauer 2013). These and other factors suggest that the functional 'miRNome' of a cell is considerably smaller than currently proposed from miRNA expression studies. Therefore, I was interested in similarities and differences of two miRNA candidates residing in the same transcriptional unit comparing miRNA expression levels versus miRNA activity.

miR-495-3p and miR-136-5p are members of the previously introduced miR-379/410 cluster. Both miRNAs yield mature miRNAs and are processed from the same transcript (**Figure 17**). Intriguingly, their miRNA expression levels differ 7-fold (**Figure 20**). One could assume that miR-495 activity does therefore exceed miR-136 activity due to its higher expression levels. Strikingly, this 7-fold difference in expression was not reflected in the miRNA activity levels. Both miRNAs displayed comparable activity

changes upon differentiation. These data suggest that miR-136-5p is more potent compared to miR-495-3p, as lower miRNA expression levels result in the same miRNA activity. This finding can probably be explained by differences in miRNA sequence composition of miR-136 and miR-495, which likely results in miRNA affinity differences.

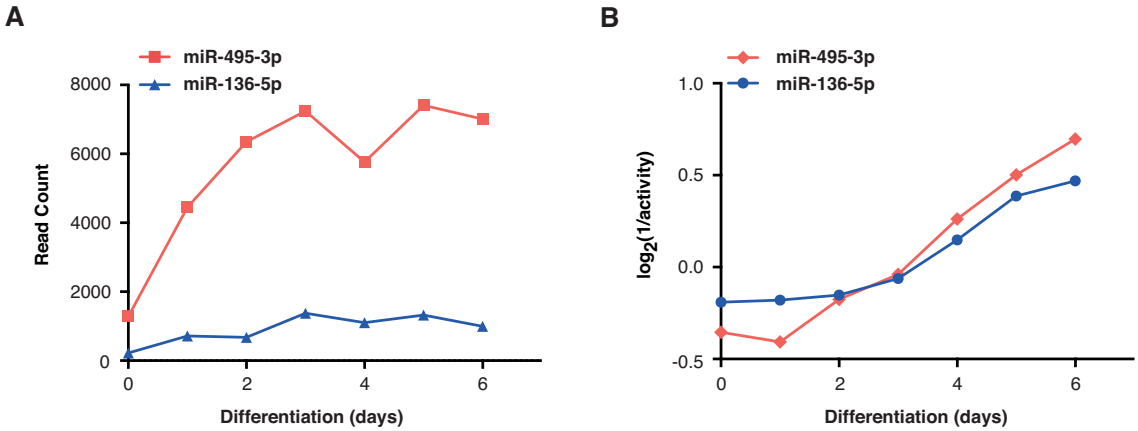

Figure 20: miRNA activity cannot be inferred from miRNA expression levels.
A) *miRNA expression levels of miR-495-3p and miR-136-5p were plotted for each day of a 6-day differentiation period towards the neuroectoderm lineage. Both miRNAs belong to the miR-379/410 cluster and are expressed from the same transcriptional unit.* ***B)*** *miRNA activity was assessed by differentiation of corresponding miRNA reporter cell lines towards the neuroectoderm lineage.*

3.10 miRNA activity and miRNA expression levels give access to miRNA affinity

In order to confirm that the miRNA reporter ratio is a direct proxy for miRNA activity, miR-142-3p reporter was calibrated by the previous PhD student. The calibration was set up as follows: the miR-142-3p reporter ratio of mESC subpopulations expressing various levels of miR-142-3p was measured by flow cytometry and subsequently FACS purified to extract total RNA. Deep sequencing was performed on FACS purified cells, and normalized miRNA detector levels were plotted over corresponding miR-142 expression levels, which resulted in a calibration curve (**Figure 21**). The dependence of the detector levels D on the miR-142-3p concentration M (miRNA levels) followed a Hill's equation

with non-cooperative binding, where K (miRNA affinity) is the binding constant and n is the Hill coefficient of the interaction.

$$D = \frac{1}{1 + M^n/K^n}$$

Adjustment of the detector mRNA expression levels as a function of miR-142-3p levels with Hill's equation resulted in $n = 1{,}07 \pm 0{,}04$. Since miRNA activity depends on both, miRNA expression and miRNA affinity, miRNA activity gave direct access to *in vivo* miRNA affinity.

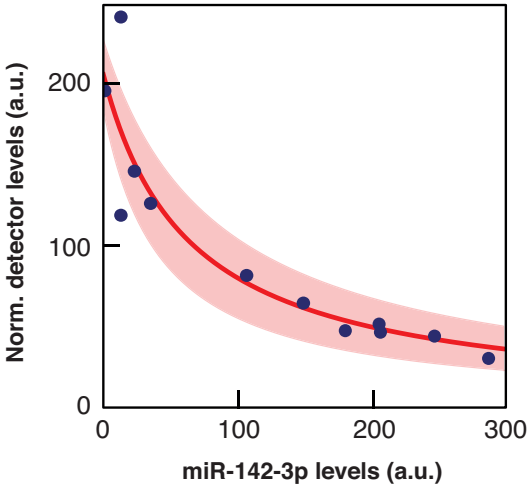

Figure 21: Calibration of the miRNA reporter.

Adjustment of the detector mRNA expression levels as a function of miR-142-3p expression levels for 12 independent biological samples (blue dots: experimental data measured by deep sequencing in FACS purified populations). Detector and miR-142-3p expression levels were quantified by RNA-Seq on matched mRNA and miRNA libraries prepared from the same total RNA sample. Data were fitted using the Hill's equation with non-cooperative binding (red line; shaded area: fit confidence interval). The calibration experiment was conducted by the previous PhD student in the lab. The figure was reprinted with permission from Sladitschek and Neveu (2015).

3.11 Expression based miRNA affinity

Having shown that miRNA reporter cell lines faithfully measure miRNA activity and the Hill function gives access to previously unrepresented miRNA affinity, I aimed to determine miRNA affinities of all conserved miRNAs in vertebrates. miRNA affinity is currently predicted from the miRNA sequence using various bioinformatic tools. Those programs apply free-energy prediction (ΔG) thermodynamic calculations in order to derive miRNA binding affinities for different targets (Sethupathy et al. 2006). This approach disregards the fact that the minority of expressed miRNAs are biologically active (Mullokandov et al. 2012). Moreover, these tools predict miRNA to target interaction based on full length miRNA complementarity. However, miRNA binding studies show that miRNAs bind through partial sequence complementarity (Grimson et al. 2007). Therefore, my aim was to experimentally determine miRNA affinities for 162 conserved and biologically active miRNAs.

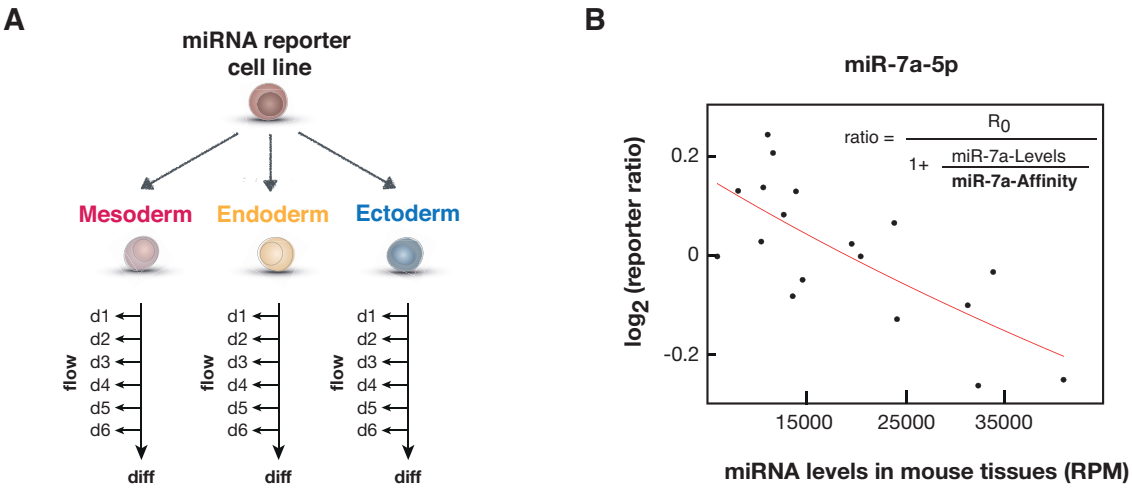

Figure 22: Expression-based miRNA affinity.

A) *Schematic representation of generating the miRNA activity dataset. 162 miRNA reporter cell lines were differentiated towards the mesoderm, endoderm and neuroectoderm lineage. The miRNA reporter ratio was measured every 24 hours, over a 6-day differentiation period using flow cytometry analysis.* ***B)*** *miR-7a-5p reporter ratios were plotted over the corresponding miR-7a-5p expression levels, for all major germ layers (6 days x 3 germ layers = 18 data points). Fitting a Hill function with non-cooperative binding gave access to the miRNA affinity for this specific miRNA.*

Since the Hill equation gives access to miRNA affinity through its binding constant (k), I postulate, that an integrative approach of miRNA expression levels and miRNA activity changes in mESC differentiation yields experimentally determined miRNA affinities for the first time. To visualize the expression-based miRNA affinity concept, I plotted the miR-7a-5p reporter ratios, as an example, over the corresponding miRNA expression levels for every day of a 6-day differentiation towards the major germ layers which resulted in 18 data points (6 days x 3 germ layers = 18 data points). These data points were fitted using the Hill function with non-cooperative binding and enabled the derivation of the miR-7a-5p affinity (**Figure 22**).

The expression-based affinity approach can derive the affinity for any miRNA with measurable changes in expression during mESC differentiation. Therefore, I generated stable transgenic reporter cell lines for 162 conserved miRNAs and differentiated those towards the mesoderm, endoderm and neuroectoderm lineage. In order to determine whether miRNAs have comparable affinities, I plotted miRNA affinities of all measurable conserved miRNAs over their respective expression levels (**Figure 23**).

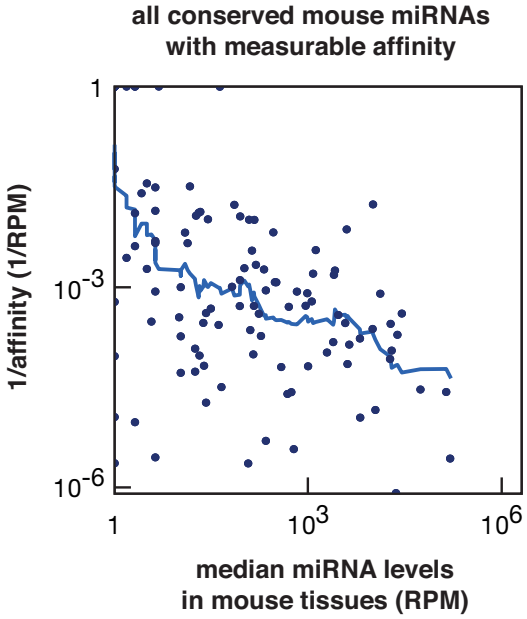

Figure 23: Expression based miRNA affinities for 96 conserved miRNAs.

Expression based miRNA affinities were plotted over their corresponding miRNA expression levels for 96 conserved miRNAs (RPM: reads per million mapped reads).

Strikingly, miRNA affinities can span several orders of magnitude, which shows that miRNAs differ vastly in their respective potency. In addition, miRNA affinity was negatively correlated with miRNA expression levels. This suggests that weakly expressed miRNAs can be as potent, or even more potent as highly expressed miRNAs. Furthermore, these data confirm that miRNA expression levels do not necessarily correlate with miRNA activity. Of note, this approach only yields the miRNA affinity for candidates with expression level changes upon differentiation. This was true for 96 miRNAs from a total of 162 candidates. The remaining miRNA affinities could not be determined as these miRNAs were either not expressed under these conditions or did not change in miRNA expression. In both cases, the expression-based method would not be applicable to derive miRNA affinities. Thus, I developed an alternative approach using miRNA KO reporter cell lines.

3.12 Knock out based miRNA affinity

In order to determine miRNA affinity for miRNAs with constitutive expression during differentiation, the miRNA expression levels have to be artificially manipulated in a controlled manner. CRISPR/Cas9 mediated deletion of miRNA alleles allows such a precise perturbation. Therefore, I established miRNA CRISPR/Cas9 knock out (KO) cell lines for a subset of miRNAs. Since the dependence of the reporter ratio on miRNA levels follow a Hill's equation (**Figure 22**, B), I postulate that miRNA affinity can be calculated from a non-linear equation consisting of two main variables: miRNA expression levels and miRNA activity in pluripotent state. Thus, the homozygous KO of a given miRNA candidate within its respective miRNA reporter cell line, would yield the miRNA affinity (**Figure 24**, B).

miRNAs entail more constraints compared to knocking out protein coding genes. Indeed, an insertion or deletion (indel) in the nucleotide sequence of a protein coding gene can result in a frame shift of the amino acid sequence, and usually introduces premature stop codons. For miRNAs, however, the entire 22 nt sequence has to be deleted as miRNAs comprise independent functional domains which can bind their respective target sequence (Broughton et al. 2016; Grimson et al. 2007). Therefore, the single strand guide RNA for CRISPR/Cas9 was designed as such that it would bind in close proximity or even within the miRNA sequence to be knocked out (**Figure 24**, A). The resulting

homozygous miRNA KO cell line was used to assess the reporter ratio of the true null of miRNA expression in pluripotent state. In addition, the unedited (wt) cell line was used to assess miRNA expression levels by deep sequencing. Having measured both, miRNA activity and miRNA expression levels, enabled me to calculate the miRNA affinity (**Figure 24**, B).

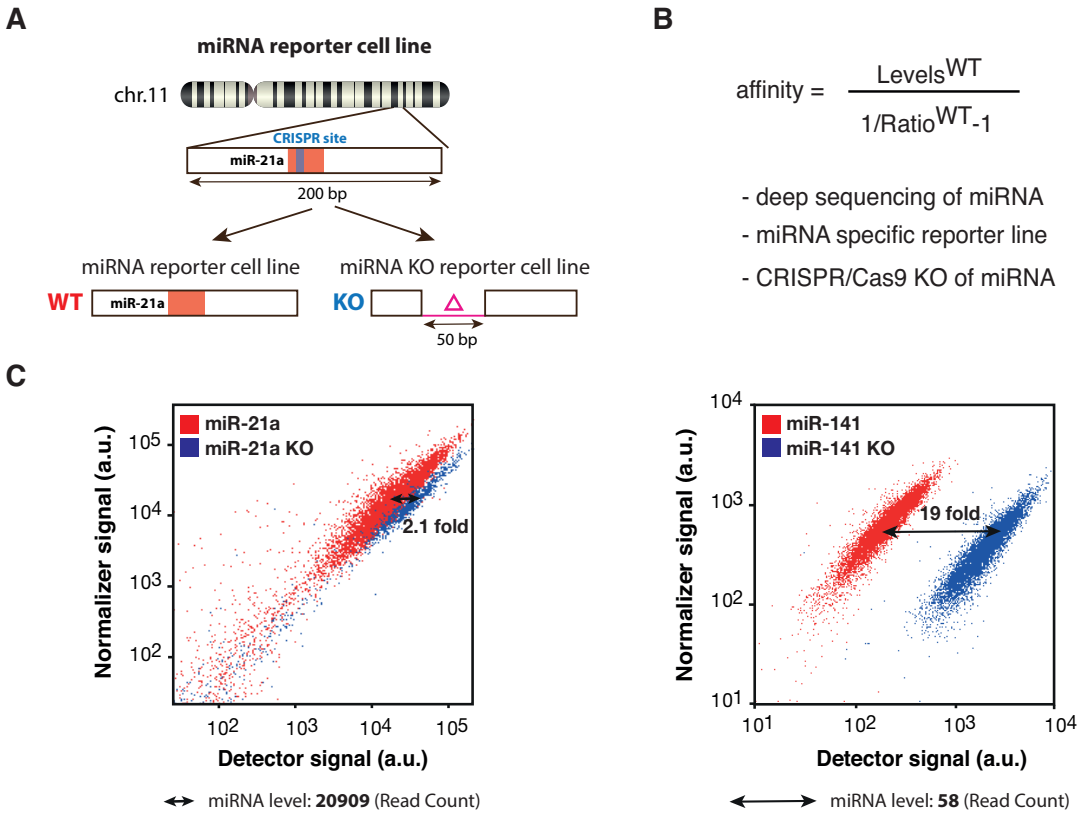

Figure 24: Direct miRNA affinity measurement.

A) *miRNA CRISPR/Cas9 KO cell lines were generated using the respective miRNA reporter cell lines. KO of the entire miRNA sequence was validated by PCR and sanger sequencing. Flow cytometry analysis was performed on reporter cell lines of both, unedited miRNA reporter cell line and miRNA KO reporter cell line.* ***B)*** *Hills equation with non-cooperative binding gave access to miRNA affinity. miRNA expression levels in pluripotent mESCs were determined by deep sequencing. miRNA activity was assessed by flow cytometry for both, unedited miRNA reporter cell line and miRNA KO reporter cell line (see C).* ***C)*** *Flow cytometry analysis was performed for unedited and KO cell lines of each miRNA in question. miRNA reporter ratio of KO cell lin was used as true null of miRNA expression.*

I chose two miRNAs with significant difference in their respective expression levels in the pluripotent state, namely miR-21 and miR-141. Interestingly, both miRNAs differ 360-fold in expression levels. Therefore, I hypothesized that the miRNA reporter repression in miR-21 KO cell lines might be more dramatic than the reporter repression in miR-141 KO cell lines. Strikingly, miR-141 KO lines showed a 19-fold miRNA reporter repression whereas miR-21 KO lines resulted in a 2-fold repression (**Figure 24**, C). This suggests, that miR-141 is more potent compared to miR-21a, despite its higher expression levels. Taken together, these data validate my previous observation that weakly expressed miRNAs can be as potent as/or even more potent then highly expressed ones. Moreover, I could show that miRNA affinity cannot be inferred from miRNA expression levels alone.

Among the 41 miRNA candidates without expression changes during differentiation, many are either members of a miRNA seed family and/or present in multiple copies in the genome. CRISPR/Cas9-mediated KO was therefore unsuited for these. Thus, I generated homozygous deletions for 23 miRNAs including candidates with up to four locations in the mouse genome. I additionally included in this set a few miRNAs for which I measured the affinity using their changes in activity during differentiation. This provided an independent validation of the measured miRNA affinity.

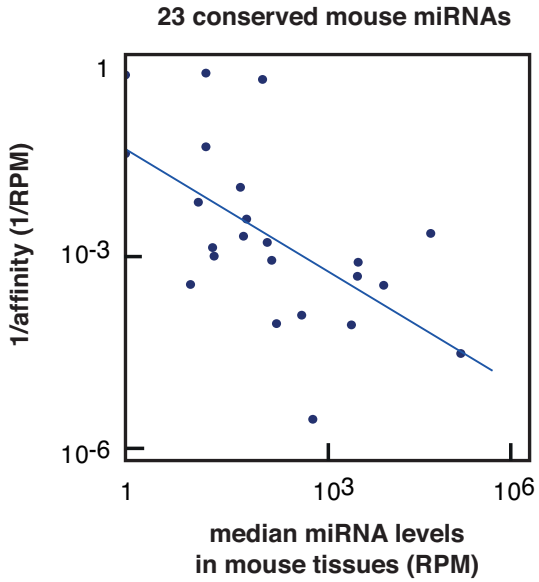

Figure 25: Knock out based miRNA affinities.

miRNA affinities of 23 conserved mouse miRNAs are plotted over their respective miRNA expression levels in mouse tissues (RPM: reads per million mapped reads).

In order to determine how miRNA affinity depends on miRNA expression levels, miRNA affinities of 23 KO cell lines were plotted over their respective miRNA expression levels (**Figure 25**). The result shows that miRNA affinity is negatively correlated with miRNA expression levels. This result confirms previous findings that lowly expressed miRNAs can be as potent or even more potent then highly expressed ones. Moreover, it indicates that miRNA affinities can span several orders of magnitude which was previously unknown.

In order to have a complete picture of experimentally determined miRNA affinities, I listed all of them in the following table. Of note, miRNA candidates are ordered alphabetically and high miRNA potency is denoted by low affinity values.

Table 2: miRNA affinities.

miRNA	Affinity	miRNA	Affinity	miRNA	Affinity	miRNA	Affinity
let-7a-5p	122114	miR-134-5p	24597	miR-218-5p	31080	miR-421-3p	806
miR-1a-3p	5849	miR-136-3p	2767	miR-219-5p	2964	miR-433-3p	757
miR-7a-5p	69423	miR-136-5p	1086	miR-221-3p	1033	miR-448-3p	n.d.
miR-9-5p	9844	miR-137-3p	59	miR-223-3p	81	miR-450a-5p	12113
miR-15a-5p	2055	miR-138-5p	1978	miR-224-5p	3523	miR-451a	127
miR-18a-5p	372	miR-141-3p	2	miR-292-5p	471839	miR-455-5p	1568
miR-19a-3p	11406	miR-143-3p	29078	miR-293-3p	81416	miR-486-5p	326
miR-21a-5p	53755	miR-144-3p	126	miR-301a-3p	n.d.	miR-487b-3p	2652
miR-22-3p	7096	miR-145a-5p	463	miR-302c-3p	40	miR-488-3p	168
miR-23a-3p	1184	miR-148a-3p	105271	miR-324-5p	61	miR-490-3p	71
miR-24-3p	1022	miR-149-5p	447	miR-328-3p	1003	miR-491-5p	n.d.
miR-26a-5p	332	miR-150-5p	1331	miR-330-5p	72	miR-495-3p	3199
miR-27b-3p	3738	miR-153-3p	32	miR-335-5p	41798	miR-496a-3p	n.d.
miR-30c-5p	224441	miR-155-5p	428	miR-338-3p	25	miR-499-5p	57
miR-31-5p	913	miR-181a-5p	5406	miR-339-5p	200370	miR-503-5p	438
miR-33-5p	ND	miR-184-3p	80	miR-340-5p	2110	miR-504-5p	23
miR-96-5p	416	miR-186-5p	1543	miR-342-3p	1551	miR-505-3p	26
miR-99b-5p	1362	miR-187-3p	383	miR-361-5p	695	miR-542-3p	965
miR-101b-3p	5982	miR-190a-5p	547	miR-365-3p	81	miR-543-3p	3972
miR-103-3p	53659	miR-192-5p	240	miR-370-3p	235	miR-544-3p	13
miR-122-5p	12434	miR-193b-3p	n.d.	miR-375-3p	8080	miR-551b-3p	n.d.
miR-124-3p	819	miR-194-5p	951	miR-376b-3p	270373	miR-590-3p	n.d.
miR-124-5p	1352	miR-196a-5p	1760	miR-376c-3p	944	miR-592-3p	n.d.
miR-125a-3p	370005	miR-199a-5p	6483	miR-377-3p	439	miR-615-3p	11
miR-125a-5p	370005	miR-200b-3p	9699	miR-378c	2856	miR-653-3p	n.d.
miR-126a-3p	2011	miR-202-3p	n.d.	miR-379-5p	11117	miR-873b	n.d.
miR-127-3p	251420	miR-208b-3p	66	miR-383-5p	n.d.	miR-875-5p	n.d.
miR-128-3p	7437	miR-214-3p	645	miR-384-3p	201	miR-876-5p	n.d.
miR-129-5p	8409	miR-216a-5p	302	miR-410-3p	4387		
miR-132-3p	89	miR-216b-3p	n.d.	miR-411-3p	51036		
miR-133b-3p	691	miR-217-3p	n.d.	miR-411-5p	331106		

n.d. = not detected (no miRNA expression levels in mouse tissues)

4 DISCUSSION

MicroRNAs act as key players in stem cell homeostasis and cell fate decisions (Bartel et al. 2004; Ong et al. 2015). They fine tune gene expression programs on the post-transcriptional level (Sevignani et al. 2006) and can therefore be seen as an additional regulatory layer during cell fate commitment (Ishikawa et al. 2017). Current studies extrapolate miRNA activity from miRNA expression levels using large RNA-Seq datasets (Li et al. 2018; Castel et al. 2018). However, miRNA activity cannot be inferred from expression analysis alone, since the bottleneck of miRNA activity is Ago loading rather than miRNA expression (Hausser et al. 2014). In addition, the presence of a given miRNA does not prove discernable activity since the 3'UTR of a potential target mRNA might not be accessible (Szostak and Gebauer 2013). Thus, miRNA expression studies do not yield meaningful insights into miRNA activity or miRNA target regulation. In addition to miRNA activity, miRNA affinity is currently underrepresented in the field of RNA biology. miRNA affinities are mostly predicted based on miRNA sequences in addition to the number of complementary sites in the 3'UTR of potential target mRNAs, without experimental validation of miRNA binding or determination of miRNA affinities. Since hundreds of miRNAs have overlapping target mRNAs, I postulate that conserved miRNAs might differ in their individual potency. In order to better understand general aspects of miRNA biology, such as miRNA activity dynamics or miRNA affinity, my PhD project aimed to determine single cell miRNA activity dynamics upon mouse embryonic stem cell differentiation in addition to miRNA affinity *in vivo*. This will provide a comprehensive picture of the miRNA complement upon mESC differentiation in addition to currently understudied miRNA affinities.

4.1 Reporter Assays to experimentally study miRNA activity

In-silico target predictions and experimental approaches are currently the two ways to study miRNA activity. In-silico approaches utilize bioinformatic target prediction tools such as TargetScan (Lewis et al. 2003), miRanda (Enright et al. 2003; John et al. 2004), PicTar (Lall et al. 2006), or miTarget (Kim et al. 2006) among others. Those tools, however, predict inconsistent miRNA targets overrating some miRNA-to-target interactions and underrating others (Lewis et al. 2003; Watanabe et al. 2007). Since

miRNAs can regulate multiple targets, prediction tools result in lists of mRNA targets, however, some of them might be false positive. Therefore, I decided to follow an unbiased experimental approach of studying the miRNA dynamics of all broadly conserved miRNAs among vertebrates upon mESC differentiation. This approach resulted in a list of 162 miRNA candidates present in the mouse genome.

Pioneering research in the field of miRNA:mRNA interactions established multiple techniques to characterize miRNA to target interaction ranging from qRT-PCR, western blot, immunoprecipitation of active RISC complexes with HITS-CLIP (Chi et al. 2009), tandem affinity purification of miRNA target mRNAs (TAP-tar) (Nonne et al. 2009), biotinylated synthetic miRNAs that bind potential mRNA targets (Ørom and Lund 2007) to luciferase reporter assays (Clément et al. 2015). All approaches have in common that they are invasive and destroys the history of a given sample. Moreover, none of these techniques are unbiased in their candidate choice, hence, the target mRNA or miRNA of interest needs to be known and decided on before characterization.

miRNA activity studies largely focused on luciferase reporter gene assays which are quantitative and determine the silencing of a possible target gene by a specific miRNA (Clément et al. 2015). This strategy relies on the ectopic expression of the predicted miRNA target cloned downstream of a luciferase reporter in addition to overexpression of the miRNA of interest, which does not mimic physiological levels. Therefore, I used a single cell ratiometric reporter, developed in our lab, which corrects for locus specific transcriptional noise by expressing a normalizer (mCherry) and miRNA sensor (Citrine). The reporter was designed as such that a perfectly complementary miRNA target site was cloned downstream of the miRNA sensor. The previous PhD student in the lab could validate that the endogenous pool of miR-142-3p molecules was not titrated by “citrine-sensor-bait molecules” over a 20-fold transgene expression range. Therefore, my approach does not face any miRNA sponging effects (Sladitschek and Neveu 2015b).

4.2 miRNA seed drives target mRNA recognition

miRNAs interact with their target mRNAs in a sequence specific manner. Mature miRNAs are loaded onto Ago proteins which results in the biologically active RISC complex. RISC specifically binds miRNA regulatory elements (MREs) in the 3’UTR of their target mRNAs. However, the regulatory interaction of miRNAs and its target seems

to be rather complex and is therefore poorly understood. It is well accepted in the field that target mRNAs are either transcriptionally repressed or degraded, depending on the degree of miRNA to target complementarity and depending on the interaction of the functional miRNA domains (anchor, seed, 3' region) with its respective Ago protein. In this study, I determined the impact of the seed sequence (nt 2-8) on target mRNA specificity. This was of interest because recent studies propose the impact of miRNA domains beyond the seed sequence (5'- and 3'-region) on target binding. (Grimson et al. 2007; Broughton et al. 2016). Moreover, structural insights into Ago bound miRNAs revealed that Ago subdivides its loaded miRNA guide into distinct functional parts that changes target binding properties compared to naked miRNAs (Wee et al. 2012).

To address this question, I generated two scrambled miRNA reporter versions for miR-136 and compared its miRNA activity to the full-length complementary control (**Figure 11**). The first scrambled construct was composed of a fully scrambled miRNA target sequence. As expected, this reporter cell line showed no sensor regulation upon miR-136 expression. The second scrambled miRNA reporter was composed of a functional seed binding region (nt 2-8) in an otherwise fully scrambled miRNA target sequence (scrambled 5'- and 3'region). Comparing the miRNA activity data of the "seed only" construct to its unedited control showed, that the seed sequence is indeed the main driver of target recognition. Strikingly, the seed-only reporter did exert almost equal miRNA activity compared to its full-length miRNA control. This confirms, that the miRNA seed alone is sufficient to regulate its target mRNA. This finding is in line with biochemistry studies showing that Ago2 masks functional miRNA domains apart from the seed sequence in order to display the seed in a pre-helical structure (Klein et al. 2017). This specific 3D arrangement lowers the entropic barrier to target binding and speeds up the target search process (Klein et al. 2017). Intriguingly, seed-only matched and full-length complementary miRNAs were found to associate and dissociate from respective mRNA targets at similar rates (Wee et al. 2012). Which confirms that the seed sequence is sufficient for target repression in mammals, as opposed to flies, where only full miRNA complementarity results in target cleavage (Wee et al. 2012).

Exposing only the seed sequence on the surface of functional RISC while other functional domains are hidden by Ago does explain the miRNA crosstalk I encountered in my miRNA activity screen. The seed sequence of miR-295 and miR-302b did overlap perfectly. Thus, the reporter cell line for miR-302b recapitulated the miRNA activity

profile of the miR-295 reporter cell line. This result was unexpected as miRNA expression levels suggested the upregulation in miR-302b activity levels. In order to measure miRNA activity for the miR-302 cluster, I identified miR-302c with its non-overlapping and unique seed sequence as representative of the cluster and repeated the activity measurements. Results of the miR-302c reporter cell lines showed the expected upregulation of miR-302 activity during endoderm differentiation. Taken together these results show, that miRNA activity can only be measured for unique miRNA sequences. Moreover, it visualizes that overlapping seed sequences are key to regulate multiple mRNA targets.

4.3 miRNAs in pluripotent state

Distinct miRNA signatures such as miR-106a, miR-200, miR-142 or miR-290 were shown to be crucial for stem cell pluripotency (Lichner et al. 2011; Sladitschek and Neveu 2015b; Balzano et al. 2018). In order to validate that the miRNA sensor faithfully measures temporal changes of miRNA activity in pluripotency, I designed the miR-295-3p sensor. The miR-290 cluster comprises seven mature miRNAs (Yuan et al. 2017) which have been shown to be implicated in pluripotency by negatively regulating Dkk-1, a known Wnt path inhibitor (Zovoilis et al. 2009), or Rbl2, a known epigenetic transcriptional repressor (Sinkkonen et al. 2008; Benetti et al. 2008). In order to differentiate, stem cells need to silence pluripotency programs and activate differentiation gene programs. Thus, miR-290 cluster expression levels are downregulated upon mESC differentiation (Lichner et al. 2011). I postulate that due to the decline of miRNA expression levels, also miR-295 activity should be downregulated. Indeed, I could show that miR-295 activity declines in all three major germ layers (**Figure 12**) upon pluripotency exit.

In addition to pluripotency associated miRNAs, I screened the deep sequencing dataset for heterogeneously expressed miRNAs in pluripotent state. Surprisingly, the dataset revealed miR-21a, which is known to have functional roles in development, cancer (Kumarswamy et al. 2011) and mesenchymal stem cell differentiation (Sekar et al. 2015) but not pluripotency. I hypothesize, that miR-21a might have functional role in pluripotency, similar to transcription factor heterogeneity (Torres-Padilla and Chambers 2014). miRNA heterogeneity might open a “window of opportunity” for external stimuli

that trigger pluripotency exit. This hypothesis is fostered by the finding that high miR-21a expression levels coincide with low Nanog expression levels (**Figure 14**). Nanog was previously shown to be heterogeneously expressed in mESCs (Singh et al. 2007), which allowed embryonic stem cells to explore pluripotency (Abranches et al. 2014). Interestingly, $Nanog^{low}$ cells were found to be prone to differentiate whereas $Nanog^{high}$ cells kept the pluripotent state (Singh et al. 2007). These findings are in line with genetic ablation studies of Nanog which triggered differentiation of mESCs towards a primitive endoderm fate, whereas Nanog overexpression enhanced stem cell self-renewal (Chambers et al. 2003; Mitsui et al. 2003). I propose that similar regulatory effects might be possible for miR-21a, where $miR\text{-}21a^{high}$ cells are prone to differentiate and $miR\text{-}21a^{low}$ cells continue to self-renew. Such potential regulatory effects would need further investigation which is beyond the scope of this thesis project.

4.4 miRNAs in differentiation

In addition to crucial roles in pluripotency, miRNAs regulate differentiation by fine tuning gene expression programs (Michaels et al. 2019). Subtle changes in gene expression have been shown to be sufficient to prime stem cells for differentiation (Yu et al. 2012). Intriguingly, miRNAs promote the transition from self-renewal to differentiation by suppressing pluripotency programs and activating differentiation genes. miR-200c, miR-203, and miR-183, for instance, cooperate to repress Sox2 and Klf4 (Wellner et al. 2009), which facilitates pluripotency exit and onset of differentiation. Pioneering work on miRNA expression levels in terminally differentiated cells has added valuable knowledge to the understanding of differentiation. miR-1 and miR-133 clusters, for instance, are highly expressed in mESCs regulating the differentiation towards cardiac muscle cells (Ivey et al. 2008; Tao et al. 2015). Furthermore, miR-214 has been shown to target Ezh2, a polycomp group protein that occupies and represses promoters of mesoderm differentiation genes among others. However, one has to keep in mind that miRNA research is largely based on sequencing datasets that reflect the population average of millions of cells, thus, potentially masks subtle changes in miRNA expression. Therefore, my miRNA activity dataset utilizes single cell resolution data which adds resolution to previously unrecognized subtle changes in miRNA activity.

This thesis project studied the temporal regulation of miRNA activity upon mESC differentiation on a global scale rather than focusing on specific miRNA candidates. I could show that miRNAs conserved among mammals are tightly regulated in their temporal miRNA activity profile. Moreover, I find that miRNAs can be classified into early, mid and late regulators of differentiation. Interestingly, most of the conserved miRNAs were upregulated throughout all germ layers, yet, their temporal profile differed vastly between mesoderm, endoderm and ectoderm lineage (**Figure 18**). This tight temporal regulation might either be crucial for cell fate commitment or for keeping cells in the trajectory they decided on. Strikingly, principle component analysis on miRNA activity could distinguish different fate choices (**Figure 19**). Divergence in miRNA profiles occurred already 48 hours after onset of differentiation, where each germ layer followed a specific trajectory. Surprisingly, once a cell has decided for its trajectory, it does not switch fate anymore. I postulate, that this tight temporal regulation of miRNA activity helps to keep differentiating cells on their committed trajectory. This finding is in line with Waddington's concept of "progressive restriction of cell differentiation potential during normal development" (Ladewig et al. 2013, p1).

Furthermore, my study shows miRNA activity of RISC loaded complexes in mESC differentiation for the first time. The data suggest that miRNA activity is very dynamic upon differentiation of stem cells, suggesting that miRNAs are another class of important regulators in facilitating the transition from pluripotency to differentiation programs by poising naïve cells for differentiation. Surprisingly, most conserved miRNAs were regulated at least in two or all three germ layers. This suggests that the majority of conserved miRNAs regulate differentiation in a cooperative manner rather than being germ layer specific, which does not exclude single miRNA clusters from being germ layer specific. Indeed, miRNA expression levels of differentiated mESCs suggest the miR-302 cluster to be endoderm specific.

The miR-302 cluster resides in an intron of the LARP7 gene and is encoded as single polycistronic transcriptional unit. The cluster is highly conserved among vertebrates and consist of five members: miR-302a, b, c, d and miR367 (Barroso et al. 2008; Chen et al. 2015). I could show that all members of the cluster are upregulated solely in endoderm but not mesoderm or neuroectoderm lineage (**Figure 15**). miR-302 is believed to repress AKT target genes and upregulate MEK expression, which in turn promotes differentiation of stem cells (Gu et al. 2016). In order to validate the necessity

if miR-302 expression for endoderm differentiation one would need a functional test. I developed a Sox17-H2B Citrine reporter cell line that marks the successful differentiation towards the endoderm lineage. This reporter cell line could be used for gain- and loss-of-function experiments of the miR-302 cluster in order to determine its necessity for endoderm specification. This approach, however, might be challenging due to miRNA redundancy. Preliminary results from my project showed that homozygous KO of miR-302c did not impair endoderm differentiation (data not shown). This suggests that other miRNAs of the cluster might buffer the miR-302c loss. The next step would be to KO the entire miR-302 cluster in order to screen for phenotypic effects in the Sox17 fate marker line. Interestingly, characterization of the miR-290 cluster in studies reported elsewhere faced similar obstacles. Only the KO of the entire miRNA cluster but not single members blocked pluripotency programs (Gu et al. 2016). Taken together, these results show that miR-302 expression is endoderm specific. However, the functionality of this finding requires further validation by gain- and loss-of-function experiments which were beyond the scope of this thesis project.

4.5 Developmentally important miR-17/92 and miR-379/410 cluster

Genomic manipulation of the miR-17/92 cluster revealed its pivotal role in fine-tuning signaling cascades and developmental pathways (Concepcion et al. 2012) throughout normal mouse development (Lu et al. 2007; Ventura et al. 2008). I could show that the affinity of the miR-17/92 cluster is overall upregulated upon mESC differentiation, which hints to a functional role in mESC differentiation. Interestingly, miR-17 is known to directly target the TGF-ß receptor II, whereas miR-18a targets SMAD2 and SMAD4 (Mogilyansky and Rigoutsos 2013). SMAD proteins are members of the TGF-ß/Nodal/Activin signaling pathway, with pivotal role in stem cell specification (Liu et al. 2018). These findings manifest the hypothesis that miR-17/92 cluster might be pivotal for mESC differentiation.

Interestingly, the temporal regulation of specific members of the miR-17/92 cluster differs among the three-germ layers. miRNA activity of miR-17 and miR-18, for instance, was upregulated from day 2 of mesoderm differentiation whereas the same

miRNAs were upregulated earliest by day 4 in the endoderm lineage (**Figure 16**). This suggests that the temporal profile of miRNA activity might be important in order to facilitate or maintain the right cell fate. It is of note that miRNA activity of all cluster members is not equally upregulated within a given germ layer. This suggests that either single miRNAs of the cluster are more important than others to the specific germ layer, or miRNA biogenesis is not equally efficient for all cluster members. miR-17/92 biogenesis studies found that the pri-miR-17/92 polycistronic transcript folds into a complex tertiary structure with solvent exposed and solvent-advert domains. This folding leads to sequential processing of the individual cluster members depending on microprocessor accessibility (Chaulk et al. 2011). Therefore, the pri-miR structure results in an autoinhibitory conformation in embryonic stem cells (Du et al. 2015) which explains why some members of the cluster are processed more efficiently than others. The germ layer specific differences in miRNA activity of cluster members are therefore probably explained by differences in miRNA biogenesis, as the expression levels do not correlate.

Another developmentally important cluster is the miR-379/410 cluster, which is the largest known placental mammal-specific miRNA cluster, and located in the *Dlk1-Dio3* locus. The cluster comprises 40 miRNAs out of which 27 are represented in the miRNA activity dataset (**Figure 17**). Interestingly, only miRNAs from the maternal allele were found to be expressed (Labialle et al. 2014). Moreover, correct dosage of the *Dlk1-Dio3* locus has been shown to be crucial for embryonic growth and neuronal development (Rocha et al. 2008). However, the biological importance of the miRNA cluster remains elusive. It might be implicated in physiological processes such as embryonic growth or placental and neuronal development (Labialle et al. 2014; Rocha et al. 2008).

Similar to miR-17/92, the miR-379/410 cluster activity is upregulated throughout differentiation, which suggests a cooperative effect. I could further show, that miR-379/410 activity cannot be inferred from miRNA expression analysis, as miRNA expression levels show a different temporal profile than miRNA activity data. Moreover, elevated expression levels do not necessarily result in elevated miRNA activity (**Figure 17**). Interestingly, Hausser *et al*. could show that the bottleneck of miRNA activity is Ago loading rather than miRNA expression (Hausser et al. 2014), which fosters the hypothesis that miRNA expression levels are not sufficient to give insights into miRNA activity. Pioneering work on miRNA sensors and decoy libraries showed that 60 % of miRNAs detected by deep-sequencing had no discernible activity (Mullokandov

et al. 2012). Therefore, miRNAs expressed below ~ 100 copies per cell had no or little regulatory activity (Brown et al. 2007). These and other results suggest that the functional 'miRNome' of a cell is considerably smaller than currently assumed from miRNA expression studies. Taken together, my data suggest that the temporal regulation of miRNA activity might have a crucial role in stem cell differentiation. The impact of miR-379/410 cluster on differentiation efficiency, however, would need to be further assessed by gain- and loss-of-function experiments in fluorescently labeled fate marker cell lines that I established for all major germ layers. Of note, KO experiments of the miR-379/410 cluster in mice aimed to elucidate the biological role of this cluster and showed that neonates deficient for miR-379/410 failed to maintain energy homeostasis and died shortly after birth (Labialle et al. 2014). This was one of the first demonstrations that miRNAs exert critical functions in the temporal activation of metabolic genes in the newborn's liver (Labialle et al. 2014) and highlights the importance of this miRNA cluster.

4.6 miRNA affinity and miRNA activity in mESCs

The mammalian genome encodes thousands of miRNAs, therefore, it is highly likely that not all of them are equally potent. The miRNA biology field is currently lacking detailed insights into basics of miRNA potency. This study finds, that miRNA potency is not dependent on miRNA expression levels. Furthermore, my results indicate that weakly expressed miRNAs can be as potent as highly expressed ones (**Figure 20**), which can probably be explained by differences in their respective miRNA affinity. As miRNA affinity determines the decay kinetics of target proteins (Breda et al. 2015), it is of interest to elucidate miRNA-levels, - activity and – affinity in order to better understand molecular basics of stem cell differentiation.

miRNA affinity is often predicted based on the miRNA sequence using various bioinformatic programs that apply free-energy prediction (ΔG) thermodynamic calculations (Sethupathy et al. 2006). However, these calculations do not reflect miRNA affinities under physiological conditions. Therefore, I plotted predicted base pair energies for both, full-length seed (nt 2-8) and sub-seed (nt 2-4) sequences over their respective experimentally determined miRNA-to-target affinities measured in my screen. The data revealed, that miRNA affinities are not correlated to base pairing energies. Therefore,

miRNA affinities cannot be predicted but need to be experimentally determined. miRNA affinity prediction methods have many pitfalls as they disregard the fact that the minority of expressed miRNAs are biologically active (Mullokandov et al. 2012). Moreover, they predict miRNA affinity based on full length miRNA to target complementarity although miRNAs largely bind their targets through partial sequence complementarity over a short sequence (Grimson et al. 2007). In addition, prediction tools treat miRNAs as naked RNA molecules, yet, Ago2 has been shown to change nucleic acid properties by making them behave more like an RNA-binding protein, rather than a free RNA (Salomon et al. 2016). *In vitro* binding kinetics for Ago bound let-7a, for instance, were 43-fold faster than for let-7a alone (Salomon et al. 2016). This shows that miRNA affinities need to be experimentally determined.

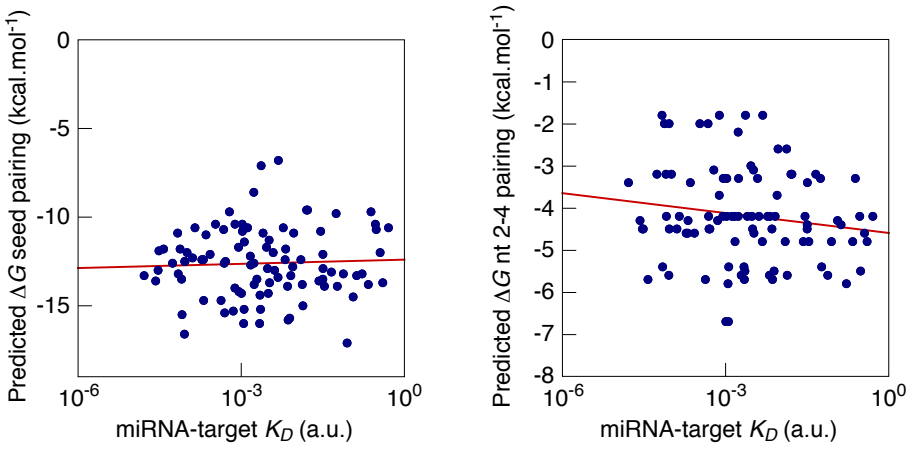

Figure 26: miRNA affinities are not correlated to predicted base pairing energy.
Free energy predictions (ΔG) for full-length seed (nt 2-8) and sub-seed (nt 2-4) were plotted over their respective miRNA affinities derived from my dataset.

This study aimed to experimentally determine miRNA affinities of 162 conserved miRNAs in mESCs. Calibration of the miRNA reporter (**Figure 21**) revealed that miRNA activity depends on both, miRNA expression and miRNA affinity. Thus, miRNA activity gives direct access to miRNA affinity. I postulate that the dependence of the miRNA detector levels D on the miRNA concentration M followed a Hill's equation with non-cooperative binding, where K (affinity) is the binding constant and n is the Hill coefficient of the interaction. With this assumption I could calculate the affinity of conserved miRNAs following two strategies, direct (miRNA KO cell lines) and indirect

(Δ expression method) miRNA affinity measurement. Affinities derived from the Δ expression method rely on an integrative approach of miRNA expression levels and miRNA activity data from differentiated mESCs. Adjustment of detector mRNA expression levels as a function of miRNA expression levels with Hill's equation enabled me to derive the affinity for 96 conserved miRNAs (**Figure 23**). This method is new to the field and enables previously uncharacterized miRNA affinity measurement *in vivo*. Of note, miRNAs not changing in the expression-based approach due constitutively active miRNAs or absence of miRNA expression, would prevent the computation of the miRNA affinity. Therefore, I developed an alternative approach using miRNA KO reporter cell lines.

The direct miRNA affinity measurement relies on the homozygous miRNA KO within its respective miRNA reporter cell line (**Figure 24**). I generated CRISPR/Cas9 KO cell lines for 23 randomly picked miRNAs and could show, that miRNA affinity is negatively correlated with miRNA expression levels. Moreover, my data reveal that weakly expressed miRNAs can be as potent or even more potent then highly expressed ones. In addition, the results indicate that miRNA affinities span several orders of magnitude, which was previously unknown. Strikingly, miRNA affinities of let-7 and miR-21 measured in my project are comparable with previous studies from Salomon and colleagues. Ago2 bound let-7 was reported to be 3-fold more potent than miR-21 (Salomon et al. 2016) which is comparable to a 2,3 fold difference measured in my affinity experiments. Taken together my dataset suggests, that conserved miRNAs differ in their respective potency due to differences in miRNA affinity.

So far experimental studies on miRNA affinity relied on purified Ago2-RISC which was used in filter-binding assays or single-molecule FRET assays using total internal reflection fluorescence microscopy (Wee et al. 2012; Chandradoss et al. 2015). Stochiometric titration showed that one mouse Ago2-miRNA molecule bound one target molecule at a time. Strikingly, direct binding assays did not find substantive differences in miRNA affinity for full miRNA complementarity versus seed only binding (Wee et al. 2012), which confirms results found in my study. Wee and colleagues further subdivided the miRNA and seed sequence into separate functional parts. They could show that central (nt 10-11) and terminal nucleotide mismatches (nt 20-21) had no detectable effect on target binding. Strikingly, mismatches within the seed sequence (nt 4-5), however, reduced target binding by 40-fold (Wee et al. 2012). This suggests, that the miRNA seed

sequence determines miRNA affinity and activity. Similar results were obtained from single-molecule FRET sensors which fosters the notion that miRNA seed sequence determines target finding, binding and silencing (Chandradoss et al. 2015; Salomon et al. 2016). Of note, there are additional factors influencing miRNA activity such as miRNA half-life (up to 72 hours) (Baccarini et al. 2011; Krol et al. 2010) and target mRNA concentration (Baek et al. 2008). Moreover, low levels of miRNA expression can still result in high miRNA activity since miRNA molecules are recycled (Baccarini et al. 2011) and one miRNA molecule per target mRNA is sufficient to facilitate target repression (Filipowicz et al. 2008)

Interestingly, target mRNAs have been shown to affect miRNA activity in a bidirectional control mechanism. Either by the competing endogenous RNA (ceRNA) (Thomson and Dinger 2016) or the target-directed miRNA degradation mechanism (TDMD) (Rüegger and Großhans 2012). The ceRNA hypotheses postulates that endogenous transcripts with shared miRNA binding sites compete for translational control. Therefore, expression changes in competing targets might influence miRNA activity on other targets since the upregulated endogenous target acts as miRNA sponge (Salmena et al. 2011). A similar hypothesis was proposed from Brown and colleagues (Brown et al. 2006) suggesting that discernable miRNA activity is only present when > 100 miRNA copies are expressed per cell.

The TDMD mechanism on the other hand postulates that the RNA target facilitates degradation of its miRNA (Bitetti et al. 2018). This process is accompanied by miRNA sequence modifications such as tailing (nt addition), trimming (nt shortening) (Ameres et al. 2010) or unloading from Ago (De et al. 2013), which would disrupt the active RISC complex. Indeed, both hypotheses are interesting and would explain how miRNA activity is modulated. Yet, they need further validation as they are highly debated in the field. Wee and colleagues for instance challenge this hypothesis by proposing that competitive mechanisms might only impact weakly expressed miRNAs. Highly abundant miRNAs, will not be regulated by seed-matched competitor transcripts (Wee et al. 2012) simply because the number of competitor targets would comprise 12 % - 50 % of all miRNAs in the cell (Islam et al. 2011). Therefore, highly abundant miRNAs are not affected by the two mechanisms described.

4.7 Outlook and Future Experiments

This PhD project determined the miRNA activity dynamics in mESC differentiation and miRNA to target affinity for 119 conserved miRNAs in vertebrates. The next step would be to identify key miRNAs or miRNA clusters, pivotal for stem cell differentiation on a global level (multilineage priming) or germ layer specification. miRNAs could be ranked according to their effective potency. Promising candidates would then be subject to gain- and loss-of-function experiments in fate marker cell lines that I have established in order to validate their functionality. Once miRNAs with phenotypic effects in germ layer specification were identified, one could investigate miRNA targets and underlying signaling cascades of mESC differentiation.

miRNA functionality is validated by measuring the efficiency of stem cell differentiation towards their respective fate, using fluorescently labeled fate marker cell lines that I established. Site directed homology recombination was used to place the coding sequence of fluorescent protein H2B-Citrine under the endogenous promoter driving the expression of Sox17 (endoderm), Vimentin (mesoderm) and Tubb3 (neuroectoderm), in independent cell lines. Once expressed, H2B-Citrine localizes in the nucleus where it is stabilized due to its H2B part. Differentiation of such fate marker cell lines towards their respective fate while measuring Citrine expression in confocal analysis or flow cytometry, would be the readout for the functionality test.

In a preliminary experiment I differentiated all three fate marker lines towards their respective germ layer and analyzed Citrine expression using confocal analysis (**Figure 27**). In order to validate the correct temporal expression of citrine, I co-stained well characterized fate marker proteins for each germ layer using immuno-fluorescence. Fate marker FoxA2 (endoderm), Vimentin (mesoderm) and Tubb3 (ectoderm) were identified from literature and AB-stained according to manufacturer's recommendation. Immunofluorescence showed that the fluorescent sensor is co-expressed with its respective fate marker in the correct temporal order.

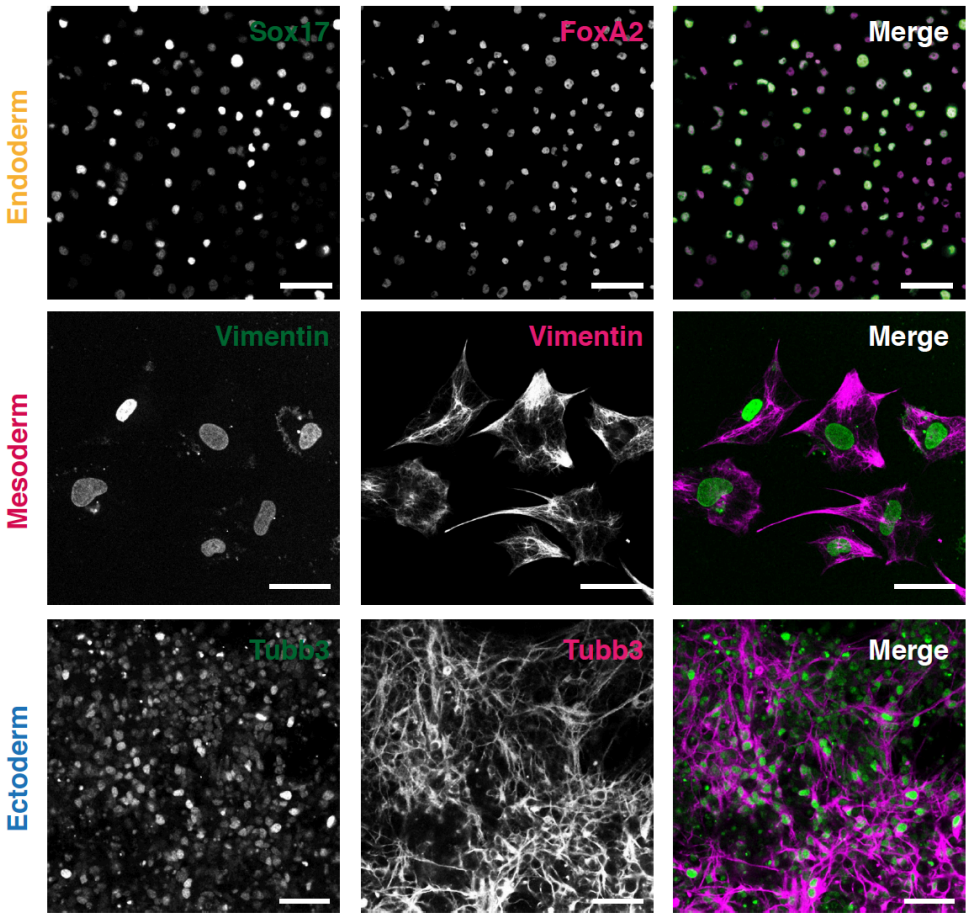

Figure 27: Confocal analysis of differentiated fate marker cell lines.
mESCs were differentiated towards the endoderm, mesoderm and neuroectoderm lineage. The fate specific H2B-Citrine reporter is expressed under the endogenous promoter of its respective fate marker gene: Sox17 (endoderm), Vimentin (mesoderm) and Tubb3 (ectoderm). Temporal expression of the fluorescent fate marker sensor was validated by immunofluorescence of well-established fate marker proteins: FoxA2 (endoderm), Vimentin (mesoderm) and Tubb3 (ectoderm). Scale bar is 50 µm.

Since immunofluorescence is laborious, expensive due to AB labeling and yields no live cell data, fluorescently labeled fate marker cell lines are the perfect alternative to allow stem cell differentiation over extended periods of time while tracking the temporal expression of their respective fate marker in live cells. Therefore, I used flow cytometry analysis which allows the measurement of millions of live cells in single cell resolution while being more cost efficient then confocal analysis (**Figure 28**). Intriguingly, differentiation of mESCs towards the three major germ layers resulted in 38 % positive cells for Sox17 (endoderm), 77 % positive cells for Vimentin (mesoderm) and 67 %

positive cells for Tubb3 (ectoderm). This result shows, that mESCs can be reliably differentiated towards any of the major germ layers.

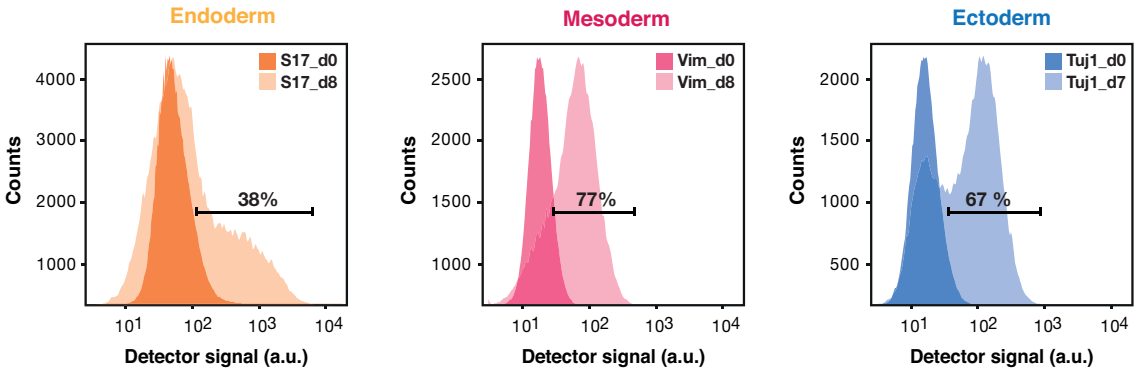

Figure 28: Flow cytometry analysis of fate marker cell lines.

mESCs were differentiated towards endoderm, mesoderm, ectoderm lineage and analyzed via flow cytometry. The H2B-Citrine sensor marks the expression of the corresponding fate marker genes: Sox17 (endoderm), Vimentin (mesoderm) and Tubb3 (ectoderm). Histograms of cells negative (day 0) and positive (day 7 or day 8) for citrine expression were overlaid according to their respective fate.

In addition to the "efficiency of differentiation test", cells positive for the respective fate marker could be subject to FACS sorting and RNA extraction in order to study the transitions from pluripotent to differentiated state. Transcriptomics of FACS sorted cells might help to delineate the molecular mechanisms that yield mature and functional differentiated cell types.

5 CONCLUSIONS

The presented study aimed to determine single cell miRNA dynamics during mouse embryonic stem cell differentiation. I established stable mESC lines expressing fluorescent reporters for the 162 miRNAs conserved among vertebrates. I could show, that the temporal miRNA activity profile is tightly regulated throughout mESC differentiation. Interestingly, miRNAs exhibit activity changes at early, mid and late stages of stem cell differentiation. Moreover, miRNAs seem to regulate differentiation in a cooperative manner on a global level rather than being germ layer specific. Strikingly, based on principle component analysis, miRNA activity diverged between germ layer fates already at 48 hours after onset of differentiation.

By integrating measurements of miRNA activity and expression levels, I experimentally determined miRNA affinities for the respective reporter construct of 119 conserved miRNAs. Surprisingly, miRNA affinities can span several orders of magnitude. Moreover, miRNA affinities are negatively correlated to miRNA expression levels, which suggests that weakly expressed miRNAs can be as potent as highly expressed ones. Knowing the affinity and expression levels in a given cell type, enables me to rank miRNAs according to their effective potency. This will potentially help to determine which genes are targets of a given miRNA. Future gain- and loss-of-function experiments of interesting miRNAs in established fate marker cell lines will aid to reveal miRNAs indispensable for stem cell differentiation.

Taken together, this thesis project provides new insights into miRNA dynamics and previously understudied miRNA potency in stem cell differentiation at single cell resolution.

6 METHODS

6.1 Mouse embryonic stem cell culture

6.1.1 General preparations before cell culture

Cell culture grade sterile reagents, plastic ware and glassware was used throughout all experiments. Experiments were performed in a laminar air flow hood which was switched on and UV-sterilized with the glass front closed for at least 15 min prior to work. The "warm up phase" of 15 min ensured a stable air flow. The working surface, in addition to any working material that entered the flow hood, was sprayed with 70 % Ethanol and wiped clean prior to work. Sterile cell culture plasticware was opened and closed exclusively under the laminar air flow. According to good cell culture practice, bottles, containers and plates would be closed during the working process whenever possible. After finishing cell culture work, the laminar air hood was cleaned and wiped with 70 % Ethanol to disinfect the working surface. The germicidal UV-lamp was switched on, with the blower running, for at least 15 min after finishing the work.

Liquid culture materials such as D-PBS, H_2O, gelatin, media or any other non-commercial and as sterile declared solution was autoclaved or sterile filtrated using a 0,22 μm Stericup Filter Unit (Millipore, SCGPU05RE). Cell culture media was sterile filtrated, aliquoted in 500 mL bottles and stored at 4 °C. Media was pre-warmed to ~ 37 °C in a water bath prior to use.

Cells were cultured at 37 °C and 5 % CO_2 in a humidified incubator. The humidity chamber was filled with water on a weekly basis. The inside of the incubator and all its stainless steel shelfs were cleaned with 70 % Ethanol once a month. The incubator was used for cell culture only after humidity and CO_2 levels were equilibrated.

6.1.2 Preparation of gelatin coated plates

0,1 % (w/v) gelatin solution was prepared as follows: 1 g pork gelatin (SIGMA; G1890) and 600 mL autoclaved water were added to a sterile 1 L beaker. The solution was swirled and microwaved till its boiling point (solution needs to boil to ensure proper solution of gelatin in water). The solution was topped up to a final volume of 1 L with H_2O (RT). After a short cooling period (till liquid reached approx. 50 °C), gelatin was sterile filtered in the laminar air hood using a 0,22 μm Stericup Filter Unit (Millipore; SCGPU05RE). Gelatin was aliquoted in 1 L bottles and stored at 4 °C.

Cell culture dishes were coated with 0.1 % gelatin (RT) latest 20 min before the experiment. The coating volume was chosen according to the culture volume of the respective dish. After checking that the entire dish surface was covered, gelatin coated plates were stored in the incubator till used. Prior to performing the experiment, gelatin was aspirated and the dish air dried before fresh media was added to the plate.

6.1.3 mES cell lines

All stable transgenic cell lines were derived from AB2.2 cell line (ATCC®SCRC-1023™). The AB2.2 cell line was regularly karyotyped and tested for mycoplasma contamination.

6.1.4 mESC maintenance and propagation

Mouse embryonic stem cells (mESCs) were maintained without feeders under standard pluripotency conditions in ES complete media (LIF+Serum) (**Table 3**) on gelatin coated plates, and maintained at 37 °C with 5 % CO_2 in a humidified incubator.

Table 3: ES complete - media composition.

Component	*Comment*	*Supplier (Number)*	*Concentration*
DMEM	high glucose, w/o glutamine	Invitrogen (11960)	80 % (v/v)
Fetal Bovine Serum	ES-qualified	Millipore (ES-009-B)	15 % (v/v)
100x Non-Essential Amino Acids	10 mM glycine 10 mM L-alanine 10 mM L-asparagine 10 mM L-aspartic acid 10 mM L-glutamic acid 10 mM L-proline 10 mM L-serine	Invitrogen (11140)	1x (100 μM)
100x L-Glutamine	200 mM	Invitrogen (25030)	1x (2 mM)
100x Sodium Pyruvate	100 mM	Invitrogen (11360)	1x (100 μM)
100x Penicillin-Streptomycin	10,000U mL^{-1} 10,000U mL^{-1}	Invitrogen (15140)	1x (100 U mL^{-1} Pen./Strep.)
2-Mercaptoethanol	55 mM in D-PBS	Invitrogen (21985)	100 μM
Murine LIF	Recombinant	EMBL PEPCore	10 ng/mL

The media was sterile filtrated using a 0,22 μm Stericup Filter Unit (Millipore; SCGPU05RE) and aliquoted in 500 mL bottles with subsequent storage at 4 °C. ES complete media was changed daily, whereas mESCs were passaged every other day. Cell dilution for passaging was chosen as such that the culture reached ~ 80 % confluency on the day of passaging. Cell culture media was replaced 2-3 hours before splitting cells. Prior to passaging, cells were washed with D-PBS (2,7 mM KCL, 1,47 mM KH_2PO_4, 137 mM NaCl, 8,1 mM N_2HPO_4, pH 7,4) (RT). Subsequently, 0,05 % Trypsin-EDTA solution (Invitrogen, 25300) was added in a dropwise manner (~ 20 μL/cm^2) to cover the entire surface of the well. Trypsin was incubated for 5 min at 37 °C. Trypsin was inactivated by addition of ES complete media (volume was chosen according the respective plate volume). Single cell suspension was generated by pipetting the cell suspension 10-15 times, while flushing the surface of the well. 50 μL of the cell suspension was diluted in 50 μL of 0,4 % (w/v) Trypan blue (Invitrogen, 15250) and cells were counted using a hemocytometer (Neubauer improved chamber). Cell viability was expected to be ≥ 98 %. Pre-prepared gelatin coated plates were aspirated, and fresh ES

complete media (37 °C) was added to the dish before cells were seeded at a density of ~ 40,000 cells/cm^2 and incubated at 37 °C with 5 % CO_2 in a humidified incubator.

6.1.5 Freezing mouse embryonic stem cells

Cells to be frozen had reached ~ 80 % of confluency with a cell viability of ≥ 98 %. Culture media was changed 2-3 hours before freezing cells. Cells were washed with D-PBS (RT) before adding 0,05 % Trypsin-EDTA solution (Invitrogen, 25300) in a dropwise manner (~ 20 μL/cm^2) to cover the entire surface of the well. Trypsin was incubated for 5 min at 37 °C and inactivated by addition of ES complete media (inactivation volume according to culture volume of the respective dish). Single cell suspension was achieved by pipetting the cell suspension 10-15 times while flushing the surface of the well. The entire cell suspension was transferred to a labeled and sterile 15 mL falcon. Cells were spun down (5 min, 500 rpm, RT), the supernatant was removed and the cell pellet resuspended in 1 mL (from a 6 well) of freezing media (10 % DMSO (v/v) (SIGMA, D8418) in ES-qualified EmbyroMax Fetal Calf Serum (Millipore, ES-009-B)). The cell suspension was transferred to a cryo-vial (1 mL per vial) and cryo-vials were placed in a polystyrene sandwich at - 80 °C, overnight. Cryo-vials were transferred to liquid nitrogen for long-term storage.

6.1.6 Thawing mouse embryonic stem cells

Prior to thawing, 15 mL falcon tubes were labeled and filled with 10 mL of pre-warmed ES complete media (~ 37 °C). Pre-prepared gelatin coated plates were aspirated and air dried in the laminar air flow hood. Cryo-vials were transported on dry ice from liquid nitrogen storage to the tissue culture room. Cryo-vials were placed in 37 °C water bath untill a small core of frozen cell solution remained. 1 mL of pre-warmed ES complete media (~ 37 °C) was added to the vial and the cell suspension was transferred to a 15 mL falcon tube. The falcon was closed and inverted multiple times to dilute the DMSO. The tube was spun down (5 min, 500 rpm, RT), the supernatant was aspirated and the cell pellet resuspended in 2 mL of pre-warmed ES complete media. Cell suspension was plated in a 6 well plate which was incubated at 37 °C with 5 % CO_2 in a humidified incubator.

6.1.7 Counting ES cells using the Neubauer chamber

Single cell suspension was generated as described previously. 50 μL of the cell suspension was diluted in 50 μL of 0,4 % (w/v) Trypan blue (Invitrogen, 15250). Neubauer improved chamber was mounted according to manufacturer recommendations and 10 μL of the cell dilution was loaded onto the chamber (Neubauer improved, depth: 0,1 mm, 0,0025 mm^2). The chamber was placed on an inverted DM IL LED microscope from Leica with an HI PLAN 10x/0,22 PH1 objective. Both, live cells (transparent) and dead cells (blue) were counted according to manufacturer recommendations in all grey shaded groups squares (one group square consist of 16 single squares) (**Figure 29**).

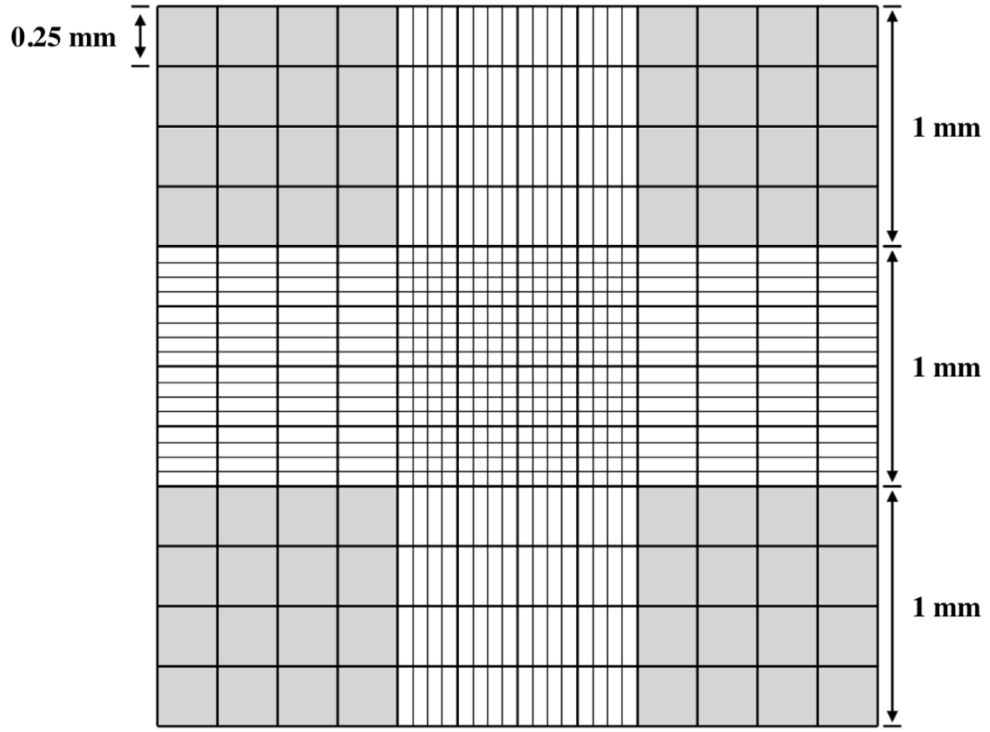

Figure 29: Counting grid of a Neubauer improved chamber.
Cells alive (transparent) and dead (blue) were counted within the grey indicated areas of the grid. One group quadrat consists of 16 smaller quadrats. The sum of all cells was counted in all four group quadrats according to manufacturer recommendations.

The final cell concentration was calculated as follows:

$$Concentration = \frac{\sum Number\ of\ cells\ x\ 10{,}000\ x\ dilution_{factor}}{N_{group\ quadrats}} \quad \left[\frac{cells}{mL}\right]$$

Cell viability was calculated as follows:

$$Viability = \frac{\sum live\ cells}{\sum all\ cells\ (live\ cells + dead\ cells)}\ x\ 100 \quad [\%]$$

6.2 Genetic modification of mESCs

6.2.1 Generation of stable transgenic miRNA reporter cell lines

The day prior to transfection, Ab2.2 wild type cells were seeded on gelatin coated plates (10 cm dish from Nunc) in ES complete media using a seeding cell number resulting in 60 - 80 % of confluency on the day of transfection (seed ~ 1.000.000 cells per 10 cm dish (Nunc)). Seeded cells were incubated overnight at 37 °C with 5 % CO_2 in a humidified incubator. The next day, culture media was replaced 2 hours prior to transfection. 25 μg of the target DNA was diluted in 1,2 mL OpiMEM. DNA dilution was mixed and 75 μL of FuGene (Promega, E2312, aquilibrated at RT) was added to the mix. The solution was mixed by pipetting and incubated for 15 min at RT without additional mixing. The transfection mix was added to the cells in dropwise manner using a 1 mL Gilson pipette. The transfected plate was incubated at 37 °C with 5 % CO_2 in a humidified incubator, overnight.

All plasmids used to generate transgenic miRNA reporter lines included a Hygromycin antibiotic selection cassette (PGK::HygroR-bGHpA). On the day after transfection, ES complete media was replaced by Hygromycin selection media (ES complete + 100 μg/mL Hygromycin B (Invitrogen, ant-hg-5)). The selection media volume was chosen according to the culture plate used. Selection media was changed on a daily basis after washing cells with D-PBS in order to remove dead cells. Seven days after selection, isolated single colonies were visible using an inverted DM IL LED

microscope (Leica). Selection media was replaced by D-PBS after washing the plate twice with D-PBS (RT). Colonies were checked for equal expression of Citrine and mCherry in all cells of a given colony, using the inverted DM IL LED microscope (Leica). Positive colonies were dislodged using a pipet tip and aspirated in 20 μL PBS. The colony was transferred to a 96 well v-bottom plate. Having picked 96 colonies per construct, 20 μL of 0,05 % Trypsin-EDTA solution (Invitrogen, 25300) was added to the wells using a multichannel pipet. The plate was incubated for 5 min in a humidified incubator (37 °C, 5 % CO_2). Cells were rescued by addition of 200 μL Hygromycin selection media (ES complete + 100 μg/mL Hygromycin B (Invivogen, ant-hg-5)). Each well was resuspended 8 - 10 times using a multichannel pipette, in order to generate single cell suspension. The entire volume was transferred to a pre-prepared gelatin coated 96 well plate and incubated at 37 °C with 5 % CO_2 in a humidified incubator. After three days (daily media change), 96 well plates were duplicated and daughter plates were measured on an HTS BD LSRFortessa™ flow cytometry analyzer, to identify clones expressing equal levels of both, Citrine and mCherry fluorescent reporter. Positive clones were expanded and frozen.

6.2.2 Generation of miRNA$^{+/-}$ and miRNA$^{-/-}$ KO cell lines

Heterozygous and homozygous miRNA KO cell lines were generated using the CRISPR/Cas9 gene editing approach. For each miRNA KO cell line a specific single guide RNA (sgRNA) was designed using the improved CRISPR sgRNA design website (Xu et al. 2015). The resulting sgRNA was cloned into the pX330-U6-Chimeric-BB-CBh-hSpCas9 backbone following Hsu *et al.* (2013). The resulting construct was cotransfected with a plasmid encoding puromycin resistance into the respective miRNA reporter cell line using FuGene transfection reagent. The day after transfection, puromycin selection media (ES complete + 1 μM puromycin) was applied to the cells. Selection media was changed on a daily basis after washing cells with D-PBS (RT) in order to remove dead cells. Cells were re-plated in a new gelatin coated 6 well dish after 2 days of puromycin selection and incubated for additional 2 days in puromycin selection media. Successfully edited clones were identified via miRNA reporter derepression and single cell sorted in 96 well plates using BD FACSAria™ Fusion flow cytometer. Clones not showing a fluorescent reporter derepression were still single cell sorted since the

respective miRNA might not be expressed in pluripotent state. miRNA$^{+/-}$ and miRNA$^{-/-}$ deletions were confirmed by sequencing of genomic PCR products.

6.2.3 Generation of stable transgenic fate marker cell lines

The homology recombination approach was used to generate stable transgenic fate marker cell lines for all three major germ layers i) endoderm (Sox17) ii) mesoderm (Vimentin) and iii) neuroectoderm (Tuj1). The Ab2.2 mESC genome was edited as such that one allele of the respective endogenous fate marker was replaced by an H_2B-Citrine fluorescent reporter. The fluorescent reporter additionally harbored an FRT flanked G418 antibiotic resistance cassette in order to select for successfully edited clones. The entire construct was placed under the endogenous promoter of the respective fate marker gene. Bacterial artificial chromosomes (BAC) of each fate marker were used to PCR-amplify DNA fragments encoding homology arms. The MXS-chaining technique (Sladitschek and Neveu 2015a) and subsequent homology recombination within the corresponding BAC was used to generate a final plasmid encoding the H_2B-Citrine fluorescent reporter flanked by 5 prime (~ 2 kb) and 3 prime (~ 8 kb) homology arms. Prior to transfection, the final construct was linearized with an AsiSI-enzyme (overnight) restriction digest in order to cut within the vector backbone, but not the insert. 25 μg of the target plasmid DNA was digested using 15 U of AsiSI enzyme in a total reaction volume of 50 μL (37 °C, overnight). Completion of the restriction digest was checked by analyzing 1/50 of the restriction digest on an analytical agarose gel (1 % (w/v) agarose in TAE buffer). The restriction digest was heat-inactivated for 20 min at 80 °C. The entire volume of the restriction digest was used for a FuGene transfection of Ab2.2 cells (**section 5.2.1**). The day after transfection, ES complete media was replaced by G418 selection media (ES complete + 1 mg/mL G418). Selection media was changed on a daily basis after washing cells with D-PBS (RT), in order to remove dead cells. Seven days after selection, single colonies were visible and dislodged as described in **section 5.2.1**. Cells were kept on 96 well plates in G418 selection media for additional 3 days. 96 well plates were duplicated and the mother plate was kept in G418 selection media (split every other day), while the daughter plate was seeded for a 6-day differentiation experiment towards the respective cell fate (**section 5.3**). Successfully edited clones were identified after 6 days of differentiation using the BD FACSAria™ Fusion flow cytometer, measuring H_2B-

Citrine expression levels. The correct reporter insertion was confirmed by genomic PCR products and southern blot. Thereafter, the FRT flanked selection cassette was removed by flipase transfection. After 4 days of flipase treatment, cells were single cell sorted into 96 well plates. Successful removal of the selection cassette was validated by duplicating the respective 96 well plates into mother and daughter plates. The mother plate was kept in ES complete media whereas the daughter plate was cultured in G418 selection media for three days. Clones negative for the selection cassette died upon G418 treatment. The corresponding mother clone, was enlarged and frozen as described in **section 5.1.5**.

6.2.4 Genomic DNA extraction

Cells were grown to ~ 80 % confluency on 12 well plates. Cells were harvested and transferred to a 1.5 mL Eppendorf tube. Cells were spun down (2 min, 4000 rpm) and the supernatant was removed. The cell pellet was covered (not mixed) with 200 μL spooling buffer (75 mM NaCl, 25 mM EDTA, 1 % SDS) containing 1 μL fresh Proteinase K and incubated at 55 °C, overnight (without shaking). The following day, 50 μL Brine (NaCl < 5 M) was added to the sample, and the sample was inverted several times during an incubation period of 5 min at 55 °C. After addition of 250 μL 2-propanol, the sample was again inverted and spun down (10 min, max speed, RT). The supernatant was removed and the pellet washed with 70 % Ethanol. The sample was spun down (10 min, max speed, RT), the supernatant removed and the cell pellet air dried at 55 °C. The resulting DNA was solubilized by addition of 200 μL EB buffer (shaking in the thermomixer, 55 °C). Samples were stored at (- 20 °C).

6.3 Differentiation of mESCs

6.3.1 Differentiation towards the endoderm germ layer

AB2.2 cells were differentiated towards endoderm progenitors following Borowiak *et al*. (2009). Cells were seeded on gelatin coated plates ~ 16 hours before starting differentiation with a seeding density of 5000 cells/cm^2 in ES complete media. Cells were incubated in a humidified incubator (37 °C, 5 % CO_2), overnight. Next day, cells were washed with D-PBS (RT) twice, before adding pre-warmed (~ 37 °C) IDE differentiation

media (**Table 4**) to the cells. Cells were incubated at 37 °C and 5 % CO_2 in a humidified incubator. Differentiation media was changed on a daily basis from day 2 of differentiation, with prior washes of D-PBS (RT) in order to remove dead cells.

Table 4: IDE1 - media composition.

Component	*Comment*	*Supplier (Number)*	*Concentration*
Advanced RPMI	w/o HEPES, w/o L-Glutamine	Invitrogen (12633)	98 % (v/v)
Fetal Bovine Serum	ES-qualified	Millipore (ES-009-B)	0,2 % (v/v)
100x L-Glutamine	200 mM	Invitrogen (25030)	1x (2 mM)
100x Penicillin-Streptomycin	10,000U mL^{-1} 10,000U mL^{-1}	Invitrogen (15140)	1x (100 U/mL Pen./Strep.)
IDE1	inducer of definitive endoderm	Tocris Bioscience (4015)	1 μM

6.3.2 Differentiation towards the mesoderm germ layer

AB2.2 cells were differentiated towards mesoderm progenitors following Torres *et al.*, (2012). Cells were seeded on gelatin coated plates ~ 16 hours before starting mESC differentiation with a seeding density of 5000 cells/cm^2 in ES complete media. Cells were incubated at 37 °C with 5 % CO_2 in a humidified incubator, overnight. The next day, cells were washed with D-PBS (RT) twice, before adding pre-warmed (~ 37 °C) GMEM differentiation media (**Table 5**). Cells were incubated at 37 °C with 5 % CO_2 in a humidified incubator. The differentiation media was changed from day 2 of differentiation every day, with prior washes of D-PBS in order to remove dead cells.

Table 5: GMEM - media composition.

Component	*Comment*	*Supplier (Number)*	*Concentration*
GMEM BHK 21		Invitrogen (21710)	96 % (v/v)
KSR		Invitrogen (10828)	10 % (v/v)
100x Non-Essential Amino Acids	10 mM glycine 10 mM L-alanine 10 mM L-asparagine 10 mM L-aspartic acid 10 mM L-glutamic acid 10 mM L-proline 10 mM L-serine	Invitrogen (11140)	1x (100 μM)
100x Sodium Pyruvate	100 mM	Invitrogen (11360)	1x (100 μM)
100x Penicillin-Streptomycin	10,000U mL^{-1} 10,000U mL^{-1}	Invitrogen (15140)	1x (100 U/mL Pen./Strep.)
2-Mercaptoethanol	55 mM in D-PBS	Invitrogen (21985)	100 μM

6.3.3 Differentiation towards the ectoderm germ layer

AB2.2 cells were differentiated towards neuroectoderm progenitors following Ying *et al.*, (2003). Cells were seeded on gelatin coated plates ~ 16 hours before starting differentiation with a seeding density of 15000 cells/cm^2 in ES complete media. Cells were incubated overnight in a humidified incubator with 5 % CO_2 at 37 °C. The next day, cells were washed with D-PBS (RT) twice, before adding pre-warmed (~ 37 °C) N2B27 differentiation media (**Table 6**). Cells were incubated in a humidified incubator with 5 % CO_2 at 37 °C. The differentiation media was changed from day 2 of differentiation every day with prior washes using D-PBS in order to remove dead cells.

Table 6: N2B27 - media composition.

Component	*Comment*	*Supplier (Number)*	*Concentration*
Neurobasal medium	w/o L-Glutamine	Invitrogen (21103)	48,4 % (v/v)
DMEM/F12 1x	w/o HEPES with L-Glutamine	Invitrogen (21041)	48,4 % (v/v)
100x L-Glutamine	200 mM	Invitrogen (25030)	0,25 mM
100x Penicillin-Streptomycin	10,000U mL^{-1} 10,000U mL^{-1}	Invitrogen (15140)	1x (100 U/mL Pen./Strep.)
B27 Supplement 50x	with vitamin A	Invitrogen (17504)	0,5 x
N2 Supplement 100x	1mM transferrin 86 μM insulin 2 μM progesterone 10 mM putrescine 10 μM selenite	Invitrogen (17502)	0,48 % (v/v)
BSA fraction V	for mouse embryo culture	SIGMA (A3311)	10 μg/mL
Insulin (human)	recombinant	SIGMA (91077C)	10 μg/mL
Retinoic Acid	inducer of ectoderm	SIGMA (R2625)	1 μM

6.4 Immunofluorescence

Cells were harvested and counted as described previously. Cells were seeded on gelatin coated 8 well μ-slides (ibidi) in ES-complete media with various seeding densities, depending on the experiment performed (pluripotent state, endoderm and mesoderm differentiation: 5000 – 10,000 cells/cm^2; neuroectoderm differentiation: 15.000 – 20.000 cells/cm^2). Cells were washed with D-PBS (RT), 12 to 16 hours after seeding and prior to addition of the corresponding differentiation media. Cells were differentiated for 6 days as described in **section 5.3**. On the final day of differentiation, cells were washed twice with D-PBS (RT), to remove debris and dead cells. Cells were fixed with 200 μL of 4 % PFA (4 % v/v PFA (16 %) in D-PBS, pH 7,4) (30 min, RT). PFA was quenched by addition of 200 μL glycine (300 mM glycine in D-PBS, pH 7,4) (1 h, RT). The fixative mix was aspirated and the entire plate gently washed (2x) in a beaker containing 400 mL TNT buffer (100 mM Tris-Cl, pH 8,0; 150 mM NaCl; 0,1 % v/v Tween-20). TNT buffer was aspirated and cells covered in 200 μL AB-buffer (0,01 % (w/v) BSA; 0,2 % (w/v) SDS; 1 % (v/v) Triton X 100), for permeabilization (1 h, RT). AB buffer was removed and cells overlaid with blocking buffer (5 % (w/v) BSA) for 1 h (RT). After blocking,

primary AB was diluted in blocking buffer (**Table 7**) and incubated overnight at 4 °C in a humidity chamber (prevents air drying of primary AB solution). Primary antibodies from different species targeting the same sample, were incubated in one reaction mix, overnight.

Table 7: Primary antibodies for immunostaining.

Antibody	*Source*	*Supplier (Number)*	*Dilution*
Oct 3/4	mouse mAb	Santa Cruz (sc-5279)	1:250
Nanog	rabbit pAb	Bethyl (A300-397A)	1:250
FoxA2	rabbit mAb	Cell Signaling (8186)	1:400
Desmin	Rabbit mAb	Cell Signaling (5332))	1:100
αSMA	mouse mAb	SIGMA (A2547)	1:800
Vimentin	rabbit mAb	Cell Signaling (5741)	1:200
Tuj1 (β-III-tubulin)	rabbit mAb	Cell Signaling (5568)	1:200

Slides were washed twice in a large volume of TNT buffer (400 mL, 5 min, RT), before adding fluorescently labeled secondary antibody, diluted in AB buffer (**Table 8**). Slides were incubated in the dark for 2 h (RT).

Table 8: Secondary antibodies for immunostaining.

Antibody	*Source*	*Supplier (Number)*	*Dilution*
anti-mouse	goat IgG, F(ab')$_2$ fragment labeled with Pacific Blue (405)	Invitrogen (P31581)	1:2000
anti-rabbit	goat IgG, F(ab')$_2$ fragment labeled with Alexa Flour 647	Cell Signaling (4414)	1:1000

Slides were washed twice in a large volume of TNT buffer (400 mL, 5 min, RT). All liquid was carefully removed and cells overlaid with fresh TNT buffer. Confocal imaging was performed on an inverted SP8 confocal microscope with a 40x PL Apo 1,1 W objective 8 (Leica).

6.5 Live cell imaging of miRNA reporter cell lines

Reporter cell lines were seeded on gelatin coated 8 well μ-slides (ibidi) with a seeding density of 5000 – 10,000 cells/cm^2. Cells were cultured up to three days in ES-complete (daily media change). The specimen was mounted onto an inverted SP8 confocal microscope with a 40x PL Apo 1,1 W objective 8 (Leica). Cells were imaged within the humidified incubation chamber at 37 °C and 5 % CO_2. The fluorescent reporters Citrine and m-Cherry were excited using 514 nm and 561 nm lasers, respectively. The emitted signals were acquired sequentially using HyD detectors and line or frame averaging in order to reduce imaging noise. Captured images were analyzed using ImageJ (Fiji).

6.6 Flow Cytometry Analysis and Single Cell Sorting

6.6.1 Flow Cytometry Analysis using LSRFortessa™ Analyzer

Samples from 96 well plates:

Samples from 96 well plates were washed with 200 μL D-PBS (RT), dislodged by addition of 25 μL 0,05 % Trypsin-EDTA (Invitrogen) per well and incubated for 4 min at 37 °C in a humidified incubator. Cells were rescued by addition of 200 μL ES-complete. Single cell solution was achieved by resuspending the cell solution 8 - 10 times. The volume was transferred to a fresh 96 well v-bottom plate. Plates were mounted onto the BD™ HTS plate reader, according to manufacturer recommendation without prior filtration of the samples.

Samples from any other culture dish but 96 well plates:

Cells were washed with D-PBS prior to addition of 0,05 % Trypsin-EDTA (Invitrogen) (volume according to plate size) and subsequent incubation for 4 min at 37 °C in a humidified incubator. Cells were rescued by addition of ES complete media. Cells were resuspended 8 - 10 times for single cell solution. Cells were spun down (2500 rpm, 2 min, RT or 500 rpm, 5 min, RT) and the supernatant was discarded. The cell pellet was resuspended in a minimum of 200 μL D-PBS (RT) or more, depending on the cell pellet size. Cells were resuspended 8 - 10 times for single cell solution and filtrated through a

40 μm cell strainer (BD Biosciences) into a polystyrene flow tube (Falcon, 352058). The sample was measured according to manufacturer recommendations.

Data acquisition and analysis:

The total cell number acquired varied between experiments. For a standard experiment 2 x 10^5 – 1 x 10^6 live single cells were recorded. Cells were analyzed using the FlowJo software. In order to gate live from dead cells, side-scatter area over forward scatter area was plotted. The resulting sub-population was plotted using side-scatter area over side-scatter width, which discriminated single-cells from doublets. The single cell population was plotted using the corresponding fluorescent colors in question. In case of miRNA-activity measurements, the fluorescent color values were exported using the *.fcs* file. The ratio of fluorescent normalizer (mCherry) over fluorescent detector (Citrine) was calculated. The resulting single cell values were plotted as a distribution function for every condition, using a customized Python script.

6.6.2 Single Cell Sorting using BD FACS Melody and Aria

Gelatin coated flat bottom 96 well plates were prepared containing 150 μL ES-complete media on the day of sorting. Cells were harvested as described earlier. Cell pellet was resuspended in 1 - 2 mL D-PBS (RT) and filtered through a 40 μm cell strainer into a polypropylene flow tube (BD Falcon, 352063). 10,000 cells were acquired prior to sorting. The target population to be sorted was gated with this preliminary acquisition. Single cells were sorted in purity mode, with one cell per well. Sorted 96 well plates were incubated for 7 days at 37 °C and 5 % CO_2 in a humidified incubator.

6.7 Molecular biology techniques

6.7.1 Kits, Buffers and Solutions

All DNA constructs for this thesis project were generated following the MXS-chaining technique (Sladitschek and Neveu 2015a). DNA purification kits were used for purification of small-scale-plasmid DNA (QIAprep Spin Miniprep Kit) and large-scale plasmid DNA (Qiagen Plasmid Plus Midi Kit) according to manufacturer

recommendations. Cloned plasmids were validated by analytical restriction digest and sanger sequencing (Eurofins GATC Biotech). All buffers and solutions used for cloning DNA constructs are listed below.

TAE-Buffer: 40 mM Tris-acetate, 1 mM EDTA, pH 8,3

LB media: 1 % w/v Tryptone, 0,5 % w/v Yeast Extract, 1 % NaCl, pH 7,0

SOB media: 2 % w/v Tryptone, 0,5 % w/v Yeast Extract, 10 mM NaCl, 2,5 mM KCL, 10 mM $MgSO_4$

SOC media: 2 % w/v Tryptone, 0,5 % w/v Yeast Extract, 10 mM NaCl, 2,5 mM KCL, 10 mM $MgSO_4$, 20 mM glucose, pH 6,8

YENB media: 0,75 % w/v Bacto Yeast Extract, 0,8 % w/v Nutrient Broth, pH 7,5

YT media: 1,6 % w/v Tryptone, 1 % w/v Yeast Extract, 0,5 % NaCl, pH 7,0

LB agar plates & antibiotics: LB media was supplemented with 1,5 % w/v agar, autoclaved and prepared as plates. Heat sensitive antibiotics were added to the solution shortly before pouring the plates. Ampicillin (100 µg/mL, SIGMA) selection was used for the standard cloning. BAC engineering was carried out using the following antibiotics and concentrations (**Table 9**).

Table 9: Antibiotics for cloning, media and plates.

Antibiotic	*Stock solution*	*Concentration liquid media*	*Concentration LB plates*
Chloramphenicol	34 mg/mL	10 µg/mL	15 µg/mL
Tetracycline	5 mg/mL	5 µg/mL)	5 µg/mL
Kanamycin	30 mg/mL	10 µg/mL	15 µg/mL
Ampicillin	100 mg/mL	50 µg/mL	100 µg/mL

6.7.2 PCR reactions

PCR primers and primer pairs were designed as such that the predicted melting temperature (TM) reached ~ 59 °C + 1,5 °C. Primers and primer pairs were checked for secondary structure formation and heterodimer formation using cloning software "Geneious" and the online "oligo analyzer tool" (idtdna.com). Primers were ordered from

SIGMA as desalted, lyophilized oligonucleotides. Primers were reconstituted in EB-buffer according to manufacturers recommendations. Standard PCR reactions were performed using Physion High Fidelity DNA polymerase (Thermo Scientific). The standard PCR reaction was set up as follows (**Table 10**).

Table 10: Standard PCR reaction mix.

Component	*1x [µL]*
H_2O	fill to 25
5x GC buffer	5
DMSO	0,75
DNTP mix	0,5
Primer forward	0,25 (500 nM)
Primer reverse	0,25 (500 nM)
DNA ≤ 250 ng	50 – 100 ng
Phusion	0,2 (0,5U)
Primer reverse	0,25

Nuclease free water was added first to the reaction tube in order to dilute small volume components. Physion DNA Polymerase was added last to the reaction mix. The PCR reaction was performed in a thermocycler (Bio-Rad, S-1000) using the following PCR program (**Table 11**).

Table 11: Standard PCR program.

Step	*Temp [°C]*	*Duration*	*Repeats*
Initial denaturation	98	2 min	1
Denaturation	98	20 sec	
Annealing	TM + 1,5	20 sec	39
Extension	72	30 sec / kb	
Final extension	72	2 min	1
End	4	∞	NA

The number of PCR cycles was decreased for BAC engineering (25 cycles). PCR products were gel purified using a 0,8 % Agarose (SIGMA) gel. Purified DNA products were excised from the gel and extracted using the QIAquick Gel Extraction Kit (Qiagen) according to manufacturer recommendations.

6.7.3 Restriction digest

Restriction digest was carried out using NEB reaction enzymes and corresponding buffers according to manufacturer's recommendations. The appropriate reaction conditions and correct combination of restriction enzymes was planned using the NEBcloner® (nebcloner.neb.com). The standard restriction digest was set up as follows (**Table 12**).

Table 12: Standard Restriction digest.

Component	*Concentration*
DNA	2 - 4 μg
Restriction enzyme buffer	1x
H_2O	fill to 30 μL
Restriction enzyme	5 U

The amount of DNA and reaction volume varied depending on the needs of the cloning experiment. The restriction digest was incubated either for 1 h at 37 °C or overnight in case of BAC engineering. Restriction digest products were gel purified using a 0,8 % Agarose (SIGMA) gel. Purified DNA products were excised from the gel and extracted using the QIAquick Gel Extraction Kit (Qiagen).

6.7.4 Ligation

The Ligation mix was prepared in an 1,5 mL Eppendorf tube where the T4 Ligase was added last. The Ligation (**Table 13**) was mixed and incubated for 15 min at RT and target DNA was transformed as described in **section 5.7.6**.

Table 13: Standard Ligation mix.

Component	*Volume [µL]*
DNA (backbone)	1
DNA (insert)	6
T4 DNA ligase buffer	1
H_2O	8
T4 DNA ligase	0,3

6.7.5 Preparation of chemically competent bacteria

Chemically competent Mach T1® bacteria were generated using the calcium-manganese based (CCMB) method (Hanahan, Jessee, and Bloom 1991). All glassware was filled with deionized water and autoclaved prior to growing cells in order to remove detergent residues. Detergent is the major inhibitor of competent cell growth and transformation efficiency.

One vial of Mach T1® competent bacteria seed stock was thawed (RT), transferred to an Erlenmeyer containing 100 mL of SOB media and incubated overnight (30 °C, shaking). 10 mL of the overnight culture was inoculated in 1 L SOB media and incubated (30 °C, shaking) till the OD600 reached 0,3. Bacteria were spun down (3000 rpm, 10 min, 4 °C) and the supernatant discarded. The bacteria pellet was resuspended in 80 mL of ice cold CCMB80 buffer. Suspension was stored for 20 min on ice, spun down (3000 rpm, 10 min, 4 °C) and the supernatant discarded. The pellet was again resuspended in ice cold CCMB80 till the OD600 matched a value of 1,0 – 1,5. Bacteria were aliquoted in Eppendorf tubes (150 μL reactions) and flash frozen in liquid nitrogen. Bacteria were stored in - 80 °C.

6.7.6 Transformation of chemically competent bacteria

During incubation of the ligation mix, Mach T1® competent bacteria were thawed on ice. 10 μL of the ligation mix was transferred to a fresh Eppendorf tube and chilled on ice for 5 min. 100 μL of competent bacteria were added to the ligation mix. The tube was flicked and incubated for 10 min on ice. Bacteria were transformed by incubation of the reaction mix in a prewarmed ThermoMixer® (Eppendorf) (1 min, 42 °C). Subsequently, bacteria were chilled on ice for 5 min. Bacteria were spun down (8000 rpm, 30 sec), the supernatant was removed, the pellet was resuspended in 50 μL LB media and subsequently plated on LB agar plates containing the respective antibiotic for selection. Transformed bacteria with ligation products > 10 kb, were allowed to recover (60 min, 37 °C, shaking 300 rpm) in 1,5 mL SOC media before plating.

6.7.7 BAC engineering

Fluorescent fate marker cell lines are based on DNA plasmids generated by BAC engineering. Bacterial artificial chromosome containing the respective fate marker for endoderm (Sox17), mesoderm (Vimentin) and neuroectoderm (Tuj1) were identified using PubMed and Ensembl. BACs were ordered from Source Bioscience and served as template to PCR-amplify DNA fragments encoding small homology arms. DNA plasmids were generated following the MXS-chaining technique (Sladitschek and Neveu 2015a). The intermediate construct was set up as such, that the H_2B-Citrine fluorescent reporter and G418 selection cassette was flanked by small homology arms (~ 200 bp – 500 bp). For homology recombination of the respective BAC, bacteria were electroporated as described in **section 5.7.8**. The final plasmid was achieved by retrieving the H_2B-Citrine fluorescent reporter flanked by the respective 5 prime (~ 2 kb) and 3 prime (~ 8 kb) homology arms. High purity plasmid DNA for transfection of embryonic stem cells was purified using the Qiagen Plasmid Plus Midi Kit.

6.7.8 Electroporation of bacteria

Bacteria were electroporated using the Bio-Rad Gene Pulser® electroporation system. Glycerol stock of the respective bacteria was inoculated the day before electroporation and grown overnight in the respective culture media supplemented with the right antibiotics (37 °C, shaking 300 rpm). 80 μL of the overnight culture was inoculated in 2 mL fresh media and incubated for 2 h at 37 °C (shaking 300 rpm). 1 mL of culture was transferred to a precooled reaction tube and spun down (30 sec, 8000 rpm, 4 °C. Supernatant was removed and the pellet resuspended in 1 mL of ice-cold glycerol (10 % (v/v) glycerol in sterile water). Bacteria were spun down (30 sec, 8000 rpm, 4 °C), the supernatant was removed and the bacteria pellet was resuspended in the corresponding ice-cold DNA mix (500 ng restriction digested and gel purified plasmid DNA in a total of 100 μL water). The solution was transferred to a chilled electroporation cuvette (without air bubbles) on ice. Bacteria were electroporated (1,8 kV; 25 μF; 200 Ω) according to manufacturer recommendations. Bacteria were rescued in 1 mL pre-warmed (~ 37 °C) SOC media and transferred to an Eppendorf tube. Bacteria were recovered for 60 min at 37 °C (shaking 300 rpm). After recovery, bacteria were spun down (30 sec,

8000 rpm) and the supernatant was removed. The bacteria pellet was resuspended in 50 μL LB media and plated onto LB Agar plates containing the respective antibiotics. Plates were incubated overnight at 37 °C. The next day a single colony was picked, inoculated in 2 mL media containing the appropriate antibiotics and prepped ~ 6 h after inoculation.

7 ACKNOWLEDGEMENTS

I would like to thank everyone who has supported and helped me in accomplishing this PhD project. In particular:

Dr. Pierre Neveu, for giving me the possibility to conduct the PhD project in his lab, to experience science in an international environment, and foster valuable skills beyond benchwork.

I would like to Thank the TAC members **Jan Ellenberg**, **Michael Knop** and **Alexander Aulehla** for great scientific advice and lively discussions during my TAC meetings. Thanks to Michael and Alexander for grading the thesis and to **Aissam Ikmi** and **Georg Stöcklin** for being members of the defense committee.

Many thanks to my lab buddies **Luigi Russo** and **Amit Mhamane.** I will always sing Italian songs when feeling down. As of now: "Lasciatemi cantare …" always helped, and hopefully will in future, thanks Russo. Amit, my lunch and coffee buddy, would have been great to have you earlier in the lab, for scientific discussion and beyond.

Special thanks to **Jerome Sinniger**, who dedicated countless hours to my project, helping me in generating and differentiating reporter lines which resulted in a great dataset. I appreciate your work, it was a great loss when you left the lab! Beyond bench work, I enjoyed spending leisure time with you! The "Horse's Neck" is now an established drink at home.

Thanks to people of my batch, the institute, and friends outside of EMBL, who detached my brain from science, not only during beer sessions but Christmas market, Schützen and countless other events. Thanks: **Jervis, Ulf, Joran, Ashna, Areeb, Sanjana, Georg, Renato, Bernhard, Sofya, Oeyvind, Rafael, Claudi, Christiene, John, Sarah, Carina, Philipp, Evelyn, Micha** and many names I probably forgot. Sorry for that.

7 ACKNOWLEDGEMENTS

Hey **Andrew**, hey **Xingsong**, I made it! Both of you are probably the toughest scientist I met during my studies. Andrew, I know it's Sunday, but where is everybody . . . ☺. Xingsong, I finally understood your lesson about science not being the pretty girl and that life has more flavors to offer than a chocolate box . . . (in any direction). I will tell you more about when we meet.

Thanks to all the people who sparked my interest for science, supported me in temporarily leaving industry and pointing the right direction. **Dr. Reiner Schiele**, you surely sparked my motivation. Thanks to **Dr. Peter Happersberger, Dr. Kay Vogel** and **Dr. Karoline Bechtold-Peters** for advice on how to leave industry, pursue a PhD and come back to do what I love. The biotech world is small and we will meet again.

Schließlich möchte ich mich bei meiner **Familie** bedanken, meinen **Geschwistern**, **Eltern** und **Großeltern**. Meinen vorherigen Beruf zu verlassen war ein Schritt in die richtige Richtung und ihr habt mich dabei unterstützt. Vielen Dank an meine Eltern die mich stets im Ausland besucht und meine Eindrücke geteilt haben. Vielen Dank an meine Geschwister für einen Rückzugsort, wenn ich ihn brauchte.

Mein Freund **Karsten**. Wir haben es geschafft! Wir sind verrückt genug gewesen unseren Job zu kündigen und jetzt ist der Abschluss endlich erreicht! Es war ein langer Weg und trotzdem ist er jetzt bereits Vergangenheit. Ich freue mich auf die Zukunft, uns fällt sicher nochmal etwas ein.

Das wichtigste zum Schluss, der Dank an meine Frau **Annika**. Für uns war das Studium sicher eine Prüfung in jeder Hinsicht. Uns hat die Zeit in Schweden, den USA und England auf einige Proben gestellt. Du hast zu keiner Zeit an uns gezweifelt und mich in antriebsarmen Momenten wieder angeschoben. Du bist mein Motor und meine Bremse, wenn ich sie brauche. Du hast mir gezeigt was Entschleunigung heißt, was neben vielen anderen Dingen zum Erfolg dieser Thesis geführt hat.

Ich Liebe Dich!

8 BIBLIOGRAPHY

Abranches, Elsa, Evguenia Bekman, and Domingos Henrique. 2013. "Generation and Characterization of a Novel Mouse Embryonic Stem Cell Line with a Dynamic Reporter of Nanog Expression." Edited by Qiang Wu. *PLoS ONE* 8 (3). Public Library of Science: e59928. doi:10.1371/journal.pone.0059928.

Abranches, Elsa, Ana M V Guedes, Martin Moravec, Hedia Maamar, Petr Svoboda, Arjun Raj, and Domingos Henrique. 2014. "Stochastic NANOG Fluctuations Allow Mouse Embryonic Stem Cells to Explore Pluripotency." *Development* 141 (14). Oxford University Press for The Company of Biologists Limited: 2770–79. doi:10.1242/dev.108910.

Alessi, D R, S R James, C P Downes, A B Holmes, P R Gaffney, C B Reese, and P Cohen. 1997. "Characterization of a 3-Phosphoinositide-Dependent Protein Kinase Which Phosphorylates and Activates Protein Kinase Balpha." *Current Biology : CB* 7 (4): 261–69. http://www.ncbi.nlm.nih.gov/pubmed/9094314.

Allison, Thomas F, Andrew J.H. Smith, Konstantinos Anastassiadis, Jackie Sloane-Stanley, Veronica Biga, Dylan Stavish, James Hackland, et al. 2018. "Identification and Single-Cell Functional Characterization of an Endodermally Biased Pluripotent Substate in Human Embryonic Stem Cells." *Stem Cell Reports* 10 (6). ElsevierCompany.: 1895–1907. doi:10.1016/j.stemcr.2018.04.015.

Ameres, Stefan L, Michael D Horwich, Jui Hung Hung, Jia Xu, Megha Ghildiyal, Zhiping Weng, and Phillip D Zamore. 2010. "Target RNA-Directed Trimming and Tailing of Small Silencing RNAs." *Science* 328 (5985). American Association for the Advancement of Science: 1534–39. doi:10.1126/science.1187058.

Ando, Hideaki, Matsumi Hirose, Gen Kurosawa, Soren Impey, and Katsuhiko Mikoshiba. 2017. "Time-Lapse Imaging of MicroRNA Activity Reveals the Kinetics of MicroRNA Activation in Single Living Cells." *Scientific Reports* 7 (1). Springer US: 1–16. doi:10.1038/s41598-017-12879-2.

Athanasiadou, Rodoniki, Dina de Sousa, Kevin Myant, Cara Merusi, Irina Stancheva, and Adrian Bird. 2010. "Targeting of De Novo DNA Methylation throughout the Oct-4 Gene Regulatory Region in Differentiating Embryonic Stem Cells." *PLoS ONE* 5 (4). Public Library of Science: e9937. doi:10.1371/journal.pone.0009937.

Baccarini, Alessia, Hemangini Chauhan, Thomas J. Gardner, Anitha D. Jayaprakash, Ravi Sachidanandam, and Brian D. Brown. 2011. "Kinetic Analysis Reveals the Fate of a MicroRNA Following Target Regulation in Mammalian Cells." *Current Biology* 21 (5): 369–76. doi:10.1016/j.cub.2011.01.067.

Baek, Daehyun, Judit Villén, Chanseok Shin, Fernando D. Camargo, Steven P. Gygi, and David P. Bartel. 2008. "The Impact of MicroRNAs on Protein Output." *Nature* 455 (7209): 64–71. doi:10.1038/nature07242.

Balzano, Francesca, Sara Cruciani, Valentina Basoli, Sara Santaniello, Federica Facchin, Carlo Ventura, and Margherita Maioli. 2018. "MiR200 and MiR302: Two Big Families Influencing Stem Cell Behavior." *Molecules* 23 (2). doi:10.3390/molecules23020282.

Bao, Siqin, Fuchou Tang, Xihe Li, Katsuhiko Hayashi, Astrid Gillich, Kaiqin Lao, and M. Azim Surani. 2009. "Epigenetic Reversion of Post-Implantation Epiblast to Pluripotent Embryonic Stem Cells." *Nature* 461 (7268). Nature Publishing Group: 1292–95. doi:10.1038/nature08534.

Barroso-delJesus, Alicia, C. Romero-Lopez, Gema Lucena-Aguilar, Gustavo J. Melen, Laura Sanchez, Gertrudis Ligero, Alfredo Berzal-Herranz, and Pablo Menendez. 2008. "Embryonic Stem Cell-Specific MiR302-367 Cluster: Human Gene Structure and Functional Characterization of Its Core Promoter." *Molecular and Cellular Biology* 28 (21). American Society for Microbiology Journals: 6609–19. doi:10.1128/mcb.00398-08.

Bartel, David P. 2009. "MicroRNAs: Target Recognition and Regulatory Functions." *Cell* 136 (2): 215–33. doi:10.1016/j.cell.2009.01.002.

Bartel, David P, Rosalind Lee, and Rhonda Feinbaum. 2004. "MicroRNAs : Genomics , Biogenesis , Mechanism , and Function." *Cell* 116: 281–97.

Benetti, Roberta, Susana Gonzalo, Isabel Jaco, Purificación Mũoz, Susana Gonzalez, Stefan Schoeftner, Elizabeth Murchison, et al. 2008. "A Mammalian MicroRNA Cluster Controls DNA Methylation and Telomere Recombination via Rbl2-Dependent Regulation of DNA Methyltransferases." *Nature Structural and Molecular Biology*. Nature Publishing Group. doi:10.1038/nsmb0908-998b.

Berdasco, María, and Manel Esteller. 2011. "DNA Methylation in Stem Cell Renewal and Multipotency." *Stem Cell Research and Therapy*. doi:10.1186/scrt83.

Berge, Derk ten, Dorota Kurek, Tim Blauwkamp, Wouter Koole, Alex Maas, Elif Eroglu, Ronald K. Siu, and Roel Nusse. 2011. "Embryonic Stem Cells Require Wnt Proteins to Prevent Differentiation to Epiblast Stem Cells." *Nature Cell Biology* 13 (9). Nature Publishing Group: 1070–75. doi:10.1038/ncb2314.

Berti, Denise A., and Rony Seger. 2017. "The Nuclear Translocation of ERK." In *Methods in Molecular Biology (Clifton, N.J.)*, 1487:175–94. doi:10.1007/978-1-4939-6424-6_13.

Bessonnard, S., L. De Mot, D. Gonze, M. Barriol, C. Dennis, A. Goldbeter, G. Dupont, and C. Chazaud. 2014. "Gata6, Nanog and Erk Signaling Control Cell Fate in the Inner Cell Mass through a Tristable Regulatory Network." *Development* 141 (19): 3637–48. doi:10.1242/dev.109678.

Bitetti, Angelo, Allison C. Mallory, Elisabetta Golini, Claudia Carrieri, Héctor Carreño Gutiérrez, Emerald Perlas, Yuvia A. Pérez-Rico, et al. 2018. "MicroRNA Degradation by a Conserved Target RNA Regulates Animal Behavior." *Nature Structural and Molecular Biology* 25 (3). Nature Publishing Group: 244–51. doi:10.1038/s41594-018-0032-x.

Boroviak, Thorsten, Remco Loos, Paul Bertone, Austin Smith, and Jennifer Nichols. 2014. "The Ability of Inner-Cell-Mass Cells to Self-Renew as Embryonic Stem Cells Is Acquired Following Epiblast Specification." *Nature Cell Biology* 16 (6): 513–25. doi:10.1038/ncb2965.

Borowiak, Malgorzata, René Maehr, Shuibing Chen, Alice E. Chen, Weiping Tang, Julia L. Fox, Stuart L. Schreiber, and Douglas A. Melton. 2009. "Small Molecules Efficiently Direct Endodermal Differentiation of Mouse and Human Embryonic Stem Cells." *Cell Stem Cell* 4 (4): 348–58. doi:10.1016/j.stem.2009.01.014.

Boyer, Laurie A., Tong Ihn Lee, Megan F. Cole, Sarah E. Johnstone, Stuart S. Levine, Jacob P. Zucker, Matthew G. Guenther, et al. 2005. "Core Transcriptional Regulatory Circuitry in Human Embryonic Stem Cells." *Cell* 122 (6): 947–56. doi:10.1016/j.cell.2005.08.020.

Breda, Jeremie, Andrzej J. Rzepiela, Rafal Gumienny, Erik van Nimwegen, and Mihaela Zavolan. 2015. "Quantifying the Strength of MiRNA–Target Interactions." *Methods* 85: 90–99. doi:10.1016/j.ymeth.2015.12.016.

Brennecke, Julius, Alexander Stark, Robert B Russell, and Stephen M Cohen. 2005. "Principles of MicroRNA–Target Recognition." Edited by James C. Carrington. *PLoS Biology* 3 (3). Public Library of Science: e85. doi:10.1371/journal.pbio.0030085.

Brons, I. Gabrielle M., Lucy E. Smithers, Matthew W.B. B. Trotter, Peter Rugg-Gunn, Bowen Sun, Susana M. Chuva de Sousa Lopes, Sarah K. Howlett, et al. 2007. "Derivation of Pluripotent Epiblast Stem Cells from Mammalian Embryos." *Nature* 448 (7150). Nature Publishing Group: 191–95. doi:10.1038/nature05950.

Broughton, James P., Michael T. Lovci, Jessica L. Huang, Gene W. Yeo, and Amy E. Pasquinelli. 2016. "Pairing beyond the Seed Supports MicroRNA Targeting Specificity." *Molecular Cell* 64 (2). Elsevier Inc.: 320–33. doi:10.1016/j.molcel.2016.09.004.

Brown, Brian D, Bernhard Gentner, Alessio Cantore, Silvia Colleoni, Mario Amendola, Anna Zingale, Alessia Baccarini, Giovanna Lazzari, Cesare Galli, and Luigi Naldini. 2007. "Endogenous MicroRNA Can Be Broadly Exploited to Regulate Transgene Expression According to Tissue, Lineage and Differentiation State." *Nature Biotechnology* 25 (12). Nature Publishing Group: 1457–67. doi:10.1038/nbt1372.

Brown, Brian D, Mary Anna Venneri, Anna Zingale, Lucia Sergi Sergi, and Luigi Naldini. 2006. "Endogenous MicroRNA Regulation Suppresses Transgene Expression in Hematopoietic Lineages and Enables Stable Gene Transfer." *Nature Medicine* 12 (5): 585–91.

doi:10.1038/nm1398.

Burdon, Tom, Austin Smith, and Pierre Savatier. 2002. "Signalling, Cell Cycle and Pluripotency in Embryonic Stem Cells." *Trends in Cell Biology* 12 (9): 432–38. http://www.ncbi.nlm.nih.gov/pubmed/12220864.

Cartwright, P. 2005. "LIF/STAT3 Controls ES Cell Self-Renewal and Pluripotency by a Myc-Dependent Mechanism." *Development* 132 (5): 885–96. doi:10.1242/dev.01670.

Castel, David, Meryem B. Baghdadi, Sébastien Mella, Barbara Gayraud-Morel, Virginie Marty, Jérôme Cavaillé, Christophe Antoniewski, and Shahragim Tajbakhsh. 2018. "Small-RNA Sequencing Identifies Dynamic MicroRNA Deregulation during Skeletal Muscle Lineage Progression." *Scientific Reports* 8 (1): 1–13. doi:10.1038/s41598-018-21991-w.

Chambers, Ian, Douglas Colby, Morag Robertson, Jennifer Nichols, Sonia Lee, Susan Tweedie, and Austin Smith. 2003. "Functional Expression Cloning of Nanog, a Pluripotency Sustaining Factor in Embryonic Stem Cells." *Cell* 113 (5): 643–55. http://www.ncbi.nlm.nih.gov/pubmed/12787505.

Chambers, Ian, Jose Silva, Douglas Colby, Jennifer Nichols, Bianca Nijmeijer, Morag Robertson, Jan Vrana, Ken Jones, Lars Grotewold, and Austin Smith. 2007. "Nanog Safeguards Pluripotency and Mediates Germline Development." *Nature* 450 (7173): 1230–34. doi:10.1038/nature06403.

Chandradoss, Stanley D., Nicole T. Schirle, Malwina Szczepaniak, Ian J. Macrae, and Chirlmin Joo. 2015. "A Dynamic Search Process Underlies MicroRNA Targeting." *Cell* 162 (1). Cell Press: 96–107. doi:10.1016/j.cell.2015.06.032.

Chaulk, Steven G, Gina L. Thede, Oliver A. Kent, Zhizhong Xu, Emily M. Gesner, Richard A. Veldhoen, Suneil K. Khanna, et al. 2011. "Role of Pri-MiRNA Tertiary Structure in MiR-17/92 MiRNA Biogenesis." *RNA Biology* 8 (6). Taylor & Francis: 1105–14. doi:10.4161/rna.8.6.17410.

Chazaud, Claire, and Yojiro Yamanaka. 2016. "Lineage Specification in the Mouse Preimplantation Embryo." *Development* 143 (7). Oxford University Press for The Company of Biologists Limited: 1063–74. doi:10.1242/dev.128314.

Chazaud, Claire, Yojiro Yamanaka, Tony Pawson, and Janet Rossant. 2006. "Early Lineage Segregation between Epiblast and Primitive Endoderm in Mouse Blastocysts through the Grb2-MAPK Pathway." *Developmental Cell* 10 (5): 615–24. doi:10.1016/j.devcel.2006.02.020.

Chen, Jian Fu, Elizabeth M Mandel, J Michael Thomson, Qiulian Wu, Thomas E Callis, Scott M Hammond, Frank L Conlon, and Da Zhi Wang. 2006. "The Role of MicroRNA-1 and MicroRNA-133 in Skeletal Muscle Proliferation and Differentiation." *Nature Genetics* 38 (2): 228–33. doi:10.1038/ng1725.

Chen, Liang, Liisa Heikkinen, K. Emily Knott, Yanchun Liang, and Garry Wong. 2015. "Evolutionary Conservation and Function of the Human Embryonic Stem Cell Specific MiR-302/367 Cluster." *Comparative Biochemistry and Physiology - Part D: Genomics and Proteomics* 16. Elsevier B.V.: 83–98. doi:10.1016/j.cbd.2015.08.002.

Chenoweth, Josh G., Ronald D. G. McKay, and Paul J. Tesar. 2010. "Epiblast Stem Cells Contribute New Insight into Pluripotency and Gastrulation." *Development Growth and Differentiation*. John Wiley & Sons, Ltd (10.1111). doi:10.1111/j.1440-169X.2010.01171.x.

Chew, J.-L., Y.-H. Loh, Wensheng Zhang, Xi Chen, W.-L. Tam, L.-S. Yeap, Pin Li, et al. 2005. "Reciprocal Transcriptional Regulation of Pou5f1 and Sox2 via the Oct4/Sox2 Complex in Embryonic Stem Cells." *Molecular and Cellular Biology* 25 (14). American Society for Microbiology (ASM): 6031–46. doi:10.1128/MCB.25.14.6031-6046.2005.

Chi, Sung Wook, Julie B. Zang, Aldo Mele, and Robert B. Darnell. 2009. "Argonaute HITS-CLIP Decodes MicroRNA-MRNA Interaction Maps." *Nature* 460 (7254). Nature Publishing Group: 479–86. doi:10.1038/nature08170.

Choi, Jiho, Aaron J. Huebner, Kendell Clement, Ryan M. Walsh, Andrej Savol, Kaixuan Lin, Hongcang Gu, et al. 2017. "Prolonged Mek1/2 Suppression Impairs the Developmental Potential of Embryonic Stem Cells." *Nature* 548 (7666). Nature Publishing Group: 219–23. doi:10.1038/nature23274.

Cisse, Ibrahim I, Hajin Kim, and Taekjip Ha. 2012. "A Rule of Seven in Watson-Crick Base-Pairing of Mismatched Sequences." *Nature Structural and Molecular Biology* 19 (6). Nature Publishing Group: 623–27. doi:10.1038/nsmb.2294.

Clément, Thomas, Véronique Salone, and Mathieu Rederstorff. 2015. "Dual Luciferase Gene Reporter Assays to Study MiRNA Function." *Methods in Molecular Biology* 1296. Humana Press, New York, NY: 187–98. doi:10.1007/978-1-4939-2547-6_17.

Cockburn, Katie, and Janet Rossant. 2010. "Making the Blastocyst: Lessons from the Mouse." *Journal of Clinical Investigation* 120 (4): 995–1003. doi:10.1172/JCI41229.

Concepcion, Carla P., Ciro Bonetti, and Andrea Ventura. 2012. "The MicroRNA-17-92 Family of MicroRNA Clusters in Development and Disease." *The Cancer Journal* 18 (3): 262–67. doi:10.1097/PPO.0b013e318258b60a.

Condic, Maureen L. 2014. "Totipotency: What It Is and What It Is Not." *Stem Cells and Development* 23 (8). Mary Ann Liebert, Inc.: 796–812. doi:10.1089/scd.2013.0364.

Cordes, Kimberly R., Neil T. Sheehy, Mark P. White, Emily C. Berry, Sarah U. Morton, Alecia N. Muth, Ting Hein Lee, Joseph M. Miano, Kathryn N. Ivey, and Deepak Srivastava. 2009. "MiR-145 and MiR-143 Regulate Smooth Muscle Cell Fate and Plasticity." *Nature* 460 (7256): 705–10. doi:10.1038/nature08195.

Czechanski, Anne, Candice Byers, Ian Greenstein, Nadine Schrode, Leah Rae Donahue, Anna-Katerina Hadjantonakis, and Laura G Reinholdt. 2014. "Derivation and Characterization of Mouse Embryonic Stem Cells from Permissive and Nonpermissive Strains." *Nature Protocols* 9 (3). Nature Publishing Group: 559–74. doi:10.1038/nprot.2014.030.

De, Nabanita, Lisa Young, Pick Wei Lau, Nicole Claudia Meisner, David V. Morrissey, and Ian J. MacRae. 2013. "Highly Complementary Target RNAs Promote Release of Guide RNAs from Human Argonaute2." *Molecular Cell* 50 (3). Cell Press: 344–55. doi:10.1016/j.molcel.2013.04.001.

Du, Peng, Longfei Wang, Piotr Sliz, and Richard I. Gregory. 2015. "A Biogenesis Step Upstream of Microprocessor Controls MiR-17~92 Expression." *Cell* 162 (4). Cell Press: 885–99. doi:10.1016/j.cell.2015.07.008.

Eldar, Avigdor, and Michael B. Elowitz. 2010. "Functional Roles for Noise in Genetic Circuits." *Nature*. doi:10.1038/nature09326.

Enright, Anton J, Bino John, Ulrike Gaul, Thomas Tuschl, Chris Sander, and Debora S Marks. 2003. "Enright-2003-Genomebiol.Pdf." *Genome Biology*. BioMed Central. doi:10.1186/gb-2003-5-1-r1.

Evans, M. J., and M. H. Kaufman. 1981. "Establishment in Culture of Pluripotential Cells from Mouse Embryos." *Nature* 292 (5819). Nature Publishing Group: 154–56. doi:10.1038/292154a0.

Faddah, Dina A., Haoyi Wang, Albert Wu Cheng, Yarden Katz, Yosef Buganim, and Rudolf Jaenisch. 2013. "Single-Cell Analysis Reveals That Expression of Nanog Is Biallelic and Equally Variable as That of Other Pluripotency Factors in Mouse ESCs." *Cell Stem Cell* 13 (1). Cell Press: 23–29. doi:10.1016/j.stem.2013.04.019.

Festuccia, Nicola, Rodrigo Osorno, Florian Halbritter, Violetta Karwacki-Neisius, Pablo Navarro, Douglas Colby, Frederick Wong, Adam Yates, Simon R. Tomlinson, and Ian Chambers. 2012. "Esrrb Is a Direct Nanog Target Gene That Can Substitute for Nanog Function in Pluripotent Cells." *Cell Stem Cell* 11 (4): 477–90. doi:10.1016/j.stem.2012.08.002.

Fidalgo, Miguel, Francesco Faiola, Carlos Filipe Pereira, Junjun Ding, Arven Saunders, Julian Gingold, Christoph Schaniel, Ihor R Lemischka, José C R Silva, and Jianlong Wang. 2012. "Zfp281 Mediates Nanog Autorepression through Recruitment of the NuRD Complex and Inhibits Somatic Cell Reprogramming." *Proceedings of the National Academy of Sciences of the United States of America* 109 (40). National Academy of Sciences: 16202–7. doi:10.1073/pnas.1208533109.

Fiedler, Stephanie D., Martha Z. Carletti, and Lane K. Christenson. 2010. "Quantitative RT-PCR Methods for Mature MicroRNA Expression Analysis." *Methods in Molecular Biology (Clifton, N.J.)* 630: 49–64. doi:10.1007/978-1-60761-629-0_4.

Filipczyk, Adam, Konstantinos Gkatzis, Jun Fu, Philipp S. Hoppe, Heiko Lickert, Konstantinos Anastassiadis, and Timm Schroeder. 2013. "Biallelic Expression of Nanog Protein in Mouse Embryonic Stem Cells." *Cell Stem Cell* 13 (1). Cell Press: 12–13. doi:10.1016/j.stem.2013.04.025.

Filipowicz, Witold, Suvendra N. Bhattacharyya, and Nahum Sonenberg. 2008. "Mechanisms of Post-Transcriptional Regulation by MicroRNAs: Are the Answers in Sight?" *Nature Reviews Genetics*. Nature Publishing Group. doi:10.1038/nrg2290.

Fu, Shijun, Qi Fei, Hua Jiang, Shannon Chuai, Song Shi, Wen Xiong, Lei Jiang, et al. 2011. "Involvement of Histone Acetylation of Sox17 and Foxa2 Promoters during Mouse Definitive Endoderm Differentiation Revealed by MicroRNA Profiling." Edited by Austin John Cooney. *PLoS ONE* 6 (11): e27965. doi:10.1371/journal.pone.0027965.

Gambardella, Gennaro, Annamaria Carissimo, Amy Chen, Luisa Cutillo, Tomasz J. Nowakowski, Diego di Bernardo, and Robert Blelloch. 2017. "The Impact of MicroRNAs on Transcriptional Heterogeneity and Gene Co-Expression across Single Embryonic Stem Cells." *Nature Communications* 8 (1). Nature Publishing Group: 14126. doi:10.1038/ncomms14126.

Gardner, R. L. 1968. "Mouse Chimaeras Obtained by the Injection of Cells into the Blastocyst." *Nature* 220 (5167). Nature Publishing Group: 596–97. doi:10.1038/220596a0.

Gaztelumendi, Nerea, and Carme Nogués. 2014. "Chromosome Instability in Mouse Embryonic Stem Cells." *Scientific Reports* 4 (June). Nature Publishing Group: 5324. doi:10.1038/srep05324.

Gillich, Astrid, Siqin Bao, Nils Grabole, Katsuhiko Hayashi, Matthew W B Trotter, Vincent Pasque, Erna Magnúsdóttir, and M. Azim Surani. 2012. "Epiblast Stem Cell-Based System Reveals Reprogramming Synergy of Germline Factors." *Cell Stem Cell* 10 (4): 425–39. doi:10.1016/j.stem.2012.01.020.

Graf, Thomas, and Matthias Stadtfeld. 2008. "Heterogeneity of Embryonic and Adult Stem Cells." *Cell Stem Cell* 3 (5). Elsevier Inc.: 480–83. doi:10.1016/j.stem.2008.10.007.

Graf, Urs, Elisa A Casanova, and Paolo Cinelli. 2011. "The Role of the Leukemia Inhibitory Factor (LIF) - Pathway in Derivation and Maintenance of Murine Pluripotent Stem Cells." *Genes*. Multidisciplinary Digital Publishing Institute (MDPI). doi:10.3390/genes2010280.

Grimson, Andrew, Kyle Kai How Farh, Wendy K. Johnston, Philip Garrett-Engele, Lee P. Lim, and David P. Bartel. 2007. "MicroRNA Targeting Specificity in Mammals: Determinants beyond Seed Pairing." *Molecular Cell* 27 (1): 91–105. doi:10.1016/j.molcel.2007.06.017.

Gritti, A, E A Parati, L Cova, P Frolichsthal, R Galli, E Wanke, L Faravelli, et al. 1996. "Multipotential Stem Cells from the Adult Mouse Brain Proliferate and Self-Renew in Response to Basic Fibroblast Growth Factor." *The Journal of Neuroscience : The Official Journal of the Society for Neuroscience* 16 (3): 1091–1100. http://www.ncbi.nlm.nih.gov/pubmed/8558238.

Gu, Kai Li, Qiang Zhang, Ying Yan, Ting Ting Li, Fei Fei Duan, Jing Hao, Xi Wen Wang, et al. 2016. "Pluripotency-Associated MiR-290/302 Family of MicroRNAs Promote the Dismantling of Naive Pluripotency." *Cell Research* 26 (3): 350–66. doi:10.1038/cr.2016.2.

Guo, G., J. Yang, J. Nichols, J. S. Hall, I. Eyres, W. Mansfield, and A. Smith. 2009. "Klf4 Reverts Developmentally Programmed Restriction of Ground State Pluripotency." *Development* 136 (7): 1063–69. doi:10.1242/dev.030957.

Guo, Guoji, Luca Pinello, Xiaoping Han, Shujing Lai, Li Shen, Ta Wei Lin, Keyong Zou, Guo Cheng Yuan, and Stuart H. Orkin. 2016. "Serum-Based Culture Conditions Provoke Gene Expression Variability in Mouse Embryonic Stem Cells as Revealed by Single-Cell Analysis." *Cell Reports* 14 (4): 956–65. doi:10.1016/j.celrep.2015.12.089.

Guo, Huili, Nicholas T. Ingolia, Jonathan S. Weissman, and David P. Bartel. 2010. "Mammalian MicroRNAs Predominantly Act to Decrease Target MRNA Levels." *Nature* 466 (7308): 835–40. doi:10.1038/nature09267.

Hackett, Jamie A., and M. Azim Surani. 2014. "Regulatory Principles of Pluripotency: From the Ground State Up." *Cell Stem Cell* 15 (4): 416–30. doi:10.1016/j.stem.2014.09.015.

Hammond, Scott M. 2015. "An Overview of MicroRNAs." *Advanced Drug Delivery Reviews*. NIH Public Access. doi:10.1016/j.addr.2015.05.001.

Han, Dong Wook, Natalia Tapia, Jin Young Joo, Boris Greber, Marcos J. Araúzo-Bravo, Christof Bernemann, Kinarm Ko, et al. 2010. "Epiblast Stem Cell Subpopulations Represent Mouse Embryos of Distinct Pregastrulation Stages." *Cell* 143 (4). Cell Press: 617–27. doi:10.1016/j.cell.2010.10.015.

Hanahan, D, J Jessee, and F R Bloom. 1991. "Plasmid Transformation of Escherichia Coli and Other Bacteria." *Methods in Enzymology* 204: 63–113. http://www.ncbi.nlm.nih.gov/pubmed/1943786.

Hanna, Jacob, Styliani Markoulaki, Maisam Mitalipova, Albert W. Cheng, John P. Cassady, Judith Staerk, Bryce W. Carey, et al. 2009. "Metastable Pluripotent States in NOD-Mouse-Derived ESCs." *Cell Stem Cell* 4 (6): 513–24. doi:10.1016/j.stem.2009.04.015.

Hassani, Seyedeh Nafiseh, Sharif Moradi, Sara Taleahmad, Thomas Braun, and Hossein Baharvand. 2019. "Transition of Inner Cell Mass to Embryonic Stem Cells: Mechanisms, Facts, and Hypotheses." *Cellular and Molecular Life Sciences*. doi:10.1007/s00018-018-2965-y.

Hassani, Seyedeh Nafiseh, Mehdi Totonchi, Ali Sharifi-Zarchi, Sepideh Mollamohammadi, Mohammad Pakzad, Sharif Moradi, Azam Samadian, et al. 2014. "Inhibition of TGFβ Signaling Promotes Ground State Pluripotency." *Stem Cell Reviews and Reports* 10 (1). Springer US: 16–30. doi:10.1007/s12015-013-9473-0.

Hastreiter, Simon, Stavroula Skylaki, Dirk Loeffler, Andreas Reimann, Oliver Hilsenbeck, Philipp S. Hoppe, Daniel L. Coutu, et al. 2018. "Inductive and Selective Effects of GSK3 and MEK Inhibition on Nanog Heterogeneity in Embryonic Stem Cells." *Stem Cell Reports* 11 (1). Elsevier: 58–69. doi:10.1016/j.stemcr.2018.04.019.

Hattori, Naoko, Yuko Imao, Koichiro Nishino, Naka Hattori, Jun Ohgane, Shintaro Yagi, Satoshi Tanaka, and Kunio Shiota. 2007. "Epigenetic Regulation of Nanog Gene in Embryonic Stem and Trophoblast Stem Cells." *Genes to Cells* 12 (3): 387–96. doi:10.1111/j.1365-2443.2007.01058.x.

Hausser, Jean, Afzal Pasha Syed, Nathalie Selevsek, E. van Nimwegen, Lukasz Jaskiewicz, Ruedi Aebersold, and Mihaela Zavolan. 2014. "Timescales and Bottlenecks in MiRNA-Dependent Gene Regulation." *Molecular Systems Biology* 9 (1). European Molecular Biology Organization: 711–711. doi:10.1038/msb.2013.68.

Hayashi, Katsuhiko, Susana M. Chuva de Sousa Lopes, Fuchou Tang, and M. Azim Surani. 2008. "Dynamic Equilibrium and Heterogeneity of Mouse Pluripotent Stem Cells with Distinct Functional and Epigenetic States." *Cell Stem Cell* 3 (4). Elsevier: 391–401. doi:10.1016/j.stem.2008.07.027.

Hemmings, Brian A, and David F Restuccia. 2012. "PI3K-PKB/Akt Pathway." *Cold Spring Harbor Perspectives in Biology* 4 (9). Cold Spring Harbor Laboratory Press: a011189–a011189. doi:10.1101/cshperspect.a011189.

Hsu, Patrick D, David A Scott, Joshua A Weinstein, F Ann Ran, Silvana Konermann, Vineeta Agarwala, Yinqing Li, et al. 2013. "DNA Targeting Specificity of RNA-Guided Cas9 Nucleases." *Nature Biotechnology* 31 (9). Nature Publishing Group: 827–32. doi:10.1038/nbt.2647.

Hu, Guang. 2018. "Cellular Self-Renewal and Differentiation." *National Institute of Environmental Health Sciences*. https://www.niehs.nih.gov/research/atniehs/labs/escbl/pi/stemcell/index.cfm.

Huang, Yali, Rodrigo Osorno, Anestis Tsakiridis, and Valerie Wilson. 2012. "In Vivo Differentiation Potential of Epiblast Stem Cells Revealed by Chimeric Embryo Formation." *Cell Reports* 2 (6). Cell Press: 1571–78. doi:10.1016/j.celrep.2012.10.022.

Huntzinger, Eric, and Elisa Izaurralde. 2011. "Gene Silencing by MicroRNAs: Contributions of Translational Repression and MRNA Decay." *Nature Reviews Genetics*. Nature Publishing Group. doi:10.1038/nrg2936.

Hupalowska, Anna, Mubeen Goolam, Sarah J.L. Graham, Thierry Voet, Iain C Macaulay, Antonio Scialdone, John C Marioni, Agnieszka Jedrusik, and Magdalena Zernicka-Goetz. 2016. "Heterogeneity in Oct4 and Sox2 Targets Biases Cell Fate in 4-Cell Mouse Embryos." *Cell* 165 (1). Elsevier: 61–74. doi:10.1016/j.cell.2016.01.047.

Hutvagner, Gyorgy, and Martin J. Simard. 2008. "Argonaute Proteins: Key Players in RNA Silencing." *Nature Reviews Molecular Cell Biology*. Nature Publishing Group. doi:10.1038/nrm2321.

Imreh, M. P., K. Gertow, J. Cedervall, C. Unger, K. Holmberg, K. Szöke, L. Csöregh, et al. 2006. "In Vitro Culture Conditions Favoring Selection of Chromosomal Abnormalities in Human ES Cells." *Journal of Cellular Biochemistry* 99 (2): 508–16. doi:10.1002/jcb.20897.

Ishikawa, Daichi, Ulf Diekmann, Jan Fiedler, Annette Just, Thomas Thum, Sigurd Lenzen, and Ortwin Naujok. 2017. "MiRNome Profiling of Purified Endoderm and Mesoderm Differentiated from HESCs Reveals Functions of MiR-483-3p and MiR-1263 for Cell-Fate Decisions." *Stem Cell Reports* 9 (5). ElsevierCompany.: 1588–1603. doi:10.1016/j.stemcr.2017.10.011.

Islam, Saiful, Una Kjällquist, Annalena Moliner, Pawel Zajac, Jian Bing Fan, Peter Lönnerberg, and Sten Linnarsson. 2011. "Characterization of the Single-Cell Transcriptional Landscape by Highly Multiplex RNA-Seq." *Genome Research* 21 (7). Cold Spring Harbor Laboratory Press: 1160–67. doi:10.1101/gr.110882.110.

Ivey, Kathryn N., Alecia Muth, Joshua Arnold, Frank W. King, Ru-Fang Yeh, Jason E. Fish, Edward C. Hsiao, et al. 2008. "MicroRNA Regulation of Cell Lineages in Mouse and Human Embryonic Stem Cells." *Cell Stem Cell* 2 (3): 219–29. doi:10.1016/j.stem.2008.01.016.

Ivey, Kathryn N., and Deepak Srivastava. 2010. "MicroRNAs as Regulators of Differentiation and Cell Fate Decisions." *Cell Stem Cell*. doi:10.1016/j.stem.2010.06.012.

Jaenisch, Rudolf, and Richard Young. 2008. "Stem Cells, the Molecular Circuitry of Pluripotency and Nuclear Reprogramming." *Cell*. doi:10.1016/j.cell.2008.01.015.

Jayme, D. W., D. A. Epstein, and D. R. Conrad. 1988. "Fetal Bovine Serum Alternatives." *Nature*. Nature Publishing Group. doi:10.1038/334547a0.

Jayme, DW, and KE Blackman. 1985. "Culture Media for Propagation of Mammalian Cells, Viruses, and Other Biologicals." *Advances in Biotechnological Processes* 5: 1–30. https://europepmc.org/abstract/med/2417609.

Jeon, Hyojung, Tsuyoshi Waku, Takuya Azami, Le Tran Phuc Khoa, Jun Yanagisawa, Satoru Takahashi, and Masatsugu Ema. 2016. "Comprehensive Identification of Krüppel-like Factor Family Members Contributing to the Self-Renewal of Mouse Embryonic Stem Cells and Cellular Reprogramming." Edited by Johnson Rajasingh. *PLoS ONE* 11 (3): e0150715.

doi:10.1371/journal.pone.0150715.

Ji, Young Lee, Soonhag Kim, Won Hwang Do, Min Jeong Jae, June Key Chung, Chul Lee Myung, and Soo Lee Dong. 2008. "Development of a Dual-Luciferase Reporter System for in Vivo Visualization of MicroRNA Biogenesis and Posttranscriptional Regulation." *Journal of Nuclear Medicine* 49 (2): 285–94. doi:10.2967/jnumed.107.042507.

John, Bino, Anton J Enright, Alexei Aravin, Thomas Tuschl, Chris Sander, and Debora S Marks. 2004. "Human MicroRNA Targets." Edited by James C. Carrington. *PLoS Biology* 2 (11). Public Library of Science: e363. doi:10.1371/journal.pbio.0020363.

Juan, Aster H., Roshan M. Kumar, Joseph G. Marx, Richard A. Young, and Vittorio Sartorelli. 2009. "Mir-214-Dependent Regulation of the Polycomb Protein Ezh2 in Skeletal Muscle and Embryonic Stem Cells." *Molecular Cell* 36 (1): 61–74. doi:10.1016/j.molcel.2009.08.008.

Kalkan, Tüzer, Nelly Olova, Mila Roode, Carla Mulas, Heather J. Lee, Isabelle Nett, Hendrik Marks, et al. 2017. "Tracking the Embryonic Stem Cell Transition from Ground State Pluripotency." *Development* 144 (7): 1221–34. doi:10.1242/dev.142711.

Kalkan, Tüzer, and Austin Smith. 2014. "Mapping the Route from Naive Pluripotency to Lineage Specification." *Philosophical Transactions of the Royal Society B: Biological Sciences* 369 (1657). The Royal Society: 20130540–20130540. doi:10.1098/rstb.2013.0540.

Kanellopoulou, Chryssa, Stefan A. Muljo, Andrew L. Kung, Shridar Ganesan, Ronny Drapkin, Thomas Jenuwein, David M. Livingston, and Klaus Rajewsky. 2005. "Dicer-Deficient Mouse Embryonic Stem Cells Are Defective in Differentiation and Centromeric Silencing." *Genes and Development* 19 (4): 489–501. doi:10.1101/gad.1248505.

Karunatilaka, Krishanthi S., Amanda Solem, Anna Marie Pyle, and David Rueda. 2010. "Single-Molecule Analysis of Mss116-Mediated Group II Intron Folding." *Nature* 467 (7318). Nature Publishing Group: 935–39. doi:10.1038/nature09422.

Keller, G M. 1995. "In Vitro Differentiation of Embryonic Stem Cells." *Current Opinion in Cell Biology* 7 (6): 862–69. http://www.ncbi.nlm.nih.gov/pubmed/8608017.

Ketting, R. F., S E.J. Fischer, E Bernstein, T Sijen, G J Hannon, and R H.A. Plasterk. 2001. "Dicer Functions in RNA Interference and in Synthesis of Small RNA Involved in Developmental Timing in C. Elegans." *Genes and Development* 15 (20): 2654–59. doi:10.1101/gad.927801.

Kim, Sung Kyu, Jin Wu Nam, Je Keun Rhee, Wha Jin Lee, and Byoung Tak Zhang. 2006. "MiTarget: MicroRNA Target Gene Prediction Using a Support Vector Machine." *BMC Bioinformatics* 7. BioMed Central: 411. doi:10.1186/1471-2105-7-411.

Kim, V. Narry, Jinju Han, and Mikiko C. Siomi. 2009. "Biogenesis of Small RNAs in Animals." *Nature Reviews Molecular Cell Biology* 10 (2). Nature Publishing Group: 126–39. doi:10.1038/nrm2632.

Kim, V. Narry, and Jin Wu Nam. 2006. “Genomics of MicroRNA.” *Trends in Genetics*. doi:10.1016/j.tig.2006.01.003.

Klein, Misha, Stanley D. Chandradoss, Martin Depken, and Chirlmin Joo. 2017. “Why Argonaute Is Needed to Make MicroRNA Target Search Fast and Reliable.” *Seminars in Cell & Developmental Biology* 65 (May). Elsevier Ltd: 20–28. doi:10.1016/j.semcdb.2016.05.017.

Kobayashi, Taeko, Hiroaki Mizuno, Itaru Imayoshi, Chikara Furusawa, Katsuhiko Shirahige, and Ryoichiro Kageyama. 2009. “The Cyclic Gene Hes1 Contributes to Diverse Differentiation Responses of Embryonic Stem Cells.” *Genes and Development* 23 (16). Cold Spring Harbor Laboratory Press: 1870–75. doi:10.1101/gad.1823109.

Kojima, Yoji, Keren Kaufman-Francis, Joshua B. Studdert, Kirsten A. Steiner, Melinda D. Power, David A.F. Loebel, Vanessa Jones, et al. 2014. “The Transcriptional and Functional Properties of Mouse Epiblast Stem Cells Resemble the Anterior Primitive Streak.” *Cell Stem Cell* 14 (1). Cell Press: 107–20. doi:10.1016/j.stem.2013.09.014.

Kong, William, Jian Jun Zhao, H. E. Lili, and Jin Q. Cheng. 2009. “Strategies for Profiling MicroRNA Expression.” *Journal of Cellular Physiology*. John Wiley & Sons, Ltd. doi:10.1002/jcp.21577.

Krichevsky, Anna M., Kai-C. Sonntag, Ole Isacson, and Kenneth S. Kosik. 2006. “Specific MicroRNAs Modulate Embryonic Stem Cell-Derived Neurogenesis.” *STEM CELLS* 24 (4): 857–64. doi:10.1634/stemcells.2005-0441.

Krol, Jacek, Inga Loedige, and Witold Filipowicz. 2010. “The Widespread Regulation of MicroRNA Biogenesis, Function and Decay.” *Nature Reviews Genetics*. doi:10.1038/nrg2843.

Kumar, Roshan M., Patrick Cahan, Alex K. Shalek, Rahul Satija, Ajay Daley Keyser, Hu Li, Jin Zhang, et al. 2014. “Deconstructing Transcriptional Heterogeneity in Pluripotent Stem Cells.” *Nature* 516 (729): 56–61. doi:10.1038/nature13920.

Kumarswamy, Regalla, Ingo Volkmann, and Thomas Thum. 2011. “Regulation and Function of MiRNA-21 in Health and Disease.” *RNA Biology* 8 (5): 706–13. doi:10.4161/rna.8.5.16154.

Labialle, Stéphane, Virginie Marty, M.-L. Bortolin-Cavaille, M. Hoareau-Osman, J.-P. Pradere, Philippe Valet, P. G. Martin, and J. Cavaille. 2014. “The MiR-379/MiR-410 Cluster at the Imprinted Dlk1-Dio3 Domain Controls Neonatal Metabolic Adaptation.” *The EMBO Journal* 33 (19): 2216–30. doi:10.15252/embj.201387038.

Ladewig, Julia, Philipp Koch, and Oliver Brüstle. 2013. “Leveling Waddington: The Emergence of Direct Programming and the Loss of Cell Fate Hierarchies.” *Nature Reviews. Molecular Cell Biology* 14 (4): 225–36. http://www.ncbi.nlm.nih.gov/pubmed/23847783.

Lagos-Quintana, Mariana, Reinhard Rauhut, Jutta Meyer, Arndt Borkhardt, and Thomas Tuschl. 2003. "New MicroRNAs from Mouse and Human." *RNA* 9 (2): 175–79. doi:10.1261/rna.2146903.

Lai, Eric C. 2003. "MicroRNAs: Runts of the Genome Assert Themselves." *Current Biology*. Cell Press. doi:10.1016/j.cub.2003.11.017.

Lall, Sabbi, Dominic Grün, Azra Krek, Kevin Chen, Yi Lu Wang, Colin N. Dewey, Pranidhi Sood, et al. 2006. "A Genome-Wide Map of Conserved MicroRNA Targets in C. Elegans." *Current Biology* 16 (5). Cell Press: 460–71. doi:10.1016/j.cub.2006.01.050.

Lanza, Robert, and Anthony Atala. 2014. *Essentials of Stem Cell Biology*. *Essentials of Stem Cell Biology: Third Edition*. Elsevier. doi:10.1016/C2012-0-06957-8.

Leitch, Harry G, Kirsten R. Mcewen, Aleksandra Turp, Vesela Encheva, Tom Carroll, Nils Grabole, William Mansfield, et al. 2013. "Naive Pluripotency Is Associated with Global DNA Hypomethylation." *Nature Structural and Molecular Biology* 20 (3). Europe PMC Funders: 311–16. doi:10.1038/nsmb.2510.

Lewis, Benjamin P., Christopher B. Burge, and David P. Bartel. 2005. "Conserved Seed Pairing, Often Flanked by Adenosines, Indicates That Thousands of Human Genes Are MicroRNA Targets." *Cell* 120 (1): 15–20. doi:10.1016/j.cell.2004.12.035.

Lewis, Benjamin P., I-hung Shih, Matthew W. Jones-Rhoades, David P. Bartel, and Christopher B. Burge. 2003. "Prediction of Mammalian MicroRNA Targets." *Cell* 115 (7). Cell Press: 787–98. doi:10.1016/S0092-8674(03)01018-3.

Li, Lu, Kai Kei Miu, Shen Gu, Hoi Hung Cheung, and Wai Yee Chan. 2018. "Comparison of Multi-Lineage Differentiation of HiPSCs Reveals Novel MiRNAs That Regulate Lineage Specification." *Scientific Reports* 8 (1): 1–15. doi:10.1038/s41598-018-27719-0.

Lichner, Zsuzsanna, Emodouble Acuteke Páll, Andrea Kerekes, Éva Pállinger, Pouneh Maraghechi, Zsuzsanna Bodouble acutesze, and Elen Gócza. 2011. "The MiR-290-295 Cluster Promotes Pluripotency Maintenance by Regulating Cell Cycle Phase Distribution in Mouse Embryonic Stem Cells." *Differentiation* 81 (1). Elsevier: 11–24. doi:10.1016/j.diff.2010.08.002.

Liu, Chang, Guangdun Peng, and Naihe Jing. 2018. "TGF-β Signaling Pathway in Early Mouse Development and Embryonic Stem Cells." *Acta Biochimica et Biophysica Sinica*. Narnia. doi:10.1093/abbs/gmx120.

Liu, Chang, Ran Wang, Zhisong He, Pierre Osteil, Emilie Wilkie, Xianfa Yang, Jun Chen, et al. 2018. "Suppressing Nodal Signaling Activity Predisposes Ectodermal Differentiation of Epiblast Stem Cells." *Stem Cell Reports* 11 (1). Cell Press: 43–57. doi:10.1016/j.stemcr.2018.05.019.

Liu, Jidong, Michelle A Carmell, Fabiola V Rivas, Carolyn G Marsden, J Michael Thomson, Ji Joon Song, Scott M Hammond, Leemor Joshua-Tor, and Gregory J Hannon. 2004. "Argonaute2 Is the Catalytic Engine of Mammalian RNAi." *Science* 305 (5689). American Association for the Advancement of Science: 1437–41. doi:10.1126/science.1102513.

Loh, Yuin-Han Han, Qiang Wu, Joon-Lin Lin Chew, Vinsensius B Vega, Weiwei Zhang, Xi Chen, Guillaume Bourque, et al. 2006. "The Oct4 and Nanog Transcription Network Regulates Pluripotency in Mouse Embryonic Stem Cells." *Nature Genetics* 38 (4): 431–40. doi:10.1038/ng1760.

Los Angeles, Alejandro De, Francesco Ferrari, Ruibin Xi, Yuko Fujiwara, Nissim Benvenisty, Hongkui Deng, Konrad Hochedlinger, et al. 2015. "Hallmarks of Pluripotency." *Nature* 525 (7570). Nature Publishing Group: 469–78. doi:10.1038/nature15515.

Lu, Yun, J. Michael Thomson, Ho Yuen Frank Wong, Scott M. Hammond, and Brigid L.M. Hogan. 2007. "Transgenic Over-Expression of the MicroRNA MiR-17-92 Cluster Promotes Proliferation and Inhibits Differentiation of Lung Epithelial Progenitor Cells." *Developmental Biology* 310 (2). Academic Press: 442–53. doi:10.1016/j.ydbio.2007.08.007.

Lund, Elsebet, Stephan Güttinger, Angelo Calado, James E Dahlberg, and Ulrike Kutay. 2004. "Nuclear Export of MicroRNA Precursors." *Science* 303 (5654): 95–98. doi:10.1126/science.1090599.

MacArthur, Ben D., and Ihor R Lemischka. 2013. "Statistical Mechanics of Pluripotency." *Cell*. Elsevier. doi:10.1016/j.cell.2013.07.024.

Macarthur, Ben D., Ana Sevilla, Michel Lenz, Franz Josef Müller, Berhard M. Schuldt, Andreas A. Schuppert, Sonya J. Ridden, et al. 2012. "Nanog-Dependent Feedback Loops Regulate Murine Embryonic Stem Cell Heterogeneity." *Nature Cell Biology* 14 (11). Nature Publishing Group: 1139–47. doi:10.1038/ncb2603.

MacDonald, Bryan T, Keiko Tamai, and Xi He. 2009. "Wnt/β-Catenin Signaling: Components, Mechanisms, and Diseases." *Developmental Cell* 17 (1). NIH Public Access: 9–26. doi:10.1016/j.devcel.2009.06.016.

Marson, Alexander, Stuart S. Levine, Megan F. Cole, Garrett M. Frampton, Tobias Brambrink, Sarah Johnstone, Matthew G. Guenther, et al. 2008. "Connecting MicroRNA Genes to the Core Transcriptional Regulatory Circuitry of Embryonic Stem Cells." *Cell* 134 (3). Cell Press: 521–33. doi:10.1016/j.cell.2008.07.020.

Martin, G R, Teng-Guo Li, Jing Hao, Jie Hu, Jing Wang, Holly Simmons, Shigeto Miura, Yuji Mishina, and Guang-Quan Zhao. 1981. "Isolation of a Pluripotent Cell Line from Early Mouse Embryos Cultured in Medium Conditioned by Teratocarcinoma Stem Cells." *Proceedings of the National Academy of Sciences* 78 (12). National Academy of Sciences:

7634–38. doi:10.1073/pnas.78.12.7634.

Martinez Arias, Alfonso, and Joshua M Brickman. 2011. "Gene Expression Heterogeneities in Embryonic Stem Cell Populations: Origin and Function." *Current Opinion in Cell Biology*. Elsevier Current Trends. doi:10.1016/j.ceb.2011.09.007.

Massagué, J. 1998. "TGF-β SIGNAL TRANSDUCTION." *Annual Review of Biochemistry* 67 (1). Annual Reviews 4139 El Camino Way, P.O. Box 10139, Palo Alto, CA 94303-0139, USA: 753–91. doi:10.1146/annurev.biochem.67.1.753.

Meister, Gunter. 2013. "Argonaute Proteins: Functional Insights and Emerging Roles." *Nature Reviews Genetics*. Nature Publishing Group. doi:10.1038/nrg3462.

Melton, Collin, Robert L Judson, and Robert Blelloch. 2010. "Opposing MicroRNA Families Regulate Self-Renewal in Mouse Embryonic Stem Cells." *Nature* 463 (7281). Nature Publishing Group: 621–26. doi:10.1038/nature08725.

Messmer, Tobias, Ferdinand von Meyenn, Aurora Savino, Fátima Santos, Hisham Mohammed, Aaron Tin Long Lun, John C. Marioni, and Wolf Reik. 2019. "Transcriptional Heterogeneity in Naive and Primed Human Pluripotent Stem Cells at Single-Cell Resolution." *Cell Reports*, January 22. doi:10.1016/j.celrep.2018.12.099.

Michaels, Yale S., Mike B. Barnkob, Hector Barbosa, Toni A. Baeumler, Mary K. Thompson, Violaine Andre, Huw Colin-York, et al. 2019. "Precise Tuning of Gene Expression Levels in Mammalian Cells." *Nature Communications* 10 (1). Nature Publishing Group: 2622. doi:10.1038/s41467-019-10615-0.

Miguel, Maria P. de, Sherezade Fuentes-Julián, and Yago Alcaina. 2010. "Pluripotent Stem Cells: Origin, Maintenance and Induction." *Stem Cell Reviews and Reports*. doi:10.1007/s12015-010-9170-1.

Mitsui, Kaoru, Yoshimi Tokuzawa, Hiroaki Itoh, Kohichi Segawa, Mirei Murakami, Kazutoshi Takahashi, Masayoshi Maruyama, Mitsuyo Maeda, and Shinya Yamanaka. 2003. "The Homeoprotein Nanog Is Required for Maintenance of Pluripotency in Mouse Epiblast and ES Cells." *Cell* 113 (5): 631–42. http://www.ncbi.nlm.nih.gov/pubmed/12787504.

Miyanari, Yusuke, and Maria-Elena Elena Torres-Padilla. 2012. "Control of Ground-State Pluripotency by Allelic Regulation of Nanog." *Nature* 483 (7390). Nature Publishing Group: 470–73. doi:10.1038/nature10807.

Mogilyansky, E, and I Rigoutsos. 2013. "The MiR-17/92 Cluster: A Comprehensive Update on Its Genomics, Genetics, Functions and Increasingly Important and Numerous Roles in Health and Disease." *Cell Death and Differentiation*. Nature Publishing Group. doi:10.1038/cdd.2013.125.

Mukherji, Shankar, Margaret S Ebert, Grace X.Y. Zheng, John S Tsang, Phillip A Sharp, and Alexander Van Oudenaarden. 2011. "MicroRNAs Can Generate Thresholds in Target Gene Expression." *Nature Genetics* 43 (9). Nature Publishing Group: 854–59. doi:10.1038/ng.905.

Mullokandov, Gavriel, Alessia Baccarini, Albert Ruzo, Anitha D Jayaprakash, Navpreet Tung, Benjamin Israelow, Matthew J Evans, Ravi Sachidanandam, and Brian D Brown. 2012. "High-Throughput Assessment of MicroRNA Activity and Function Using MicroRNA Sensor and Decoy Libraries." *Nature Methods* 9 (8): 840–46. doi:10.1038/nmeth.2078.

Murayama, Hideyuki, Hideki Masaki, Hideyuki Sato, Tomonari Hayama, Tomoyuki Yamaguchi, and Hiromitsu Nakauchi. 2015. "Successful Reprogramming of Epiblast Stem Cells by Blocking Nuclear Localization of β-Catenin." *Stem Cell Reports* 4 (1): 103–13. doi:10.1016/j.stemcr.2014.12.003.

Nair, Gautham, Elsa Abranches, Ana M.V. Guedes, Domingos Henrique, and Arjun Raj. 2015. "Heterogeneous Lineage Marker Expression in Naive Embryonic Stem Cells Is Mostly Due to Spontaneous Differentiation." *Scientific Reports* 5 (1). Nature Publishing Group: 13339. doi:10.1038/srep13339.

Najm, Fadi J., Josh G. Chenoweth, Philip D. Anderson, Joseph H. Nadeau, Raymond W. Redline, Ronald D.G. McKay, and Paul J. Tesar. 2011. "Isolation of Epiblast Stem Cells from Preimplantation Mouse Embryos." *Cell Stem Cell* 8 (3). NIH Public Access: 318–25. doi:10.1016/j.stem.2011.01.016.

Nakanishi, Momo, Koji Hayakawa, Kunio Shiota, and Satoshi Tanaka. 2010. "Establishment of Cell Lineage-Specific DNA Methylation Profile Follows the Morphological Differentiation of Trophoblast and Embryonic Cell Lineages." *Biology of Reproduction* 83 (Suppl_1). Narnia: 32–32. doi:10.1093/biolreprod/83.s1.32.

Navarro, Pablo. 2018. "2i, or Not 2i: The Soliloquy of Nanog-Negative Mouse Embryonic Stem Cells." *Stem Cell Reports*. Cell Press. doi:10.1016/j.stemcr.2018.06.017.

Niakan, K. K., J. Han, R. a. Pedersen, C. Simon, and R. a. R. Pera. 2012. "Human Pre-Implantation Embryo Development." *Development* 139 (5): 829–41. doi:10.1242/dev.060426.

Nichols, J, D Davidson, T Taga, K Yoshida, I Chambers, and A Smith. 1996. "Complementary Tissue-Specific Expression of LIF and LIF-Receptor MRNAs in Early Mouse Embryogenesis." *Mechanisms of Development* 57 (2): 123–31. http://www.ncbi.nlm.nih.gov/pubmed/8843390.

Nichols, J, B Zevnik, K Anastassiadis, H Niwa, D Klewe-Nebenius, I Chambers, H Schöler, and A Smith. 1998. "Formation of Pluripotent Stem Cells in the Mammalian Embryo Depends on the POU Transcription Factor Oct4." *Cell* 95 (3): 379–91.

http://www.ncbi.nlm.nih.gov/pubmed/9814708.

Nichols, Jennifer, and Austin Smith. 2009. "Naive and Primed Pluripotent States." *Cell Stem Cell* 4 (6). Elsevier Inc.: 487–92. doi:10.1016/j.stem.2009.05.015.

———. 2012. "Pluripotency in the Embryo and in Culture." *Cold Spring Harbor Perspectives in Biology* 4 (8): a008128–a008128. doi:10.1101/cshperspect.a008128.

Niwa, Hitoshi, Jun-ichi Ichi Miyazaki, and Austin G Smith. 2000. "Quantitative Expression of OCT3 / 4 Defines Differentiation , Dedifferentiation or Self-Renewal of ES Cells." *Nature Genetics* 24 (4): 372–76. doi:10.1038/74199.

Niwa, Hitoshi, Kazuya Ogawa, Daisuke Shimosato, and Kenjiro Adachi. 2009. "A Parallel Circuit of LIF Signalling Pathways Maintains Pluripotency of Mouse ES Cells." *Nature* 460 (7251). Nature Publishing Group: 118–22. doi:10.1038/nature08113.

Nonne, Nora, Maya Ameyar-Zazoua, Mouloud Souidi, and Annick Harel-Bellan. 2009. "Tandem Affinity Purification of MiRNA Target MRNAs (TAP-Tar)." *Nucleic Acids Research* 38 (4). Narnia: e20–e20. doi:10.1093/nar/gkp1100.

Nusse, Roel. 2008. "Wnt Signaling and Stem Cell Control." *Cell Research* 18 (5). Nature Publishing Group: 523–27. doi:10.1038/cr.2008.47.

Ochiai, Hiroshi, Takeshi Sugawara, Tetsushi Sakuma, and Takashi Yamamoto. 2014. "Stochastic Promoter Activation Affects Nanog Expression Variability in Mouse Embryonic Stem Cells." *Scientific Reports* 4 (1). Nature Publishing Group: 7125. doi:10.1038/srep07125.

Ogawa, Kazuya, Ryuichi Nishinakamura, Yuko Iwamatsu, Daisuke Shimosato, and Hitoshi Niwa. 2006. "Synergistic Action of Wnt and LIF in Maintaining Pluripotency of Mouse ES Cells." *Biochemical and Biophysical Research Communications* 343 (1): 159–66. doi:10.1016/j.bbrc.2006.02.127.

Ohnishi, Yusuke, Wolfgang Huber, Akiko Tsumura, Minjung Kang, Panagiotis Xenopoulos, Kazuki Kurimoto, Andrzej K. Oleå, et al. 2014. "Cell-to-Cell Expression Variability Followed by Signal Reinforcement Progressively Segregates Early Mouse Lineages." *Nature Cell Biology* 16 (1). Nature Publishing Group: 27–37. doi:10.1038/ncb2881.

Oliveira, Pedro H., Cláudia Lobato Da Silva, and Joaquim M.S. Cabral. 2014. "Concise Review: Genomic Instability in Human Stem Cells: Current Status and Future Challenges." *Stem Cells* 32 (11). John Wiley & Sons, Ltd: 2824–32. doi:10.1002/stem.1796.

Ong, Sang Ging, Won Hee Lee, Kazuki Kodo, and Joseph C. Wu. 2015. "MicroRNA-Mediated Regulation of Differentiation and Trans-Differentiation in Stem Cells." *Advanced Drug Delivery Reviews* 88: 3–15. doi:10.1016/j.addr.2015.04.004.

Onishi, Kento, and Peter W Zandstra. 2015. "LIF Signaling in Stem Cells and Development." *Development* 142 (13). Oxford University Press for The Company of Biologists Limited: 2230–36. doi:10.1242/dev.117598.

Ørom, Ulf Andersson, and Anders H. Lund. 2007. "Isolation of MicroRNA Targets Using Biotinylated Synthetic MicroRNAs." *Methods* 43 (2): 162–65. doi:10.1016/j.ymeth.2007.04.007.

Paling, Nicholas R. D., Helen Wheadon, Heather K. Bone, and Melanie J. Welham. 2004. "Regulation of Embryonic Stem Cell Self-Renewal by Phosphoinositide 3-Kinase-Dependent Signaling." *Journal of Biological Chemistry* 279 (46): 48063–70. doi:10.1074/jbc.M406467200.

Parker, James S., Eneida A. Parizotto, Muhan Wang, S. Mark Roe, and David Barford. 2009. "Enhancement of the Seed-Target Recognition Step in RNA Silencing by a PIWI/MID Domain Protein." *Molecular Cell* 33 (2): 204–14. doi:10.1016/j.molcel.2008.12.012.

Pauklin, Siim, and Ludovic Vallier. 2015. "Activin/Nodal Signalling in Stem Cells." *Development* 142 (4). Oxford University Press for The Company of Biologists Limited: 607–19. doi:10.1242/dev.091769.

Pratt, Ashley J, and Ian J MacRae. 2009. "The RNA-Induced Silencing Complex: A Versatile Gene-Silencing Machine." *Journal of Biological Chemistry*. American Society for Biochemistry and Molecular Biology. doi:10.1074/jbc.R900012200.

Qi, Xiaoxia, T.-G. Teng-Guo T.-G. Li, Jing Hao, Jie Hu, Jing Wang, Holly Simmons, Shigeto Miura, Yuji Mishina, and G.-Q. Guang-Quan Zhao. 2004. "BMP4 Supports Self-Renewal of Embryonic Stem Cells by Inhibiting Mitogen-Activated Protein Kinase Pathways." *Proceedings of the National Academy of Sciences* 101 (16). National Academy of Sciences: 6027–32. doi:10.1073/pnas.0401367101.

Raj, Arjun, and Alexander van Oudenaarden. 2008. "Nature, Nurture, or Chance: Stochastic Gene Expression and Its Consequences." *Cell*. Cell Press. doi:10.1016/j.cell.2008.09.050.

Rocha, Simao Teixeira da, Carol A. Edwards, Mitsuteru Ito, Tsutomu Ogata, and Anne C. Ferguson-Smith. 2008. "Genomic Imprinting at the Mammalian Dlk1-Dio3 Domain." *Trends in Genetics*. doi:10.1016/j.tig.2008.03.011.

Rüegger, Stefan, and Helge Großhans. 2012. "MicroRNA Turnover: When, How, and Why." *Trends in Biochemical Sciences*. Elsevier. doi:10.1016/j.tibs.2012.07.002.

Saitou, M., S. Kagiwada, and K. Kurimoto. 2012. "Epigenetic Reprogramming in Mouse Pre-Implantation Development and Primordial Germ Cells." *Development* 139 (1): 15–31. doi:10.1242/dev.050849.

Salmena, Leonardo, Laura Poliseno, Yvonne Tay, Lev Kats, and Pier Paolo Pandolfi. 2011. "A CeRNA Hypothesis: The Rosetta Stone of a Hidden RNA Language?" *Cell*. Elsevier. doi:10.1016/j.cell.2011.07.014.

Salomon, William E E., Samson M M. Jolly, Melissa J J. Moore, Phillip D D. Zamore, and Victor Serebrov. 2016. "Single-Molecule Imaging Reveals That Argonaute Reshapes the Binding Properties of Its Nucleic Acid Guides." *Cell* 166 (2). Elsevier: 517–20. doi:10.1016/j.cell.2016.06.048.

Schirle, Nicole T, Jessica Sheu-Gruttadauria, and Ian J. MacRae. 2014. "Structural Basis for MicroRNA Targeting." *Science* 346 (6209): 608–13. doi:10.1126/science.1258040.

Sekar, Durairaj, Subramanian Saravanan, Kulandaivelu Karikalan, Krishnaraj Thirugnanasambantham, Perumal Lalitha, and Villianur I H Islam. 2015. "Role of MicroRNA 21 in Mesenchymal Stem Cell (MSC) Differentiation: A Powerful Biomarker in MSCs Derived Cells." *Current Pharmaceutical Biotechnology* 16 (1): 43–48. http://www.ncbi.nlm.nih.gov/pubmed/25564252.

Sethupathy, Praveen, Molly Megraw, and Artemis G Hatzigeorgiou. 2006. "A Guide through Present Computational Approaches for the Identification of Mammalian MicroRNA Targets." *Nature Methods* 3 (11). Nature Publishing Group: 881–86. doi:10.1038/nmeth954.

Sevignani, Cinzia, George A Calin, Linda D Siracusa, and Carlo M Croce. 2006. "Mammalian MicroRNAs: A Small World for Fine-Tuning Gene Expression." *Mammalian Genome*. Springer. doi:10.1007/s00335-005-0066-3.

Silva, Jose, Jennifer Nichols, Thorold W. Theunissen, Ge Guo, Anouk L. van Oosten, Ornella Barrandon, Jason Wray, Shinya Yamanaka, Ian Chambers, and Austin Smith. 2009. "Nanog Is the Gateway to the Pluripotent Ground State." *Cell* 138 (4): 722–37. doi:10.1016/j.cell.2009.07.039.

Sim, Ye Ji, Min Seong Kim, Abeer Nayfeh, Ye Jin Yun, Su Jin Kim, Kyung Tae Park, Chang Hoon Kim, and Kye Seong Kim. 2017. "2i Maintains a Naive Ground State in ESCs through Two Distinct Epigenetic Mechanisms." *Stem Cell Reports* 8 (5). Elsevier: 1312–28. doi:10.1016/j.stemcr.2017.04.001.

Singer, Zakary S. S., John Yong, Julia Tischler, Jamie A. A. Hackett, Alphan Altinok, M. Azim Azim Surani, Long Cai, and Michael B. B. Elowitz. 2014. "Dynamic Heterogeneity and DNA Methylation in Embryonic Stem Cells." *Molecular Cell* 55 (2). Elsevier Inc.: 319–31. doi:10.1016/j.molcel.2014.06.029.

Singh, Amar M., Matthew Bechard, Keriayn Smith, and Stephen Dalton. 2012. "Reconciling the Different Roles of Gsk3β in 'Naïve' and 'Primed' Pluripotent Stem Cells." *Cell Cycle* 11 (16): 2991–96. doi:10.4161/cc.21110.

Singh, Amar M., James Chappell, Robert Trost, Li Lin, Tao Wang, Jie Tang, Hao Wu, Shaying Zhao, Peng Jin, and Stephen Dalton. 2013. "Cell-Cycle Control of Developmentally Regulated Transcription Factors Accounts for Heterogeneity in Human Pluripotent Cells." *Stem Cell Reports* 1 (6). Cell Press: 532–44. doi:10.1016/j.stemcr.2013.10.009.

Singh, Amar M., Takashi Hamazaki, Katherine E. Hankowski, and Naohiro Terada. 2007. "A Heterogeneous Expression Pattern for Nanog in Embryonic Stem Cells." *Stem Cells* 25 (10): 2534–42. doi:10.1634/stemcells.2007-0126.

Sinkkonen, Lasse, Tabea Hugenschmidt, Philipp Berninger, Dimos Gaidatzis, Fabio Mohn, Caroline G Artus-Revel, Mihaela Zavolan, Petr Svoboda, and Witold Filipowicz. 2008. "MicroRNAs Control de Novo DNA Methylation through Regulation of Transcriptional Repressors in Mouse Embryonic Stem Cells." *Nature Structural and Molecular Biology* 15 (3). Nature Publishing Group: 259–67. doi:10.1038/nsmb.1391.

Sladitschek, Hanna L., and Pierre A. Neveu. 2015a. "MXS-Chaining: A Highly Efficient Cloning Platform for Imaging and Flow Cytometry Approaches in Mammalian Systems." *PLoS ONE* 10 (4). doi:10.1371/journal.pone.0124958.

———. 2015b. "The Bimodally Expressed MicroRNA MiR-142 Gates Exit from Pluripotency." *Molecular Systems Biology* 11 (12): 850–850. doi:10.15252/msb.20156525.

———. 2016. "Bidirectional Promoter Engineering for Single Cell MicroRNA Sensors in Embryonic Stem Cells." *PLoS ONE* 11 (5): 1–16. doi:10.1371/journal.pone.0155177.

Smith, Austin. 2013. *Nanog Heterogeneity: Tilting at Windmills? Cell Stem Cell*. Vol. 13. Elsevier. doi:10.1016/j.stem.2013.06.016.

Smith, Austin G., John K. Heath, Deborah D. Donaldson, Gordon G. Wong, J. Moreau, Mark Stahl, and David Rogers. 1988. "Inhibition of Pluripotential Embryonic Stem Cell Differentiation by Purified Polypeptides." *Nature* 336 (6200): 688–90. doi:10.1038/336688a0.

Smith, Zachary D., Michelle M. Chan, Kathryn C. Humm, Rahul Karnik, Shila Mekhoubad, Aviv Regev, Kevin Eggan, and Alexander Meissner. 2014. "DNA Methylation Dynamics of the Human Preimplantation Embryo." *Nature* 511 (7511): 611–15. doi:10.1038/nature13581.

Sokol, Sergei Y. 2011. "Maintaining Embryonic Stem Cell Pluripotency with Wnt Signaling." *Development* 138 (20). Company of Biologists: 4341–50. doi:10.1242/dev.066209.

Song, Ji Joon, Jidong Liu, Niraj H Tolia, Jonathan Schneiderman, Stephanie K Smith, Robert A Martienssen, Gregory J Hannon, and Leemor Joshua-Tor. 2003. "The Crystal Structure of the Argonaute2 PAZ Domain Reveals an RNA Binding Motif in RNAi Effector Complexes." *Nature Structural Biology* 10 (12). Nature Publishing Group: 1026–32. doi:10.1038/nsb1016.

Song, Ji Joon, Stephanie K. Smith, Gregory J. Hannon, and Leemor Joshua-Tor. 2004. "Crystal Structure of Argonaute and Its Implications for RISC Slicer Activity." *Science* 305 (5689). American Association for the Advancement of Science: 1434–37. doi:10.1126/science.1102514.

Sulzbacher, Sabine, Insa S. Schroeder, Thuy T. Truong, and Anna M. Wobus. 2009. "Activin A-Induced Differentiation of Embryonic Stem Cells into Endoderm and Pancreatic Progenitors-the Influence of Differentiation Factors and Culture Conditions." *Stem Cell Reviews and Reports* 5 (2): 159–73. doi:10.1007/s12015-009-9061-5.

Suter, David M., Nacho Molina, David Gatfield, Kim Schneider, Ueli Schibler, and Felix Naef. 2011. "Mammalian Genes Are Transcribed with Widely Different Bursting Kinetics." *Science* 332 (6028): 472–74. doi:10.1126/science.1198817.

Szostak, Emilia, and Fátima Gebauer. 2013. "Translational Control by 3'-UTR-Binding Proteins." *Briefings in Functional Genomics* 12 (1). Oxford University Press: 58–65. doi:10.1093/bfgp/els056.

Tai, C.-I., Eric N Schulze, and Q.-L. Ying. 2014. "Stat3 Signaling Regulates Embryonic Stem Cell Fate in a Dose-Dependent Manner." *Biology Open* 3 (10). Company of Biologists: 958–65. doi:10.1242/bio.20149514.

Tanaka, Tetsuya S. 2009. "Transcriptional Heterogeneity in Mouse Embryonic Stem Cells." In *Reproduction, Fertility and Development*, 21:67–75. CSIRO PUBLISHING. doi:10.1071/RD08219.

Tanzer, Andrea, and Peter F Stadler. 2004. "Molecular Evolution of a MicroRNA Cluster." *Journal of Molecular Biology* 339 (2): 327–35. doi:10.1016/j.jmb.2004.03.065.

Tao, Lichan, Yihua Bei, Yanli Zhou, Junjie Xiao, and Xinli Li. 2015. "Non-Coding RNAs in Cardiac Regeneration." *Oncotarget*. doi:10.18632/oncotarget.6073.

Tay, Yvonne M.-S., Wai-Leong Tam, Yen-Sin Ang, Philip M. Gaughwin, Henry Yang, Weijia Wang, Rubing Liu, et al. 2007. "MicroRNA-134 Modulates the Differentiation of Mouse Embryonic Stem Cells, Where It Causes Post-Transcriptional Attenuation of Nanog and LRH1." *Stem Cells* 26 (1): 17–29. doi:10.1634/stemcells.2007-0295.

Tay, Yvonne, Jinqiu Zhang, Andrew M. Thomson, Bing Lim, and Isidore Rigoutsos. 2008. "MicroRNAs to Nanog, Oct4 and Sox2 Coding Regions Modulate Embryonic Stem Cell Differentiation." *Nature* 455 (7216). Nature Publishing Group: 1124–28. doi:10.1038/nature07299.

Tee, Wee Wei, Steven S. Shen, Ozgur Oksuz, Varun Narendra, and Danny Reinberg. 2014. "Erk1/2 Activity Promotes Chromatin Features and RNAPII Phosphorylation at Developmental Promoters in Mouse ESCs." *Cell* 156 (4). Cell Press: 678–90. doi:10.1016/j.cell.2014.01.009.

Tesar, Paul J., Josh G. Chenoweth, Frances A. Brook, Timothy J. Davies, Edward P. Evans, David L. Mack, Richard L. Gardner, and Ronald D.G. McKay. 2007. "New Cell Lines from Mouse Epiblast Share Defining Features with Human Embryonic Stem Cells." *Nature* 448 (7150). Nature Publishing Group: 196–99. doi:10.1038/nature05972.

Thomson, Daniel W., and Marcel E. Dinger. 2016. "Endogenous MicroRNA Sponges: Evidence and Controversy." *Nature Reviews Genetics* 17 (5). Nature Publishing Group: 272–83. doi:10.1038/nrg.2016.20.

Thomson, Matt, Siyuan John Liu, Ling Nan Zou, Zack Smith, Alexander Meissner, and Sharad Ramanathan. 2011. "Pluripotency Factors in Embryonic Stem Cells Regulate Differentiation into Germ Layers." *Cell* 145 (6). Elsevier Inc.: 875–89. doi:10.1016/j.cell.2011.05.017.

Tompkins, Joshua D, Christine Hall, Vincent Chang Yi Chen, Arthur Xuejun Li, Xiwei Wu, David Hsu, Larry A Couture, and Arthur D Riggs. 2012. "Epigenetic Stability, Adaptability,and Reversibility in Human Embryonic Stem Cells." *Proceedings of the National Academy of Sciences of the United States of America* 109 (31). National Academy of Sciences: 12544–49. doi:10.1073/pnas.1209620109.

Torres-Padilla, M.-E., and Ian Chambers. 2014. "Transcription Factor Heterogeneity in Pluripotent Stem Cells: A Stochastic Advantage." *Development* 141 (11). Oxford University Press for The Company of Biologists Limited: 2173–81. doi:10.1242/dev.102624.

Torres, Josema, Javier Prieto, Fabrice C. Durupt, Simon Broad, and Fiona M. Watt. 2012. "Efficient Differentiation of Embryonic Stem Cells into Mesodermal Precursors by BMP, Retinoic Acid and Notch Signalling." *PLoS ONE* 7 (4): 1–11. doi:10.1371/journal.pone.0036405.

Tosolini, Matteo, and Alice Jouneau. 2015a. "Acquiring Ground State Pluripotency:Switching Mouse Embryonic Stem Cells from Serum/LIF Medium to 2I/LIF Medium." *Methods in Molecular Biology* 1341: 41–48. doi:10.1007/7651_2015_207.

———. 2015b. "From Naive to Primed Pluripotency: In Vitro Conversion of Mouse Embryonic Stem Cells in Epiblast Stem Cells." *Methods in Molecular Biology* 1341: 209–16. doi:10.1007/7651_2015_208.

Toyooka, Y., D. Shimosato, K. Murakami, K. Takahashi, and H. Niwa. 2008. "Identification and Characterization of Subpopulations in Undifferentiated ES Cell Culture." *Development* 135 (5): 909–18. doi:10.1242/dev.017400.

Treiber, Thomas, Nora Treiber, and Gunter Meister. 2019. "Regulation of MicroRNA Biogenesis and Its Crosstalk with Other Cellular Pathways." *Nature Reviews Molecular Cell Biology* 20 (1). Springer US: 5–20. doi:10.1038/s41580-018-0059-1.

Trott, Jamie, and A. Martinez Arias. 2013. "Single Cell Lineage Analysis of Mouse Embryonic Stem Cells at the Exit from Pluripotency." *Biology Open* 2 (10): 1049–56. doi:10.1242/bio.20135934.

Ventura, Andrea, Amanda G. Young, Monte M. Winslow, Laura Lintault, Alex Meissner, Stefan J. Erkeland, Jamie Newman, et al. 2008. "Targeted Deletion Reveals Essential and Overlapping Functions of the MiR-17~92 Family of MiRNA Clusters." *Cell* 132 (5). Cell Press: 875–86. doi:10.1016/j.cell.2008.02.019.

Viswanathan, Srinivas R., George Q. Daley, and Richard I. Gregory. 2008. "Selective Blockade of MicroRNA Processing by Lin28." *Science* 320 (5872): 97–100. doi:10.1126/science.1154040.

Wang, Gang, Xiao Yan Dong, Jian Yang Hu, Wen Hong Tian, Jie Yuchi, Yue Wang, and Xiao Bing Wu. 2011. "Long-Term Ex Vivo Monitoring of in Vivo MicroRNA Activity in Liver Using a Secreted Luciferase Sensor." *Science China Life Sciences* 54 (5): 418–25. doi:10.1007/s11427-011-4171-0.

Wang, Yangming, Scott Baskerville, Archana Shenoy, Joshua E Babiarz, Lauren Baehner, and Robert Blelloch. 2008. "Embryonic Stem Cell-Specific MicroRNAs Regulate the G1-S Transition and Promote Rapid Proliferation." *Nature Genetics* 40 (12). Nature Publishing Group: 1478–83. doi:10.1038/ng.250.

Wang, Yanli, Gang Sheng, Stefan Juranek, Thomas Tuschl, and Dinshaw J. Patel. 2008. "Structure of the Guide-Strand-Containing Argonaute Silencing Complex." *Nature* 456 (7219). Nature Publishing Group: 209–13. doi:10.1038/nature07315.

Wang, Zhong, Mark Gerstein, and Michael Snyder. 2009. "RNA-Seq: A Revolutionary Tool for Transcriptomics." *Nature Reviews. Genetics* 10 (1). Nature Publishing Group: 57–63. doi:10.1038/nrg2484.

Watanabe, S, H Umehara, K Murayama, M Okabe, T Kimura, and T Nakano. 2006. "Activation of Akt Signaling Is Sufficient to Maintain Pluripotency in Mouse and Primate Embryonic Stem Cells." *Oncogene* 25 (19): 2697–2707. doi:10.1038/sj.onc.1209307.

Watanabe, Yuka, Masaru Tomita, and Akio Kanai. 2007. "Computational Methods for MicroRNA Target Prediction." *Methods in Enzymology*. Academic Press. doi:10.1016/S0076-6879(07)27004-1.

Wee, Liang Meng, C. Fabián Flores-Jasso, William E. Salomon, and Phillip D. Zamore. 2012. "Argonaute Divides Its RNA Guide into Domains with Distinct Functions and RNA-Binding Properties." *Cell* 151 (5): 1055–67. doi:10.1016/j.cell.2012.10.036.

Wei, Zhang, and Hui Tu Liu. 2002. "MAPK Signal Pathways in the Regulation of Cell Proliferation in Mammalian Cells." *Cell Research*. Nature Publishing Group. doi:10.1038/sj.cr.7290105.

Weidgang, Clair E., Thomas Seufferlein, Alexander Kleger, and Martin Mueller. 2016. "Pluripotency Factors on Their Lineage Move." *Stem Cells International*. doi:10.1155/2016/6838253.

Weinberger, Leehee, Muneef Ayyash, Noa Novershtern, and Jacob H. Hanna. 2016. "Dynamic Stem Cell States: Naive to Primed Pluripotency in Rodents and Humans." *Nature Reviews Molecular Cell Biology* 17 (3). Nature Publishing Group: 155–69. doi:10.1038/nrm.2015.28.

Wellner, Ulrich, Jörg Schubert, Ulrike C. Burk, Otto Schmalhofer, Feng Zhu, Annika Sonntag, Bettina Waldvogel, et al. 2009. "The EMT-Activator ZEB1 Promotes Tumorigenicity by Repressing Stemness-Inhibiting MicroRNAs." *Nature Cell Biology* 11 (12): 1487–95. doi:10.1038/ncb1998.

Williams, R. Lindsay, Douglas J. Hilton, Shirley Pease, Tracy A. Willson, Colin L. Stewart, David P. Gearing, Erwin F. Wagner, Donald Metcalf, Nicos A. Nicola, and Nicholas M. Gough. 1988. "Myeloid Leukaemia Inhibitory Factor Maintains the Developmental Potential of Embryonic Stem Cells." *Nature* 336 (6200): 684–87. doi:10.1038/336684a0.

Winter, Julia, Stephanie Jung, Sarina Keller, Richard I. Gregory, and Sven Diederichs. 2009. "Many Roads to Maturity: MicroRNA Biogenesis Pathways and Their Regulation." *Nature Cell Biology* 11 (3): 228–34. doi:10.1038/ncb0309-228.

Wobus, Anna M., and Kenneth R. Boheler. 2005. "Embryonic Stem Cells: Prospects for Developmental Biology and Cell Therapy." *Physiological Reviews* 85 (2). American Physiological Society: 635–78. doi:10.1152/physrev.00054.2003.

Xu, Han, Tengfei Xiao, Chen-Hao Chen, Wei Li, Clifford A. Meyer, Qiu Wu, Di Wu, et al. 2015. "Sequence Determinants of Improved CRISPR SgRNA Design." *Genome Research* 25 (8). Cold Spring Harbor Laboratory Press: 1147–57. doi:10.1101/gr.191452.115.

Xu, Na, Thales Papagiannakopoulos, Guangjin Pan, James A. Thomson, and Kenneth S. Kosik. 2009. "MicroRNA-145 Regulates OCT4, SOX2, and KLF4 and Represses Pluripotency in Human Embryonic Stem Cells." *Cell* 137 (4): 647–58. doi:10.1016/j.cell.2009.02.038.

Yamaji, Masashi, Jun Ueda, Katsuhiko Hayashi, Hiroshi Ohta, Yukihiro Yabuta, Kazuki Kurimoto, Ryuichiro Nakato, Yasuhiro Yamada, Katsuhiko Shirahige, and Mitinori Saitou. 2013. "PRDM14 Ensures Naive Pluripotency through Dual Regulation of Signaling and Epigenetic Pathways in Mouse Embryonic Stem Cells." *Cell Stem Cell* 12 (3). Elsevier: 368–82. doi:10.1016/j.stem.2012.12.012.

Yamanaka, Yojiro, and Amy Ralston. 2010. "Early Embryonic Cell Fate Decisions in the Mouse." *The Cell Biology of Stem Cells*. Springer, Boston, MA, 1–13. doi:10.1007/978-1-4419-7037-4_1.

Yasuda, Shin Ya, Tatsuhiko Ikeda, Hosein Shahsavarani, Noriko Yoshida, Bhavana Nayer, Motoki Hino, Neha Vartak-Sharma, Hirofumi Suemori, and Kouichi Hasegawa. 2018. "Chemically Defined and Growth-Factor-Free Culture System for the Expansion and Derivation of Human Pluripotent Stem Cells." *Nature Biomedical Engineering* 2 (3). Nature

Publishing Group: 173–82. doi:10.1038/s41551-018-0200-7.

Yeom, Kyu Hyeon, Inha Heo, Jinwoo Lee, Sungchul Hohng, V Narry Kim, and Chirlmin Joo. 2011. "Single-Molecule Approach to Immunoprecipitated Protein Complexes: Insights into MiRNA Uridylation." *EMBO Reports* 12 (7): 690–96. doi:10.1038/embor.2011.100.

Ying, Qi-Long Long, and Austin Smith. 2017. *The Art of Capturing Pluripotency: Creating the Right Culture*. *Stem Cell Reports*. Vol. 8. Cell Press. doi:10.1016/j.stemcr.2017.05.020.

Ying, Qi-Long Long, Jason Wray, Jennifer Nichols, Laura Batlle-Morera, Bradley Doble, James Woodgett, Philip Cohen, and Austin Smith. 2008. "The Ground State of Embryonic Stem Cell Self-Renewal." *Nature* 453 (7194): 519–23. doi:10.1038/nature06968.

Ying, Qi Long, Jennifer Nichols, Ian Chambers, and Austin Smith. 2003. "BMP Induction of Id Proteins Suppresses Differentiation and Sustains Embryonic Stem Cell Self-Renewal in Collaboration with STAT3." *Cell* 115 (3). Elsevier: 281–92. doi:10.1016/S0092-8674(03)00847-X.

Ying, Qi Long, and Austin G. Smith. 2003. "Defined Conditions for Neural Commitment and Differentiation." *Methods in Enzymology*. doi:10.1016/S0076-6879(03)65023-8.

Ying, Qi Long, Marios Stavridis, Dean Griffiths, Meng Li, and Austin Smith. 2003. "Conversion of Embryonic Stem Cells into Neuroectodermal Precursors in Adherent Monoculture." *Nature Biotechnology* 21 (2): 183–86. doi:10.1038/nbt780.

Yoshida, Kanji, Ian Chambers, Jennifer Nichols, Austin Smith, Mikiyoshi Saito, Kiyoshi Yasukawa, Mohammed Shoyab, Tetsuya Taga, and Tadamitsu Kishimoto. 1994. "Maintenance of the Pluripotential Phenotype of Embryonic Stem Cells through Direct Activation of Gp130 Signalling Pathways." *Mechanisms of Development* 45 (2): 163–71. doi:10.1016/0925-4773(94)90030-2.

Yu, Zuoren, Yuan Li, Huimin Fan, Zhongmin Liu, and Richard G. Pestell. 2012. "MiRNAs Regulate Stem Cell Self-Renewal and Differentiation." *Frontiers in Genetics* 3 (SEP). Frontiers: 191. doi:10.3389/fgene.2012.00191.

Yuan, Kai, Wen Bing Ai, Lin Yan Wan, Xiao Tan, and Jiang Feng Wu. 2017. "The MiR-290-295 Cluster as Multi-Faceted Players in Mouse Embryonic Stem Cells." *Cell and Bioscience*. BioMed Central. doi:10.1186/s13578-017-0166-2.

Yue, Xuetian, Lihua Wu, and Wenwei Hu. 2015. "The Regulation of Leukemia Inhibitory Factor." *Cancer Cell & Microenvironment* 2 (3). NIH Public Access. doi:10.14800/ccm.877.

Zhao, Yong, Eva Samal, and Deepak Srivastava. 2005. "Serum Response Factor Regulates a Muscle-Specific MicroRNA That Targets Hand2 during Cardiogenesis." *Nature* 436 (7048): 214–20. doi:10.1038/nature03817.

Zheng, Xiaoyang, Haven Baker, William S. Hancock, Farah Fawaz, Michael McCaman, and Erno Pungor. 2006. "Proteomic Analysis for the Assessment of Different Lots of Fetal Bovine Serum as a Raw Material for Cell Culture. Part IV. Application of Proteomics to the Manufacture of Biological Drugs." *Biotechnology Progress* 22 (5): 1294–1300. doi:10.1021/bp060121o.

Zimmerlin, Ludovic, Tea Soon Park, and Elias T. Zambidis. 2017. "Capturing Human Naïve Pluripotency in the Embryo and in the Dish." *Stem Cells and Development* 26 (16): 1141–61. doi:10.1089/scd.2017.0055.

Zovoilis, Athanasios, Lukasz Smorag, Angeliki Pantazi, and Wolfgang Engel. 2009. "Members of the MiR-290 Cluster Modulate in Vitro Differentiation of Mouse Embryonic Stem Cells." *Differentiation* 78 (2–3). Elsevier: 69–78. doi:10.1016/j.diff.2009.06.003.